CALIBRATION AMONG THE SEPARATE TRAWL SURVEY PROGRAMS TO EXTEND THE TIME SERIES FOR JUVENILE SNAPPER INDEXES

Scott Nichols
NMFS Pascagoula

INTRODUCTION

Trawl survey programs relevant to juvenile indexes for red snapper are best described as several separate time series (Nichols 2004a). Statistics from these separate segments could be used as independent tuning indexes in the stock assessment, each with its own catchability coefficient (q). However, any systematic errors in any other data sets or model structures used in the assessment might affect estimation of these separate q's differentially. The assessment might be made stronger then, if the separate trawl survey segments could be united analytically first, using just the survey data. The idea is to develop longer time series that could be expected to be proportional to standing stock, *i.e.* have the same q throughout each lengthened time series.

This paper explores two models to extract longer time series from the available survey segments. Both use a Bayesian, Markov Chain Monte Carlo (MCMC) approach, using the freely available 'BUGS' software (Spiegelhalter *et al.* 1996). Depending on the data set and the structure, the models must "solve" up to 3 problems:

1) account of any "missing" observations
2) adjust for differences in coverage among cruise programs
3) deal with observations of zero catch.

The models considered share similar strategies: impute values and uncertainties for missing observations, calibrate among surveys based on ratios between the most complete surveys and the portions of the most complete surveys that approximate the less complete surveys, and model error within strata with negative binomial distributions. The two models differ in the information used to predict catch rates, and in the assumptions about the structure of survey error above the level of within-stratum variation.

The raw materials are the same data summarized by Nichols 2004a, used to calculated the "base indexes" of that paper. The end products here are a single summer time series, and a single fall time series spanning the years with data present. The survey segments FS (Fall SEAMAP), FF (First Fall), and FG (Fall groundfish described in Nichols 2004a are combined into a single Fall Index for 1972-2002, and the segments SS (Summer SEAMAP), ES (Early SEAMAP), and TC (Texas Closure) are combined into a single Summer Index for 1981-2003. Results are expressed in number per hour, scaled to the FS and SS time series. At this time, analyses have been done only for red snapper, catch in numbers, all sizes (ages) combined.

Although Bayesian models are used here, "Bayesianism" is not the message of this paper. It is really the MCMC portion of the approach that I am making the most use of. Similar analyses could be carried out in a Frequentist structure, but the MCMC approach allows more flexibility for considering structural alternatives for modeling uncertainty. The MCMC also allows estimates of uncertainty, and any hidden correlations among the parameter estimates, to be carried forward very conveniently into any statistics that are functions of the parameter estimates. This "carrying forward" can sometimes be done analytically in a Frequentist structure, but can become difficult or even impossible for functions of any complexity. In an MCMC approach, you actually simulate the processes or structures that are believed to give rise to the data, rather than solving a set of "normal equations" to fit a statistical model that is assumed up front to approximate the consequence of those processes. I believe that the increased flexibility of the MCMC gives more insight into the problems underlying development of statistical models. The cost is greatly increased computing time, so much so that it limits the number of alternatives that can be considered.

METHODS

The Data

The surveys and their data are as described in Nichols 2004a. The only additional processing required was conversion from SAS to BUGS format; simple proportional adjustment of fishing time to standard speeds (for stations where speed was recorded); and attachment of indicator variables for the stratification used in this analysis.

The First Fall (FF) time "series" was for one year only (1987), and was the first attempt to apply the SEAMAP design to the traditional fall sampling window. It differed from the FS series only in the order of stations. The FF survey went "counterclockwise," but encountered problems working during passage of cold fronts off the Texas coast. For 1988, the survey was reversed, allowing completion of the sampling off Texas before the full progression of seasonal cold fronts began. We have very little information to compare surveys with order difference. There was one repeat in the summer of 1984 (C2 in Nichols 2004a), which showed virtually no difference in average catch rate of red snapper. For this paper, the FF results have been combined with FS, without any adjustments. All further references to FS in this paper imply FS plus FF in the Nichols 2004a designations.

The SEAMAP designs (FS, SS, and ES) are very finely stratified (to guarantee full distributional information each year), with one sample per stratum. The 'method of collapsed strata' (Cochran 1977) was the intended vehicle for more rigorous estimates of variance. (Recognition that 'collapsed strata' could be extended to mean 'collapse over all strata' as in the base indexes (Nichols 2004a) was a bit belated.) For these Bayesian models, I returned to the original collapsed strata concept, as without some combination of strata, some of the parameters of the Bayesian models will be completely confounded, with the potential for unpredictable results. (This was confirmed with some preliminary runs that deliberately ignored this confounding.) Choices for collapsing strata are arbitrary. The surveys had many strata in depth, and relatively few alongshore. I chose to collapse adjacent depth strata, to six new strata of 5- 9 fm, 9-13 fm, 13-17 fm, 17-22 fm, 22-35 fm, and 35-50 fm. I retained the separate day/night stratification in FS and SS, in part because series ES and TC are night-only, and the separation will be needed for calibration. The larger strata usually meant 3 or 4 stations per stratum if no stations were missing. The collapsed strata were selected without regard to missing stations. As a results 3 strata for FS (out of 960) are missing; for SS, 15 of 1020; and for ES, 2 of 150. No collapsing is necessary for TC and FG, which have multiple stations in the original strata (our most strata, for TC), with none empty.

Multiple vessels are used in SEAMAP surveys, and data from all vessels using the SEAMAP standard net are included in this analysis, with vessel identity ignored. There is a separate analysis being prepared at the same time as this paper, to evaluate possible vessel differences. Earlier, preliminary results presented to the SEAMAP participants indicated little consistent difference among vessels. Non-Oregon II stations make up fairly small fractions of FS, SS, and ES surveys when the full ranges of the surveys are examined, suggesting there would be little effect on the full index even if differences are found. However, more significant impacts might be felt in the calibration for FG to FS, and for indexes developed for smaller areas, if vessel differences turn out to be important.

The Models

I began by developing 2 models for the Fall SEAMAP (FS) survey, and then started applying the lessons learned to the other surveys. Unfortunately some of the model details that worked for FS did not work for SS, largely due to the lower snapper abundances during the summer period. ("Did not work" in this case meant nonsensical predictions and enormous variances.) Diagnosing the problems, and determining what model structures will work turned out to be important steps in getting access to the flexibility of a Bayesian / MCMC approach, and I will spend some time on those considerations. Listings of the models in the BUGS programming language (which is not difficult to figure out) are collected in the Appendix. Readers

are encouraged to "follow along" using the listings, as the written explanations below proved impossible to make very concise.

The two models examined differ primarily in the structures that estimate the individual stratum abundances which in turn predict the catch data. Model 01 is basically a "mu-sub-ij" model in the sense of Searle (1971), with each cell considered individually, whereas model 02 is a "main effects plus local term" model much like the model 02 of the bycatch analysis reported in Nichols 2004b.

In model 01, each cell is given a lognormal prior on abundance (catch per hour), with the mean and precision terms for that prior given lognormal hyperpriors. With that structure, the data largely determine the parameters of the abundance priors. The prior is the same for all cells within a year, so no information about a cell's geographic location or average spatial distribution of snapper is used. The data will relocate the posterior for each cell's abundance, sometimes by a sizeable amount. The data also tighten spread of each posterior for abundance compare to the (fitted) prior, but with only a few observations per cell, not by a large amount. Abundance for any cell without data is imputed by the prior, as the mean abundance over all cells with precision determined directly by the fitted prior, again incorporating no information about location or average distribution of snapper over cells. This model is intended to use only very simple assumptions, with minimal transfer of information across cells. The cost is that information that does exist is left unused.

Model 02 does make use of location information, and the snapper distribution averaged over each time series. Broad normal priors are placed on factors for year, stratum, and time of day (day vs night). These factors are treated as additive on a log scale, as is a cell-specific "Local" factor assumed to be normal with prior mean zero, and precision determined by the data and a lognormal hyperprior. Abundance for cells without data are imputed by the main effects for year, spatial stratum, and time of day, with variance imputed by the uncertainty contained in the posterior for each of those factors, and by the Local term treated as a random effect. The variation in Local for missing cells is determined by the hyperpriored precision, and thus is largely determined by the spread of Local factor values occuring throughout the time series.

In model 02, stratum factors could potentially be partitioned into alongshore and depth terms, but this structure would presume the abundance distributions were the same at each level of the other factor, at least until the Local term was applied. I decided not to use this "crossed" spatial structure, and thus no spatial stratum "knows" anything about its spatial relationships to the other strata.

Both models use the geographic areas of the strata as weighting factors for calculating index values, much as described by Nichols (2004a) for the "base indexes." I made one change from the weightings described in Nichols 2004a. As I am now going to calibrate the ES time series to an SS standard, I used the stratum areas of SS. The difference is in the "east of the River" area, where we had to discontinue sampling east of 88 W as described in Nichols 2004a. The areas of strata east of the river here do not include any contribution from shrimp statistical zone 10.

Both models used assume that a negative binomial distribution applies to trawls within each stratum. The motivation for this came from the work I had been doing at that same time on bycatch estimation (Nichols 2004b). The negative binomial was chosen because it is a commonly used distribution that allows a finite probability for a catch of zero, and because it can describe patchy populations. Our surveys, like many, are stratified random. The simplest analyses are 'design based,' often using arithmetic means with normal expectations (although other approaches have been considered), and are nearly unique (the base indexes of Nichols 2004a follow that theme, with minor variation). Only data from within any space / time 'cell' affects estimates for that cell. However, a design-based approach may not be appropriate for all surveys and applications. Some years, it is not be possible to complete all stations. One can either ignore the gaps, or turn to model-based estimation, at least to fill the holes. Additionally, survey results may be too sparse for some uses, such that better estimates might be expected from borrowing information from other cells, again by considering a more model-based approach. However, a problem arises with a shift to a more model-based structure. At least to first order, we expect multiplicative effects from any auxiliary variable, but catch=0 is often a common observation (sometimes even for means) and an observed zero probably

rarely means total absence, even locally. There have been several approaches to dealing with the expectation of multiplicative effects combined with observations of zero (Table 1), but none have ever proved completely satisfactory. The negative binomial structure is not perfect, either (expanded discussion in Nichols 2004b), but appears to be at least as reliable as the other methods of Table 1.

Implementing the negative binomial in BUGS proved a bit tricky, requiring a number of 'trial and error' adjustments. BUGS' internal negative binomial distribution was slow, and plagued by poor mixing in the bycatch analysis project, so I switched to a procedure suggested by B Jones (Duke / SAMSI), and used a combination of BUGS' gamma and poisson distributions. Two parameters, r and mu are set by the predicted abundances in each cell. A gamma distribution with the r and mu parameters is sampled in the MCMC to produce a lambda parameter for a Poisson distribution, essentially changing lambda for every trawl. The lambda drawn is in catch per hour units, so that lambda is multiplied by the hours fished for each tow to obtain the Poisson parameter that predict the value of catch in numbers to compare with the data. . Neither gamma parameter is independently related to the cell mean (gamma mean=r/mu). To set the mean to the value predicted by the main effects parameters, only r is taken as a free parameter, and mu is set to be r/(predicted mean cpue for each simulation iteration). I initially considered two different structures for setting the r parameter. The first idea was to use a common value of r for all space and time strata, which was the approach taken in the bycatch analysis (Nichols 2004b). The second was to consider r to be determined by a power function of (predicted) abundance. I began this trawl survey analysis with the first structure, but switched to the second when some preliminary runs with partial data suggested a tighter fit to the data using the second approach. The two structures are related, in that the first is a special case of the second, the case where the exponent in the power function is zero. The first case corresponds to a relation between log variance and log mean with slope of approximately 2. In trawl surveys, empirical fits for this slope tend to be slightly less than 2 (often visible only when a large number of species are considered at once, increasing the range of means examined), so it seemed reasonable to consider the greater flexibility of the second alternative.

Both structures were implemented through prior distributions on variables determining r, but some of my first choices led to numerical problems. Using too broad a prior on a common r caused the analyses to crash if that prior allowed the MCMC to explore very low values of r. There appeared to be two sources to the numerical crashes: 1) less frequently, a draw from the gamma with low r would produce a lambda numerically indistinguishable from zero by the computer, which crashed the Poisson portion of the routine, and 2) more frequently, the adapative strategy (first 4000 iterations) for BUGS dropped the trial parameters for r to extremely low levels, and caused a numerical error even when the final posterior might not have been a problem. A solution to both problems is to constrain r either via a prior (common r case) or a max( ) function (power function case) to keep r in a numerically acceptable range. These survey data supported r values as low as 0.05 without numerical problems. (The bycatch dataset of Nichols 2004b was able to support r as low as 0.03). I chose to use a uniform prior on r on the interval 0.05 to 5. For red snapper in the fall survey, this choice of prior appeared to have little impact, as even the lower tail of the r posterior tended to be above 0.05 in any of the models considered. At that point, I decided to stop exploration of the "common r" structure, in favor of a prior structure that spanned both alternatives

An r prior is not specified directly – power function parameters are given priors, and their posterior distributions determine the posterior distribution for r. I used a normal prior on the exponent, centered on 1.2, with a precision chosen to put the -3 standard deviation value just above zero. The intent was to allow the data to determine whether a common r or an r changing with abundance was more appropriate via the posterior on the exponent. (The prior for the proportionality coefficient was lognomal, with log mean of 0 and variance 1). I concentrated on the FS survey first, and the normal power function version worked well for both FS models, and for SS model 01. However, for the SS data set with model 02, the normal prior on the exponent returned a nonsense component to the abundance predictions. Most of the parameters related to abundance came out strongly bimodal, with a component associated with the exponent for the r power function about –0.4 (over 5 standard deviations from the center of the prior). This component was most strongly expressed in cells with catches very near zero. Catch data near zero were mathematically compatible with very high mean estimates and enormous variances under the normal prior assumption of this model applied to the SS data set. This problem was not observed with any of the other time series.

To solve this problem, I switched to a lognormal prior on the exponent to r vs abundance function in the SS analyses. (I also relaxed the prior on the proportionality term, trying to add back some flexibility.) This allowed the analysis to express posteriors on the exponent centered anywhere in a wide range between zero and well over one, but exponent=0 is structurally excluded. I decided to retain the normal prior on the exponent for FS and SS model 01. Because the ES and TC series are calibrated against SS, I matched the prior used in those analyses to the one used in the corresponding SS model.

The analysis of the FG time series also failed with the normal prior on b, in this case with a crash of the BUGS run, rather than production of nonsense results. I switched to a lognormal prior on b for the FG analysis.

Actual indexes associated with each time series, and with calibrations among series, are calculated as functions of the cell by cell abundance posteriors. The cells do not cover equal spatial areas, so area weights as described in Nichols 2004a are applied. Time series FS and SS are the most complete in space and time of day, and the indexes dervied for those surveys are taken as the standards. To "calibrate" the other time series in each season to FS and SS scales, calibration factors are derived from the FS and SS results, and treated as random variables, with variation "carried forward" into the estimates of each index value on the FS and SS scales.

A set of reasonably obvious assumption must be applied to derive the calibration factors. (We do not have simultaneous observations under different designs.) The assumptions are:

1) different nominal vessel speeds are presumed to act proportionally, *i.e.* area covered is the real effort variable. There are no comparative data, and speed was not measured with much accuracy until very recently (Nichols 2004a).
2) Day/night difference as are assumed to be consistent over years, determined by the average difference between the log of the FS or SS index and the log of an index calculated using only the night strata from those analysis. Variation in this calibration determined by variations among years for this difference in log values. This calibration is applied to ES and TC indexes, which involved night sampling only. For FG, stations were taken without reference to time of day. The dense sampling and near balance is presumed to make a day/night factor unnecessary.
3) After speed and time of day are taken into account, surveys with different designs, but covering the same spatial area were assumed to have the same expected values for the area-weighted means of catch rate, with no calibration needed.
4) Surveys designed to cover smaller spatial ranges than FS and SS were rescaled to FS or SS using a ratio expectation determined in the FS and SS data. The difference in the log of the FS or SS index and an index for each reduced area (TC and FG spatial areas) was calculated for each year in the FS and SS data. The mean of that difference over the FS and SS surveys (separately) became the (log) mean for a lognormal distribution of calibration factor to be used in the FG and TC series, respectively. Variances for each calibration parameter in the FG, ES, and TC series were set to the variance observed among years in the FS or SS series (i.e. standard deviation, not standard error).

This 4th assumption is probably the most vulnerable of the four, in that it presumes the mean and variance of the calibration factors remained the same back to 1981 for the combined Summer Index, and back to 1972 for the Fall Index. Treating calibration as a random variable, with variance, does capture some of the "cost" of not having surveyed the full range, but cannot defend against any unknown, large changes in distribution of fish prior to the FS and SS series.

The "Primary Area" of the FG series (88 W to 91 30 W, 5 – 50 fm; Nichols 2004a) does not have the same boundaries as the strata of the FS survey. This wrinkle was handled by assuming that the FS samples out to 92 W, the FS boundary, were representative of the West stratum in FG, which goes only to 91 30 W. However, to calculate the facsimile of the FG index in the FS data, the FG area weights were used.

Separate East and West indexes, bounded by the Mississippi River, were requested. These were estimated by summing only over appropriate spatial strata in the FS and SS analyses. The r vs abundance power function, and in model 02, the main affects; are still used across both regions. However, the presence of the

Local term in model 02 implies that the influence of West data on East estimates (and vice versa) will be small, and assuming different r vs abundance curves East and West appears to be an unnecessary complication. However, I expected that the effect of restricting the spatial range could sizeable effects on the calibration factor variances, so I calculated east and west calibration factors for the east and west FS and SS indexes separately.

Criteria for examining mixing and convergence, and deciding on number of iterations were very similar to those used in the bycatch analysis (Nichols 2004b), where there is a more extended discussion. In this index analysis, I never encountered any results indicating convergence or mixing problems, so duration was chosen mainly by noting the relative smoothness of the posterior densities. Two-chain runs for 20k iterations were taken as standard, which was probably a bit of an overkill. I developed a fairly standard series of graphs to examine the results of each analyses. These are developed in the Results section.

All FS and SS runs were completed on a Dell computer of September 2003 vintage, equipped with Dual 2.6 GHz XEON Processors and 2 GB RAM. The operating system was Windows 2000. The version of BUGS software used was WinBUGS 1.4. The standard 20k iteration runs took about 10 hours for FS and SS data. The TC and ES analyses were small enough to run, albeit slowly, on my older IBM laptop under Windows 98, and for convenience some runs were made on that machine. No compatibility problems were noted in moving the same BUGS codes between the 2 computers and operating systems. Additional analysis and graphic summarizations used SAS for Windows (v 8.00) and Excel 97 software, run on the Windows 98 machine. [Declaration of trade names does not imply a product endorsement by the government.]

RESULTS

Fall Index

Fall SEAMAP (FS)

Figure 1 shows the index results for Fall SEAMAP (FS) time series estimated via model 01. The figure uses a convention repeated several times in this paper, with boxplot format for the model under discussion; and lines for central tendency, without distribution information , for results from other analytical approaches. (Graphs with several years and several sets of confidence intervals each seemed ineffective as presentation tools.) Box plots in this document (whether prepared using BUGS or Excel) follow the BUGS convention: the thick bar covers the interquartile range, and the thinner vertical line covers the 95% confidence band. A solid line was usually added to connect the medians in plots constructed with Excel. Box plots prepared using BUGS also show a horizontal dash at the mean value of each distribution; the Box plots produced using Excel do not. BUGS plots also have an overall mean as a horizontal line; the plots constructed in Excel do not.

The central tendencies for all three indexes shown in Figure 1 capture much the same pattern. I have not shown confidence intervals (CI's) for all three on the same graph, but generally they were of comparable in size as well, with the ordering of size of the CI's among models differing in different years.

FS Model 1 Details

Figure 2 shows examples of the posterior marginal densities for the index values, using a single year. On an arithmetic scale, a slight skew is evident (present, but not easily seen in Figure 1). The distribution is more symmetric on the log scale.

Posterior marginals for the parameters of the power function relating gamma parameter r to predicted abundance are shown in Figure 3. Examination of BUGS "history" plots (not shown) suggests that the b parameter is the slowest at mixing in any of the models, consistent with the irregular edge in Figure 3a. (This figure was probably the most jagged posterior for any parameter in any of the models.) I did not investigate correlation between the a and b parameters in individual models, but the pattern seen among models suggests that there probably is some. These posterior distribution are quite narrowed and relocated

compared to their prior (I return to that topic in more detail in the TC results section), and the parameters appear to be doing the job intended for them.

Results for the parameter later used to adjust the Fall Groundfish (FG) time series to the FS scale are shown in the Figure 4 box plot. Perhaps a more easily understood statistic based on the same information appears in Figure 5, which is a box plot of the percent of the population estimated to be in the area covered by the FG surveys (the "Groundfish Primary Area"). In the BUGS box plots, years are identified sequentially, with [1] being 1987 and [16] being 2002 for the FS series. Both statistics are highly variable among years; and there appears to be a pattern over years, with the highest percentages early in the FS time series. This pattern will ultimately limit our confidence about using the FG series as an indicator of stockwide abundance.

The posterior distributions of the annual precision parameters used in the priors for the abundances in each cell are shown in Figure 6. The variation among the annual posteriors demonstrates relocation and some narrowing with respect to the hyperprior, but the spreads on the individual year values are still quite broad, suggesting the data do not pin down the values for these parameters all that tightly. The extent of the spreads may thus be more influenced by the hyperprior itself than desired, although other options are limited. Past experience with similar structures suggests that much broadening this particular hyperprior would soon lead to "numerical analysis – type" trouble. Considering only a single parameter common to all years would increase the influence of the data, but the differences among years seen in Figure 6 argue against that approach. Fortunately, the index results are not strongly affected by these parameters (variation among cells is more important than the magnitude of the variation within), so I elected to leave the structure and the prior at my original choice.

A goodness of fit plot for predicted abundances vs cell means appears on the arithmetic scale in Figure 7. Replotting the same information (less the points with observed means of zero) on the log scale gives a different perspective to the same information (Figure 8). Both figures show a pleasingly tight fit. Departures from a 1:1 line reflect more the structural assumptions than any difficulty for model 01 in fitting the data. On the arithmetic plot, the predicted values increasingly scatter away from a 1:1 situation as abundance increases. I interpret this to be model 01 increasingly 'writing off' the higher observations as more random fluctuations than as indicators of underlying higher abundance in proportion to the mean. At the low end, points on the arithemetic plot are above a 1:1 relationship, but all are 'small.' The log plot does a better job of communicating the curvature of the model away from a pure mean prediction, and this is primarily the impact of the increasing frequency of observations of zero. Model 01 says observations of zero come from an underlying positive abundance, and the structure of model 01 estimates those underlying abundance to be fairly flat, relative to observed means, on the log scale. I will contrast this later with the pattern from model 02, which stays linear with the observed means to much lower (log) values.

FS Model 02 Details

As already seen in Figure 1, model 02 captures essentially the same pattern of variation in central tendency as model 01, and the "Base Index" of Nichols 2004a. Figure 9 includes the box plot depiction specifically for model 02. Comparing Figs. 1 and 9 finds the spreads (uncertainty) to be slightly tighter with model 02 most of the time. This is not surprising, as there are more terms in model 02, and distributional information external to each cell is used in the few cases where data are missing.

Although a slight skew is present on the arithmetic scale, the posterior distributions of the index values are nearly symmetric on both the arithmetic and log scales (example in Figure 10.)

The posteriors for the a and b pararmeters are a bit smoother than for model 01, and the distributions are in slightly different locations (Figure 11 vs Figure 2). However, given the similarity of the index results, the impacts of the differences in a and b on the indexes must minor. Most of the other differences in results between models 01 and 02 probably stem more from other aspects of the different structural assumptions rather than from the minor a and b differences, but I did not verify this.

Model 02 explicitly incorporates main effects for stratum and time of day (day/night). Figure 12 show a box plot for the stratum effects, and Figure 13 shows the box plot for the day vs night effect. Levels for both effects were centered about their means. The central tendency for day vs night differences has night samples averaging about 40% above day catch rates, although this figure is not well pinned down even by this extensive set of data (95% CI about 20-60%).

Box plots for the model 02 results relevant to adjusting the FG time series to the FS scale are presented in Figures 14 and 15, paralleling the results for model 01 of Figures 4 and 5. Model 02 returned results very similar to the model 01 results, although some small differences can be found.

Model 02 contains a single precision parameter common to all cells as a prior to the Local effects (which can be thought of as perturbations from the sum of the year, stratum, and time of day main effects). Thus, variation in the value of Local throughout the data set is captured. The posteriors of Figure 16 are markedly relocated and narrowed compared to the hyperprior used, suggesting dominance by the data despite the fairly precise prior used to insure numerical stability.

The goodness of fit plots (Figures 17 and 18) for model 02 were similar to the plots for model 01, with a few pertinent exceptions. On the arithmetic scale, the spread around any level of abundance appears a bit greater than the spread in model 01, at least through the mid-range of abundances. However, the predicted value vs observed mean seems to be more centered around a 1:1 relationship than was the case for model 01, especially at lower values of abundance. The partitioning of the (log) cell abundance prediction into main effects appears to allow the model to consider much lower values of predicted abundance than the cell by cell approach of model 01 could.

Fall Groundfish (FG)

The Fall Groundfish sampling was very different in character than the SEAMAP sampling. Only the "Primary Area" was covered, but it was covered by very dense sampling compared to the SEAMAP work. There were effectively only two strata (east and west of the river, 5-50 fm, time of day not considered), so several of the modeling structures used in the FS analysis would not make much sense here. A single model was used to fit the data, without the main effects or precision hyperpriors used in FS. The model used does resemble FS model 01 more closely than FS model 02, but there are no missing cells to be filled. Later in the paper, I refer to two models for FG, but these differ only in the source of the calibration distributions used to rescale FG to FS. The distributions for these calibration parameters are not narrowed by the FG data.

The box plot for the FG index (Fig. 19) and the distribution examples (Fig. 20) show much the same patterns as the FS figures. However, one interesting feature emerges from comparing Fig. 20b with Figs. 2b and 10b -- the spreads of the distributions of Figs. 2b and 10b are smaller than for 20b. These are not the same years in these example figures, of course, but examining the tabled values in the BUGS output confirmed that this pattern held across the board. The result is surprising, because Figure 20 is based on very dense sampling in a much smaller area compared to the sampling that generated the other two figures. I would expect narrower spreads for FG index values than for FS.

I have already discussed in the Methods section that the FG data would not support the normal prior for the "b" parameter of the power function for r, so a lognormal prior was used. Figure 21 shows the posteriors for the power function parameters. Both are much relocated from the centers of their lognormal priors. The median for the "b" posterior here had the lowest value of any analysis in this paper. The resulting r from these distributions centered near 0.2 whatever the predicted abundance was. That pattern would suggest that a value of b=0 would be justifiable, but that the posterior has probably been pulled back from that by the precision of prior. That is, a less precise prior might allow the posterior of b to be centered closer to zero (centering<=0 is structurally excluded, of course). However, the impact on the overall analysis would be minor, as the r posteriors were already very close to constant, with 95% spreads on the order of 0.18 to 0.22.

The goodness of fit plots (Figs 22 & 23) are very tight, but this should be expected given that there are about 100 samples behind each point.

Combining FS and FG

The distribution for the calibration factor to convert FG to the FS scale is shown in Fig. 24. Recall that these distributions are products of the two FS analyses; the FG analysis just applies them. The distributions are broad and highly skewed, which will carry forward into the FS-calibrated indexes from the FG era. Figure 25 shows that central tendencies of the "base index," the FG index, and the two calibration versions all capture much the same signal, but that a major change in scale must be made when inferring SEAMAP wide abundance from the relatively low abundance of the Primary Area. The two index choices for the extended time series are shown in Figs. 26 & 27. The two are very similar, with the CI's on the second slightly broader by virtue of a larger spread to the calibration statistic derived from FS model 02. There is about a 20-fold range between the maximum and minimum years based on the central tendencies, but the most obvious feature is the dwarfing of the CI's from the FS period by the CI's produced by attempting to infer SEAMAP-wide abundance from surveying only the groundfish "primary area." (And, this still ignores the concern about trends over years in Figures 4, 5, 14, and 15.) It is hard to imagine a better illustration of why sampling as much of the range of a stock as possible is an important principle in developing fishery independent surveys.

Summer Index

Summer SEAMAP (SS)

Figure 28 shows the index results for the Summer SEAMAP (SS) time series estimated via model 01 in box plot format. Central tendencies for two other indexes (medians for SS model 02, means for the Nichols 2004a "Base index") are plotted as lines. As was the case with the Fall analysis, the 3 analytical choices are all capturing much the same pattern.

SS Model 01 Details

Arithmetic and log scale posterior marginals for the index value resulting from SS model 01 are shown in Figure 29. (Only a single year is shown as an example). The distribution in Fig. 29a is the same one summarized by 5 points in the box plot's bars for 1990, but the 32k points of Figure 29 makes the full shape of the distribution much more evident. As in Fall, there is a modest skew on the arithmetic scale, and near symmetry on the log scale.

Posterior marginals for the "a" and "b" parameters (Fig. 30) show nothing surprising. These parameters had the same normal priors as used in the fall analysis, and there is no indication of any bimodality that required the switch a lognormal prior for b in SS model 02.

The calibration factor to be used to rescale ES to SS based on the log of the SS index minus the log of an index using only SS night data. Posterior marginals for the annual values of that statistic are shown in Figure 31. There is a modest scatter, without indication of trends. Calibration of TC to the SS will be based on the statistics plotted in Figure 32. There appears to be some tendency for the higher values to be clustered in the earlier years (1987-1992). This information is re-expressed as estimates of the "percent of the population off Texas" (the TC survey area) in Figure 33. This description is in quotes because there are really two effects captured in the plot. SS day and night combined is being compared with night only for the TC area, which makes the values above 100% seen in the tail of one distribution mathematically possible.

Figure 34 shows a box plot of the annual precision parameters for the priors on log abundances. The same comments I made in discussing FS model 01 apply here as well. The goodness of fit plots (Figs. 35 & 36) likewise resemble the FS model 01 patterns, and I have no additional comments on them.

SS Model 02 Details

The box plot featuring the index results from SS model 02 is shown in Figure 37, complementing Figure 28. The spreads are slightly smaller for model 02 compared to model 01 for most years, but you would have to study the two figures for a long time to notice it. The full posteriors exemplified by Figure 38 may be a bit more symmetrical in the arithmetic compared to those from model 01, but again the difference is minor. The posterior for the b parameter (Fig. 39) is surprisingly symmetric, despite the lognormal prior.

Stratum effects (Fig. 40) suggest a dome-shaped distribution of abundance with depth, much like in the Fall results, although a bit less consistent among the 5 alongshore zones than in Fall. The day vs night effects (Fig. 41) are remarkably similar to the Fall results (central tendency about 40% higher at night), which need not be expected a priori.

Day night differences also determine the calibration factor between ES and SS (Fig. 42), in this case calculate by comparing the full SS index with one based on only night samples. The agreement between the calibration factor averaged over years and the time of day effect of Figure 41 is reasonable (median values of -0.1439 vs -0.1716 on a log scale; difference well below the CI's around each). This agreement is reassuring but not surprising for this fairly well balanced data set. However, the central values from the two relevant values in model 02 imply quite a bit more difference between day and night than estimated by model 01 (33-40% vs about 15%). I consider the model 02 estimates more reliable, as the model 01 procedure for imputing catches where missing will tend to reduce any actual day night difference.

The two figures describing statistics related to calibrating TC to SS (Figs. 43 & 44) have properties similar to the results from model 01 (Figs. 32 & 33). The 'run' of values over the first 6 years is troublesome given we would like to use the assumption that uncertainty in the TC year can be modeled by the variation throughout the SS years; but unlike the more troublesome FS/FG case, values near those in the first 6 years of SS do occur in the later SS years as well.

The discussion of the precision parameter for the Local effects priors put forth in the FS model 02 section applies here as well. Numerically, the results were quite similar, too (compare Fig. 45 with Fig. 16). The goodness of fit plots for SS model 02 (Figs. 46 & 47) likewise share the properties discussed for FS model 02.

Early SEAMAP (ES)

ES model 01 (Figs. 48-52) and ES model 02 results (Figs. 53-59) do not contain many features not already discussed. The broad confidence intervals for the 1982 index values in Figures 48 and 53 of probably result from the particularly poor spatial coverage of the survey that year. The box plot of stratum effects from model 02 (Fig. 56) shows a number of differences from the similar plot for the SS time period (Fig. 40). Neither the South Texas nor the east of the River segments (first and last 6 points) seem to have the dome-shaped relationship between depth and abundance, and the confidence bands for shallowest strata (stratum number mod 6 = 1) suggest that there may be considerable variation among years in the fraction of the population found near shore. The different pattern for ES compared to SS might have arisen in part from the different order, and thus timing, of stations during the cruises (ES cruises took stations "counterclockwise); and in part from the relatively few years of data available to establish the patterns (5 in ES vs 17 in SS).

The two distributions for the factor calibrating ES to the SS scale (Fig. 60) do have noticeably different centers, as discussed in the SS model 02 section, but the difference is seen to be small compared to the uncertainty established by the year to year variation seen in the SS years. A case could be made based on the similarities among years in Figure 42 to use the standard error rather than the standard deviation to model the uncertainty in the calibration factor. However, Figure 31 does not make a strong case for that narrowing, and the difference between the centers from models 01 and 02 suggests retaining the choice to use the more conservative confidence band is justified. Figure 61 shows that much the same signal is being captured by the central tendencies of all the index versions. Only a modest rescaling is required to go between the night only surveys of ES and the day and night of SS. The amount of rescaling is centered on a value of about half the day to night differences discussed in the SS model 02 section.

Texas Closure (TC)

The TC survey occurred only one year (1981) and sampling took place only at night, so there is really only one underlying structure used to model the data, essentially the same structure used in model 01 in the FS, SS , and ES series. There are two models here, however, but for data fitting, they differ only in the choice of priors used for the parameters of the r vs abundance power function. (They also differ in whether the calibration factor was based on SS model 01 or 02, but that difference enters only 'downstream' from the use of the data.) Recall the ES and TC priors for b were matched to those in the SS model providing the calibration parameters. I will take a different route in presenting TC results, using the TC survey as a 'laboratory' for investigating the impacts of the choice of prior.

Figure 62 shows the index estimated specifically for the TC survey from the two models differing only in the priors on the power function. There is very little practical difference. Figure 63 shows the two posteriors for the "a" parameter compared with their priors, using box plots on both arithmetic and log scales. The centers of the posteriors have been relocated and narrowed considerably compared to the priors. A similar plot for b (Fig. 64, arithmetic only) shows similar behavior. I have always considered changes in the relationship between r and abundance to be most easily understood as changing the relationship between the variance and the mean for a set of estimates. Figure 65 shows the implications of the different medians of the posteriors for a and b associated with each choice of prior on the variance vs mean relationship. There appears to be no practical difference.

The goodness of fit plots (Figs. 66-69) have much the same features discussed for the other time series, although they may be harder to see given that there are so few points. Reflecting the minimal impact of the choice of priors, the paired figures are almost identical.

I made no plot for the calibration between the TC and SS surveys (it would be only one year with one point for each model. Given the higher abundance in Texas and higher catch rates at night, the TC index numbers must be adjusted downward to go to the SS scale. The median values for the factors are 0.88 for model 01, and 0.74 for model 02.

Combining SS, ES, and TC

The indexes obtained by applying the calibration distributions to the ES and TC surveys and attaching the results to the SS time series are shown in Figures 71 and 72. There does not appear to be much practical difference between the two choices. Like the FG case, the cost of not covering the full SEAMAP range is evident in the confidence band for the first year. However, because a larger fraction of the stock was surveyed than appears to have been the case for FG, the confidence bands are nowhere near as "dwarfing" to the SS confidence bands as the FG-derived bands were to the FS bands.

East and West Indexes

I decided not to extend this paper by presenting details of the results for deriving separate indexes for east and west of the Mississippi River. I have included the final results for each season using model 02 throughout, as Figures 73-74 and 76-77. More details are available should the SEDAR wish to consider

them. I did not notice anything new issues in deriving the separate indexes, save for effects expected from the smaller sample sizes of the separated areas. I included the results here mainly because there is some information that could be relevant to considering separate (sub)stocks. Figures 75 and 78 plot east vs west index values against one another, and correlation is readily apparent. Had there been none, it would have been an argument for separation. With the correlation shown, the results do not much support either the separation or combination argument in preference to the other. There is support for interpreting the two sides as a single stock; or the two sides could be essentially separate, but with year class strengths influenced by factors correlated on a spatial scale larger than the ranges of the two putative (sub)stocks.

Perhaps a more surprising finding, present but not obvious in the figures, is the apparent higher reduction between fall and spring in the east compared to the west. Averaged over years with both present, the Fall indexes are about the same east and west. By summer, the east index average is nominally about one-half the value of the west index average. I did not notice this until after all runs were completed, so I had not built anything into the programs to assess the uncertainty around that observation, but I plan to look at this further. However, I am also concerned that the east index may be covering only a small fraction of a putative eastern stock or substock, because we cannot survey effectively with trawls east of 88 W. I have generally not worried about that in the other indexes, because the full SEAMAP survey probably does cover the bulk of any single northern Gulf stock. However, if the east alone should be considered in separation, we may or may not be covering a large fraction of its population, and the problems described for the FG series may apply.

Relationships Between Summer and Fall

I have not tried to unite the Fall and Summer indexes into a single year class strength indicator, believing that step is better left for the full stock assessment. It is evident, however, that the precisions estimated during the SEAMAP portions of the time series (1987 on) might support estimating the rate of change between successive surveys. I will compare the Fall survey with the following Summer, and describe the (exponential) rate as Z', with the prime meant to stress that the rate will include any changes in catchability as well as total mortality. I wrote a short BUGS program (listing in the Appendix) to get annual estimates of Z' and its uncertainty from lognormal distributions based on the index results. The results appear as Figure 79. The average value is probably in rough agreement with Z values from past stock assessments, but the individual year estimates are scattered, with confidence intervals suggesting real differences. Whatever is causing the differences appears not to be related to shrimping effort (Figure 80).

There may be several causes, not mutually exclusive, for the scattered pattern:

1) Z is truly that variable
2) The prime part of Z' is truly that variable
3) The variation in the age 1 fraction in the fall surveys is too much for this simple analysis
4) The widths of the confidence bands for individual index points are underestimated
5) There are large-scale sources of error that affect most or all samples of an entire survey

I will consider each of these at more length in the Discussion section, as the problem is relevant to evaluating just how much reliance we can put on individual survey results. I will say now that I believe 4) is probably the dominant factor behind the scatter of Figure 79.

DISCUSSION:

For all the effort required to get the details of a Bayesian/MCMC approach working, there was not much change within the individual series from the information implied by the "base indexes." However, this is generally a good thing. The issue of missing stations has now been addressed two different ways, but it would appear that missing stations have not in general been a serious issue. The Bayesian index distributions show some skew on the arithmetic scale, and appear to be fundamentally lognormal. Lognormal uncertainty is not surprising for the individual cell predictions, given the with multiplicative structures and the negative binomial error, but it may surprise some to find that this skew carries over into indexes that are weighted means of a large number of observations. (In the base indexes, normality of the

mean is assumed at the outset.) Even if the results for Z' cause one to question the accuracy of the variance estimates, the relative cost to precision caused by surveying only a portion of the range is probably well estimated. For the FG case, that cost was very high, and even the cost seen may be underestimated because of the likelihood of trends over years. Nevertheless, as is often the case for surveys of juveniles, year to year variation is large (to 20x max to min in these surveys). That large a signal tends to come through for any reasonable sampling design or choice of analytical method.

I have not presented much on the details about mixing, convergence, or (except for a few cases) impacts of priors, largely because extensive inspections of BUGS histories and distributional results indicated no appreciable problems beyond the ones already discussed. This has not always been the case for other applications I have tried using BUGS, so here the omission reflects the relative simplicity of these models and probably too, the high degree of balance in the data sets. I have also not included much commentary here on Bayesian approaches per se, or on the utility of BUGS. I included much more of that in my bycatch paper which also prepared for the red snapper SEDAR (Nichols 2004b), and many of the comments I might make here would simply repeat those.

The negative binomial portion of this modeling effort was the most difficult, and least satisfying. Based on experience with king mackerel in the bycatch analysis, I anticipate further problems (requiring ad hoc adjustments) if I extend the analysis in this paper to less common species. Currently, the negative binomial seems to be getting the job done for red snapper, but there must be room for improvement.

The final results from the model 01 and model 02 structures were not very different. I recommend model 02 however, as I believe its use of information from outside an individual cell is preferable for dealing with missing data. I expect model 02 to be more accurate for the few years with the highest missing fractions, and cases may arise in other studies where this advantage could be more important than it was here. Model 02 predictions also remained linear with the observed values to much lower abundances in the goodness of fit plots than model 01 predictions did.

What can we infer from the apparent poor performance in estimation of Z? Implausible disagreements between successive surveys are frequent topics for discussion among survey practitioners worldwide, and it may have become fashionable to invoke the cause I listed as 5) -- unknown sources of error affecting an entire year's results -- as the cause. Certainly there are candidate factors could act like that: changes in vessel noise over years, changes in skill of the operators, undetected gear problems, etc. However, the high frequency to the fluctuations of Figure 79 make those issues seem unlikely to be dominant factors. The large geographic area and duration of our surveys probably rule out weather or sea conditions as serious candidates for "cause 5" impactors for the results here. I have no reason to anticipate any particular level of variation in real Z from year to year, but the fact that the variation in Figure 79 looks so totally unrelated to a measure of one of its components, shrimping effort, make cause 1) suspect. (I did note, however, that the range of shrimp effort values over the years having Z' estimates is rather small.) Like cause 1), we really have little basis to expect any particular level of variation in the 'prime' portion of Z'. Causes 2) and 3) are related, distinguished by cause 2) impacting the rate sometime between fall and the next summer, whereas 3) implies a potential for bias in the initial point. Cause 3) is potentially addressable with our size composition data, but that was beyond the scope of this paper. However, unless the 'prime' portion of Z' rises to effectively infinity on those that were age 1 in the fall, there should be little bias, as there would still be a trace of that cohort the following summer.

Support for cause 4) is found in the unusual situation noted on page 8 in comparing the variance between the FG and FS surveys. The FG surveys sampled a small area very densely, yet the variance was higher there than in the broader, sparser FS surveys. This pattern was also found to hold for the "base index" result, so it is not a consequence of the Bayesian approach or the different stratifications used in the two surveys (both time series are analyzed in the "base index" approach as if they were completed randomized designs). One would expect that the ~200 samples of the FS series would be enough to characterize the variance fairly accurately, but that expectation might be wrong if the underlying population contained relatively rare, extremely high densities that appeared very rarely in the actual sampling. The current FS sampling density may encounter those rare samples in none to a few strata a most, resulting in variances for most strata or years being underestimated. The higher density FG sampling may contain some of these rare

samples in almost every year and stratum, resulting in consistently higher variance estimates. It would not take a great deal more variation to make the separate confidence bands of Figure 79 overlap to a major degree – maybe a standard deviation about twice what is reported. The estimated levels of variation suggest that index values differing by about 20-30% are distinguishable – that seems unusually high for work in the marine environment, where 'factor of 2' is the rule of thumb. This has the feel of a productive area for further research.

Although we may doubt our ability to distinguish annual indexes down to the level indicated by the precisions reported, we have no reason to doubt our surveys at the level useful for assessment, where indications of year class differences to resolutions of 2x, 3x, or even more may be valuable. We might, however, want to think very carefully before setting up programs using individual cruise results as management triggers.

REFERENCES

Cochran W G. 1977. Sampling Techniques. (Wiley) Section 5a.12

Nichols S. 2004a. Derivation of red snapper time series from SEAMAP and Groundfish trawl surveys. Report to the Gulf of Mexico Fishery Management Council. Red Snapper data SEDAR, April 2004.

Nichols S. 2004b. Some Bayesian approaches to estimation of shrimp fleet bycatch. Report to the Gulf of Mexico Fishery Management Council. Red Snapper data SEDAR, April 2004.

Spiegelhalter D J, Best N G, Gilks W R, & Inskip H. 1996. Hepatitis B: a case study in MCMC methods. In: Gilks W R, Richardson S, & Spiegelhalter D J. Markov Chain Monte Carlo in Practice. (Chapman & Hall / CRC) pp.21-44.

Searle S R. 1971. Linear Models. (Wiley). Chapter 7 & 8.

{BUGS stands for **B**ayesian inference **U**sing **G**ibbs **S**ampling, and there is now a fairly sizeable literature on its use. The Gilks *et al.* book containing the Spiegelhalter *et al.* citation has several other references to BUGS as well. The BUGS software is available at www.mrc-bsu.cam.ac.uk/bugs/ }

Table 1. Techniques for dealing with the "zero problem" in multiplicative models.

Log (x + c)	(several suggestions for c)
Delta distribution	(several variations)
Treat zeros as censored observations	
Discrete distribution at last stage	
Other transformations	

Figure 1. The FS index from model 01. Error bars follow the BUGS convention, with the thick bar covering the interquartile range, and the thin line spanning the 95% confidence interval. The solid line labeled FS 01 connects the medians. For comparisons with other results, the medians from the FS 02, and the means of the "Base Index" of Nichols 2004a are also plotted.

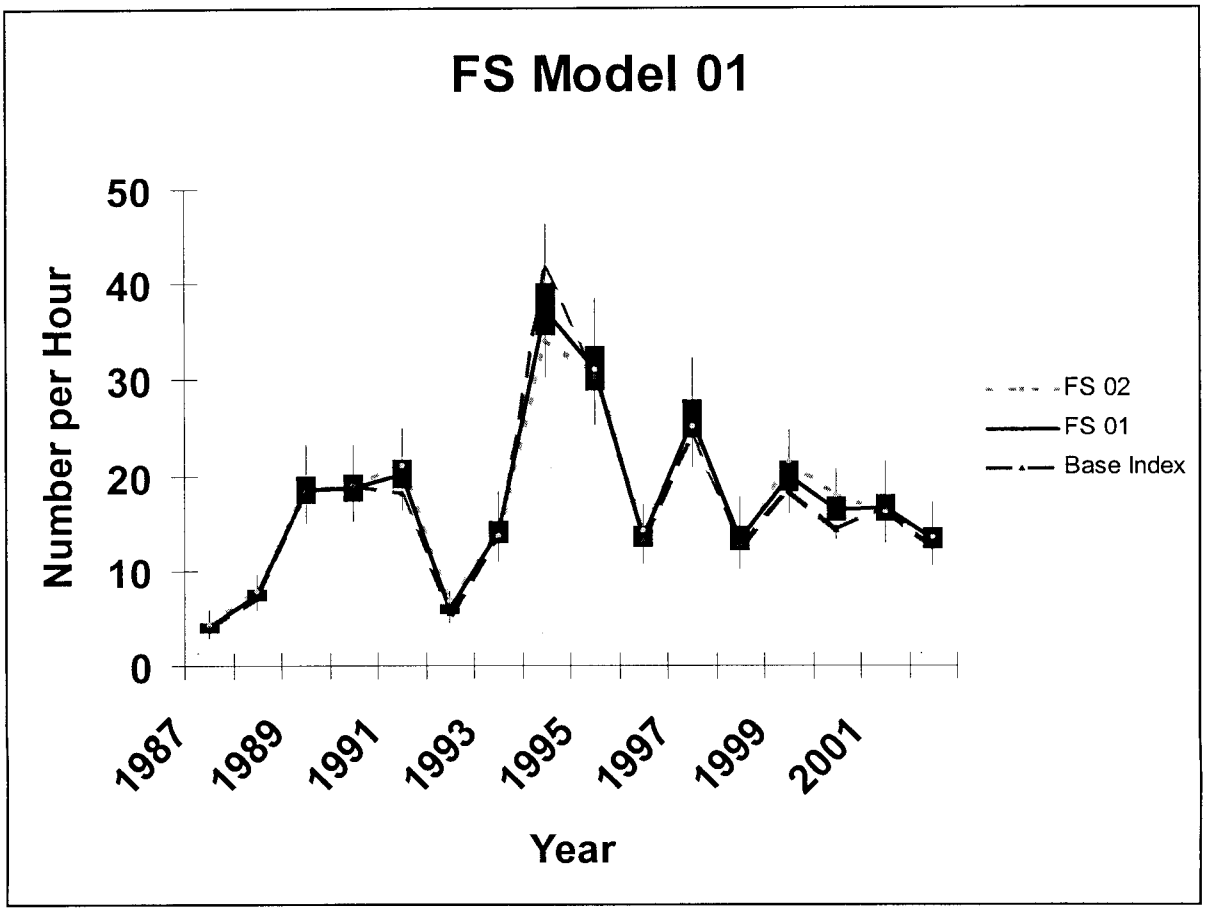

Figure 2. Examples of posterior marginal distributions for the 1990 FS index from model 01. a) arithmetic value. b) log value. The year chosen was just picked to be an example. The shapes for other years are very similar.

2a)

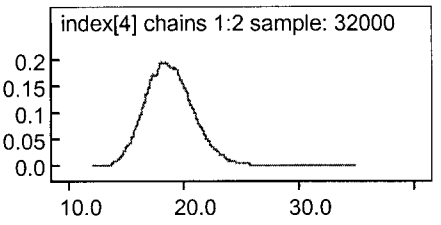

2b)

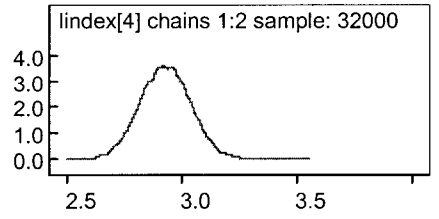

Figure 3. Posterior marginal distributions of the power function parameters relating gamma parameter r to predicted abundance in cell for FS model 01. A functional form $r = a * \text{abundance}^{b}$ is assumed a) the a (proportionality) parameter. b) the b parameter (exponent). (b had a normal prior in this version)

3a)

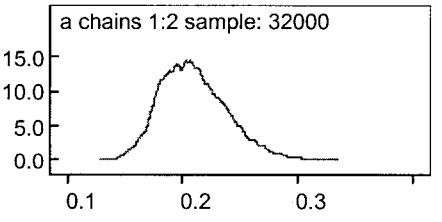

3b)

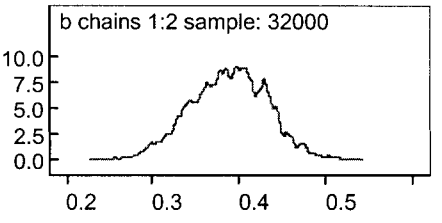

Figure 4. BUGS box plot of the calibration parameter relating FS and FG, model 01. The value is the log of the FS index (full spatial range) minus the log of an index calculated for the Primary Area covered by the FG surveys.

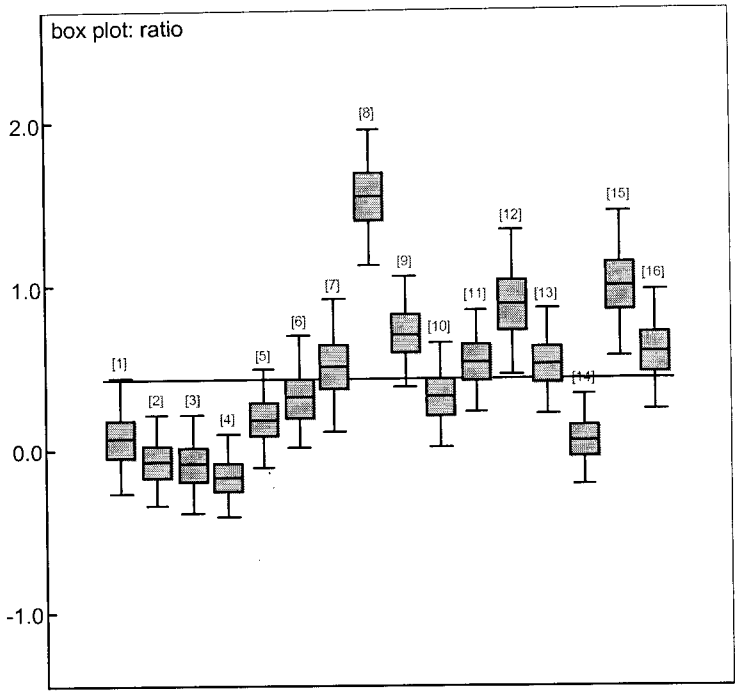

Figure 5. Box plot of the percent of the population estimated to be in the Groundfish Primary Area, compared to the population in the entire FS survey area. Model 01.

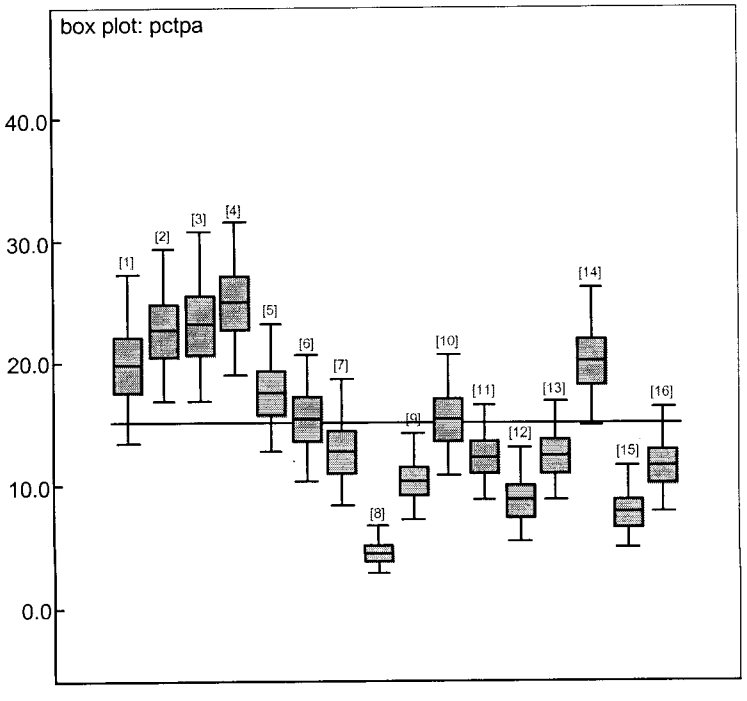

Figure 6. Box plot of the annual precision parameters for the priors for the (log) abundance in each cell. (FS model 01).

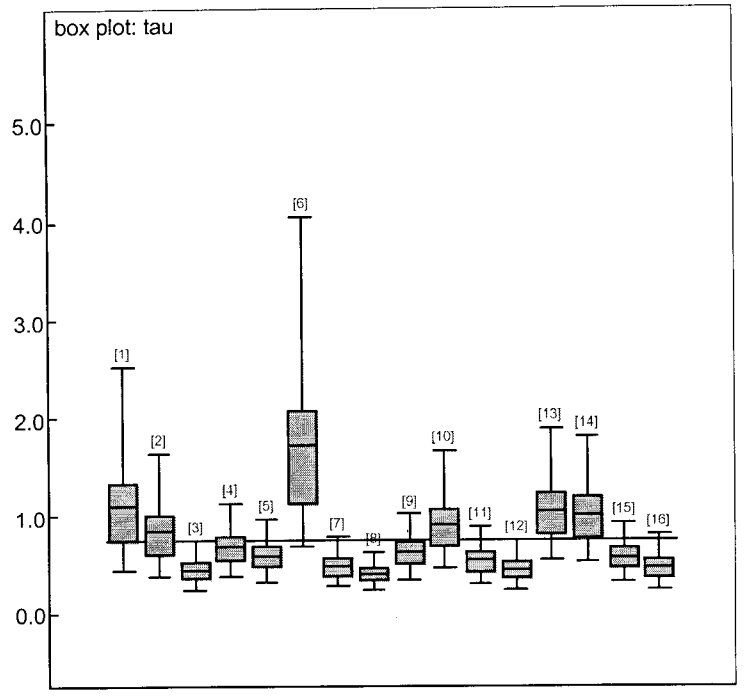

Figure 7. Goodness of fit plot for FS model 01. Predicted abundance vs mean of cell observations. Arithmetic scale. Different symbols identify the 6 depth bands of the stratification.

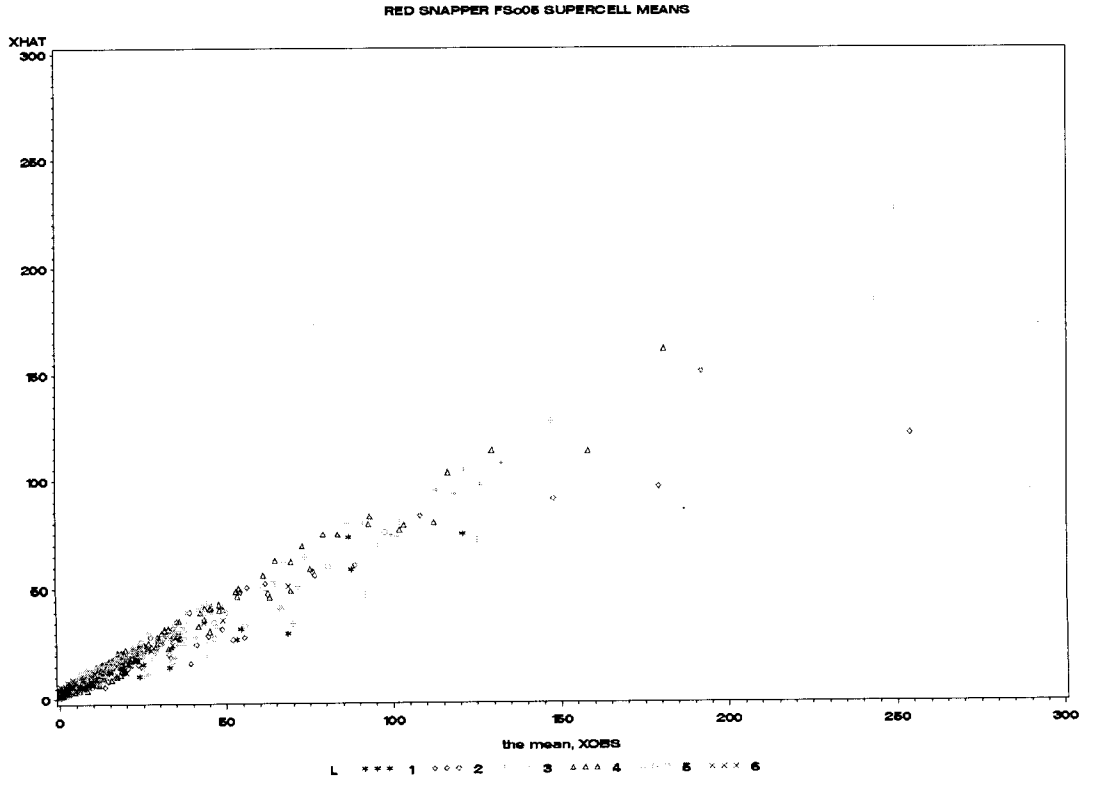

Figure 8. Goodness of fit plot for model FS 01. Predicted abundance vs mean of cell observations. Log scale; observations of zero cannot be plotted. Symbols identify depth bands of stratification.

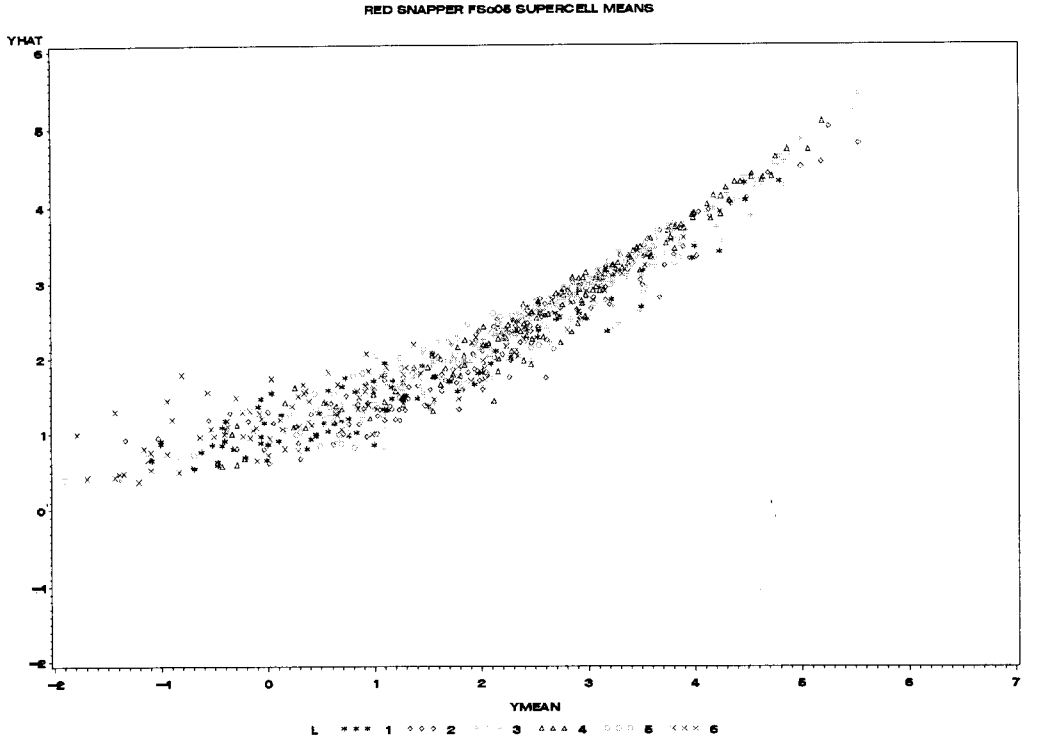

Figure 9. The FS index from model 02. The solid line labeled FS 01 connects the medians. For comparisons with other results, the medians from the FS 01, and the means of the "Base Index" of Nichols 2004a are also plotted.

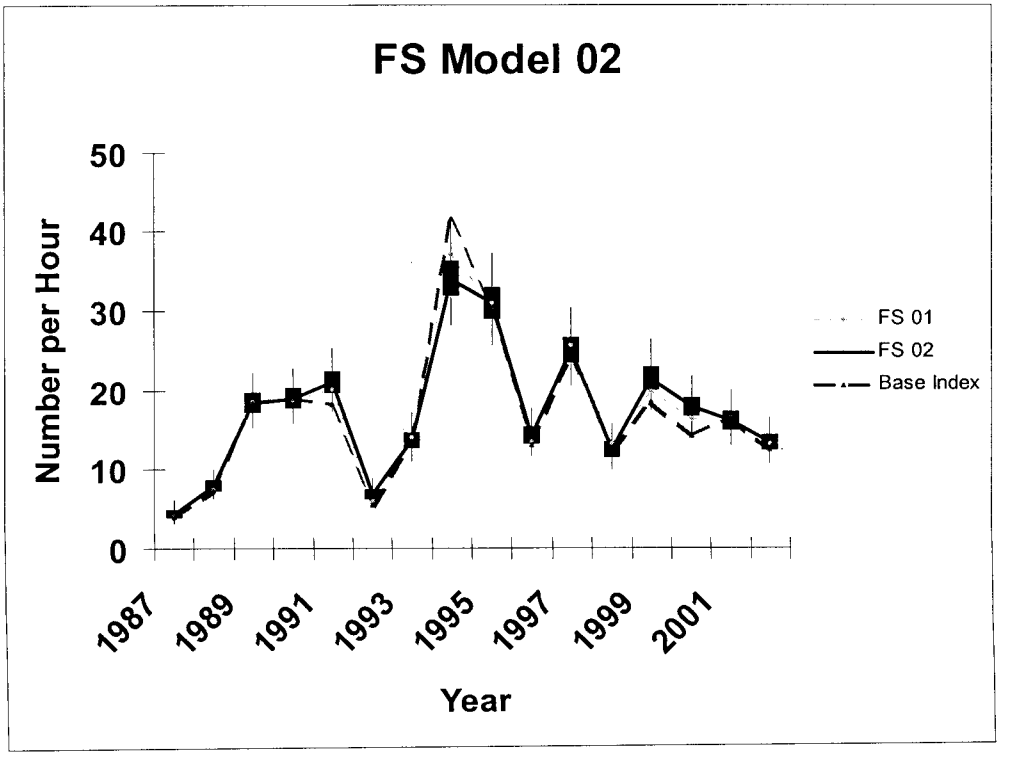

Figure 10. Examples of posterior marginal distributions for the 1990 FS index from model 02. a) arithmetic value. b) log value. The year chosen was just picked to be an example. The shapes for other years are very similar.

10a)

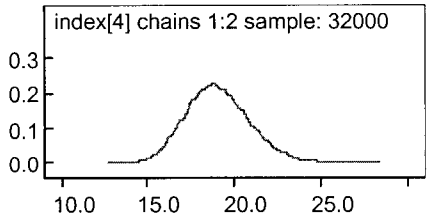

10b)

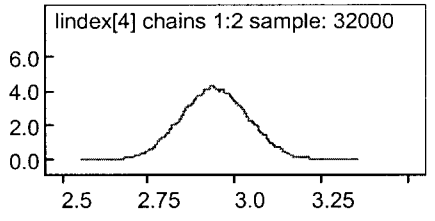

Figure 11. Posterior marginal distributions of the power function parameters relating gamma parameter r to predicted abundance in cell for FS model 02. A functional form r = a * abundance b is assumed a) the a (proportionality) parameter. b) the b parameter (exponent). (b had a normal prior in this version)

11a)

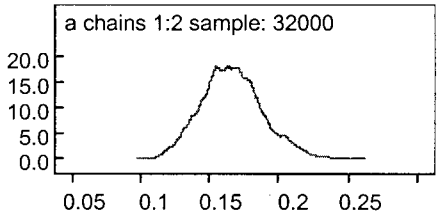

11b)

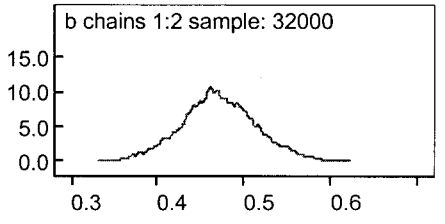

Figure 12. Box plot of marginal posteriors for the stratum effects (FS model 02). Strata were numbered sequentially through the 6 depth zones, then by alongshore zone, then depth w, starting in South Texas, and ending east of the River. The patterning reflects the general dome-shaped distribution of snapper with depth.

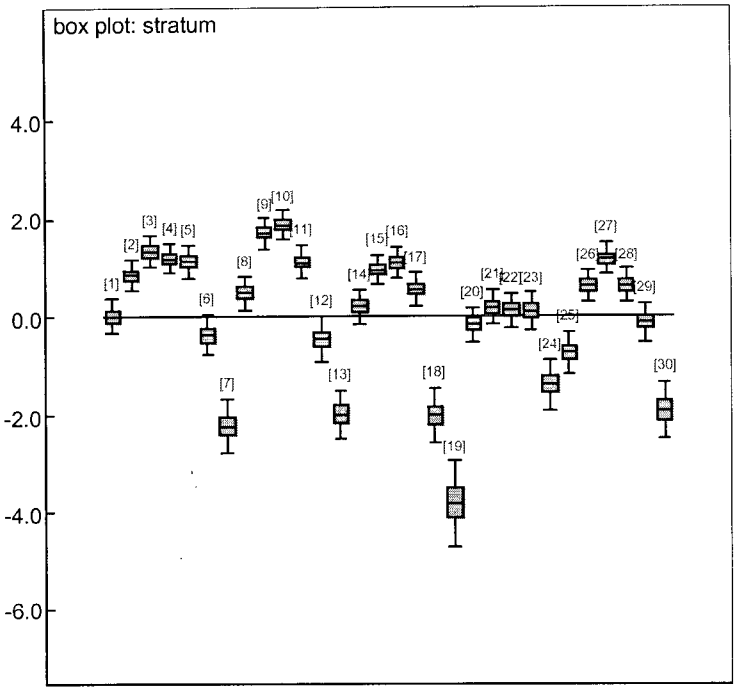

Figure 13. Box plot of the marginal posteriors for the time of day effects (FS model 02). [1] is day; [2] is night.

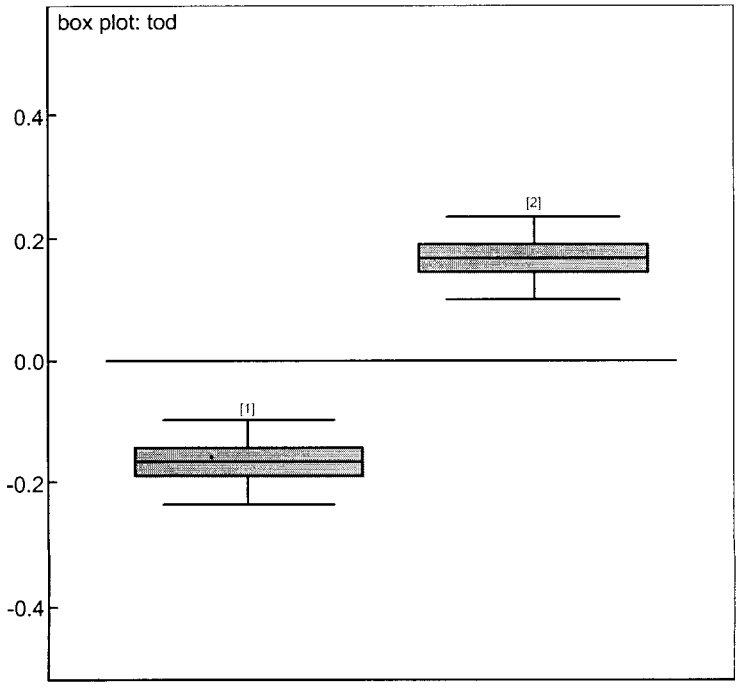

Figure 14. Box plot of the calibration parameter relating FS and FG, model 02. The value is the log of the FS index (full spatial range) minus the log of an index calculated for the Primary Area covered by the FG surveys.

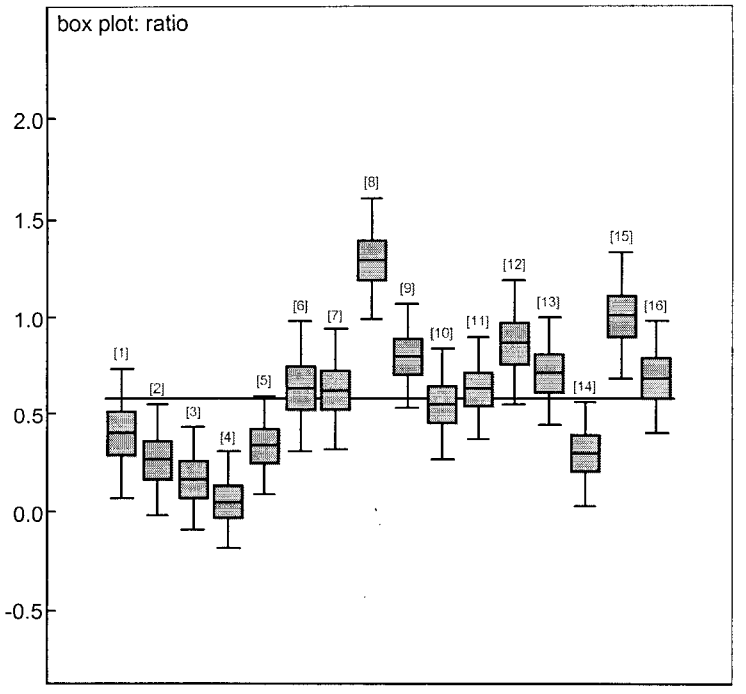

Figure 15. Box plot of the percent of the population estimated to be in the Groundfish Primary Area, compared to the population in the entire FS survey area. Model 02.

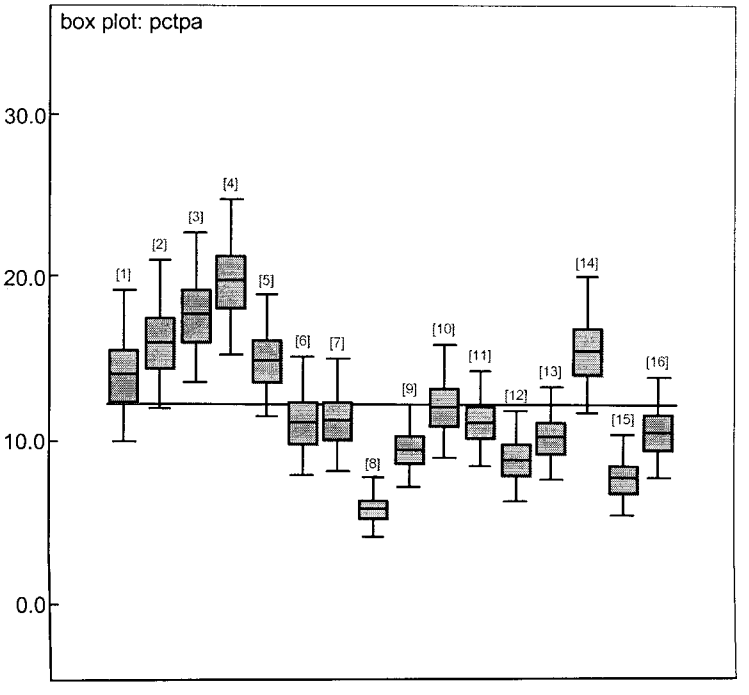

Figure 16. Marginal posterior distribution of the precision parameter for the priors on the Local effects. There is one common parameter for this precision in FS model 02, determined primarily by the deviations from main effects only predictions over the entire time series. a) arithmetic scale b) log scale. The prior on this parameter was lognormal.

16a)

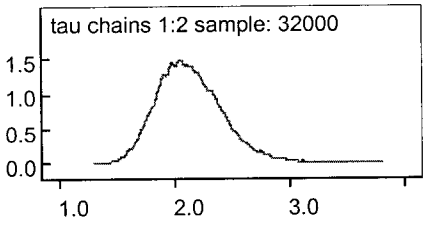

16b)

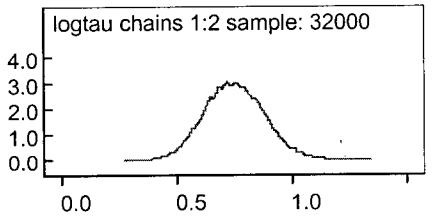

Figure 17. Goodness of fit plot for FS model 02. Predicted abundance vs mean of cell observations. Arithmetic scale. Different symbols identify the 6 depth bands of the stratification.

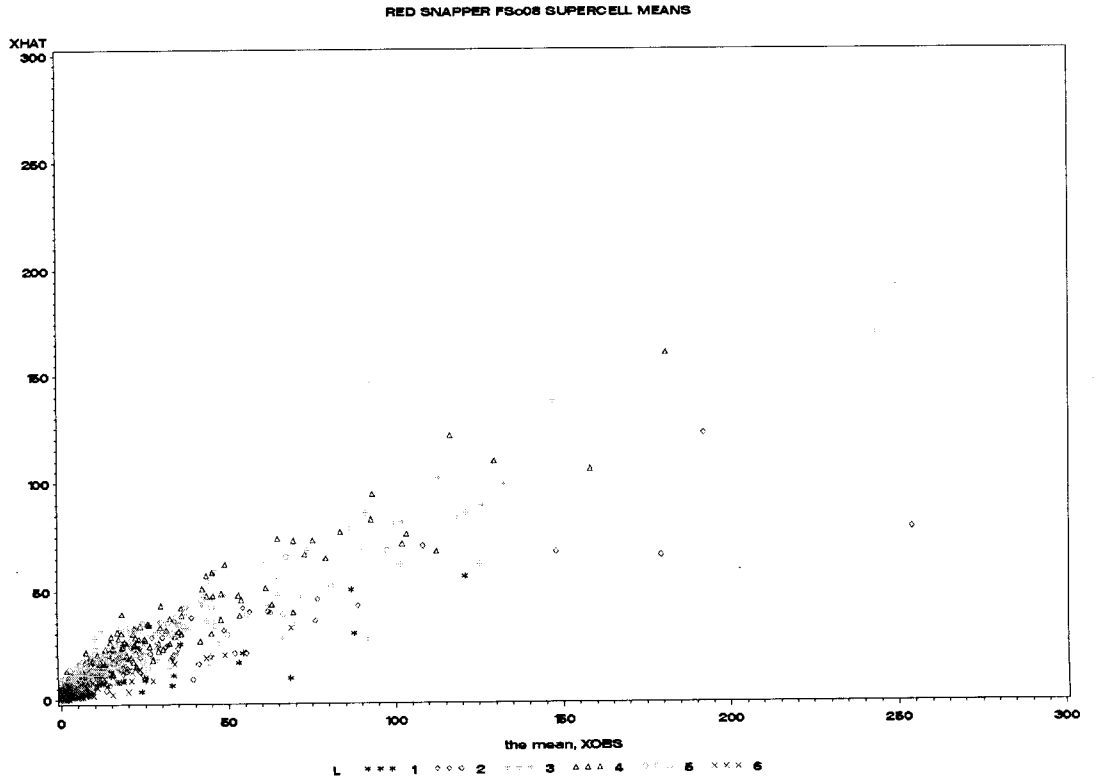

Figure 18. Goodness of fit plot of FS model 02. Predicted abundance vs mean of cell observations. Log scale; observations of zero cannot be plotted. Symbols identify depth bands of stratification.

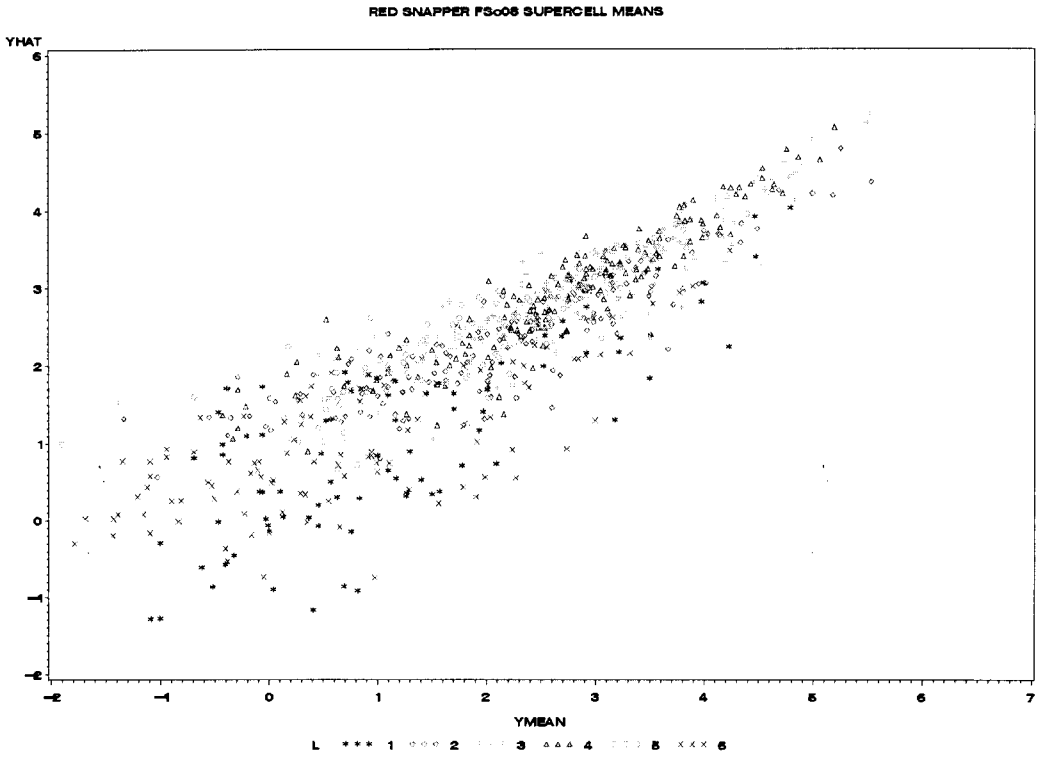

Figure 19. Box plot of FG index. This index applies to the "Primary Area" of the groundfish surveys. The dotted line is the "Base Index" of Nichols 2004a.

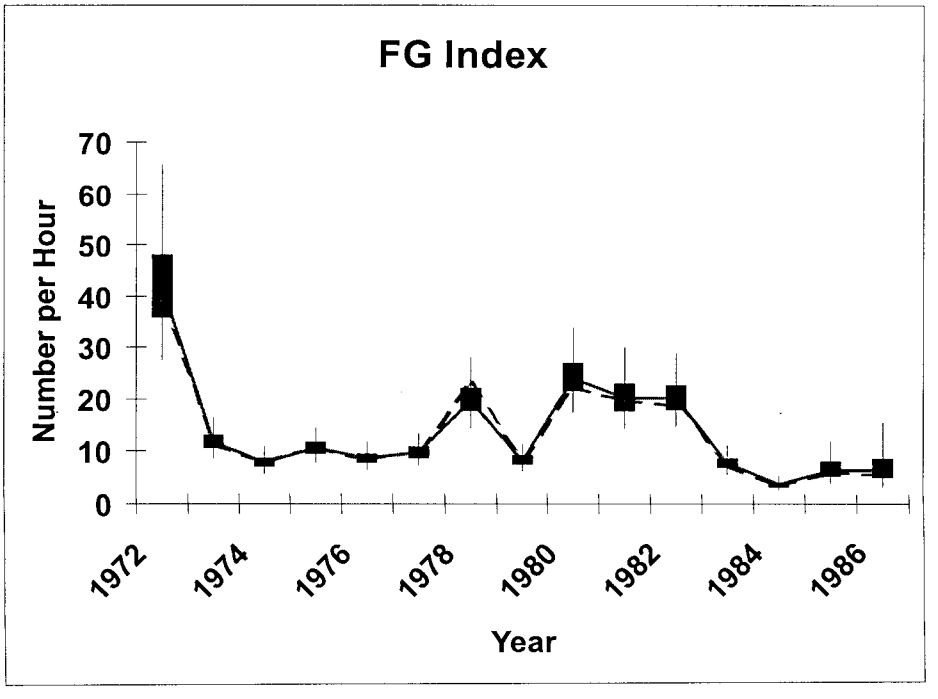

Figure 20. Examples of posterior marginal distributions for the 1975 FG index. a) arithmetic value. b) log value. The year chosen was just picked as an example. The shapes for the other years are similar.

20a)

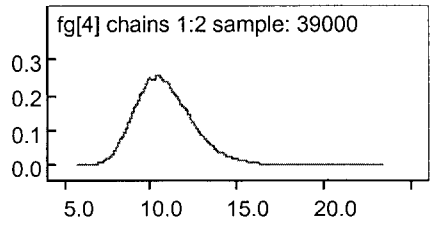

20b)

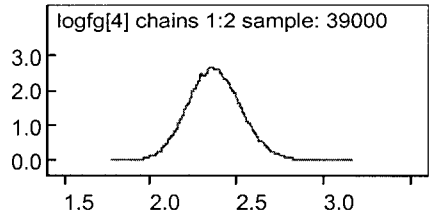

Figure 21. Posterior marginal distributions of the power function parameters relating gamma parameter r to predicted abundance in cell for the FG model. A functional form $r = a * abundance^{b}$ is assumed. a) the a (proportionality) parameter. b) the b parameter (exponent). (b had a lognormal prior in this version)

21a)

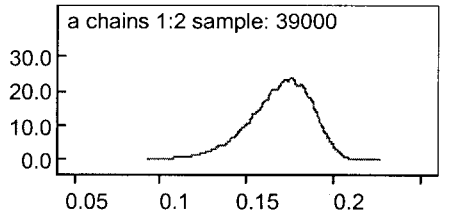

21b)

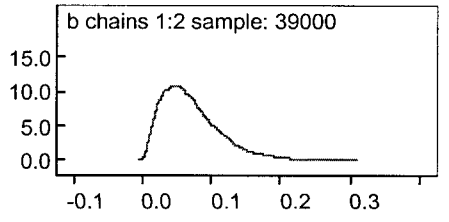

Figure 22. Goodness of fit plot for the FG model. Predicted abundance vs mean of cell observations. Arithmetic scale. Different symbols identify the 6 depth bands of the stratification.

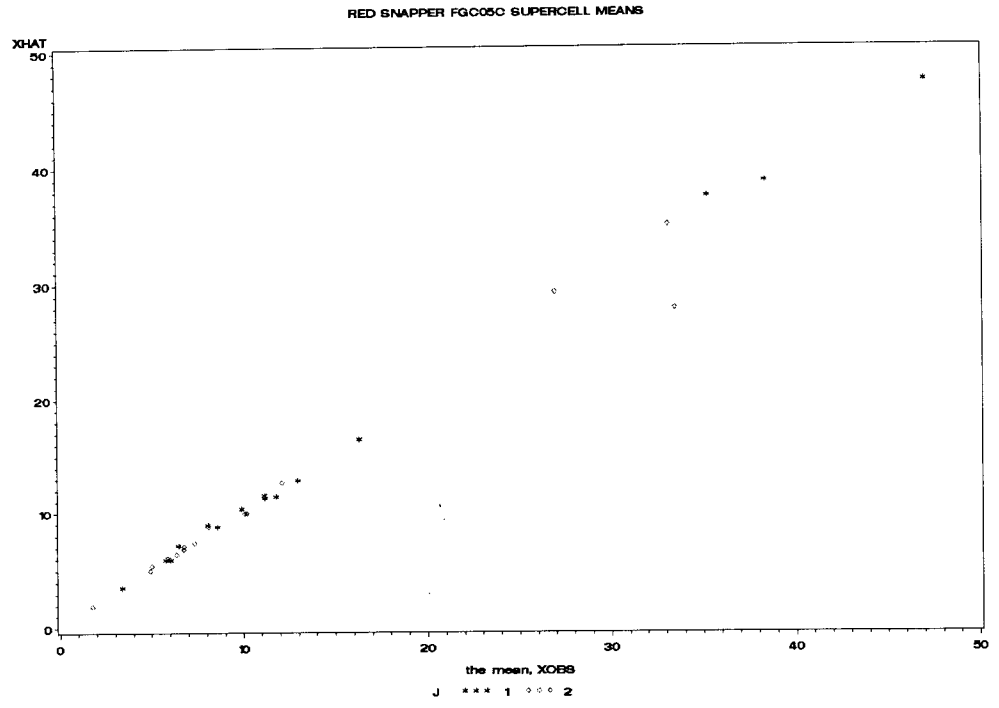

Figure 23. Goodness of fit plot for the FG model. Predicted abundance vs mean of cell observations. Log scale. Different symbols identify the 6 depth bands of the stratification.

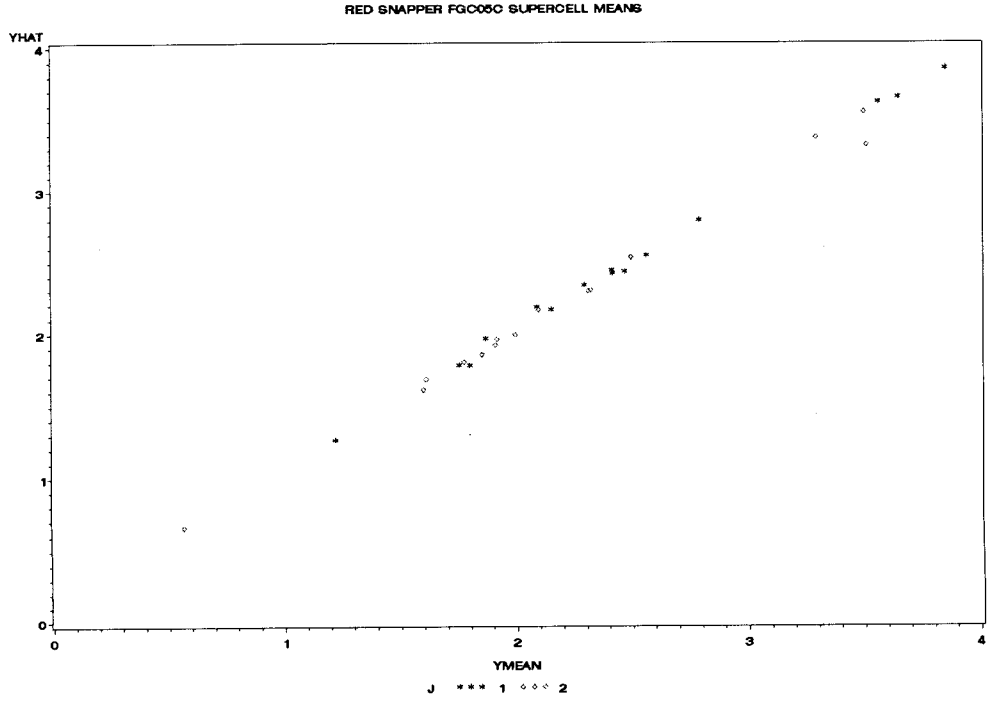

Figure 24. Posterior marginal distributions for the calibration factor to convert FG to the FS scale. a) from the FS 01 model. b) from the FS 02 model.

24a)

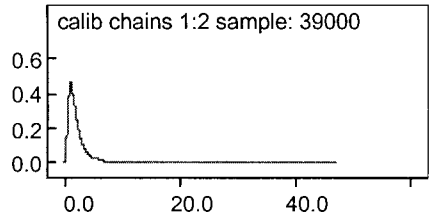

24b)

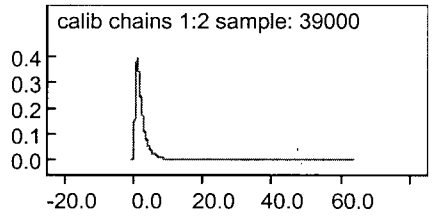

Figure 25. Median values of the FG index, and the rescalings to FS based on FS models 01 and 02. The mean value of the "Base Index" of Nichols 2004a is also shown.

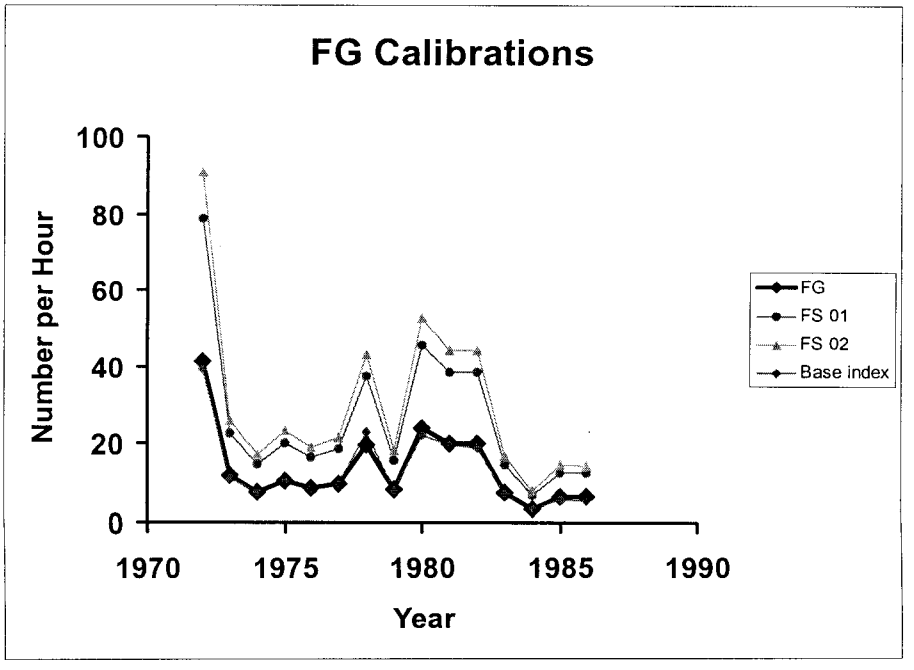

Figure 26. The combined Fall Index based on FS model 01 for 1987-2002, and FG for 1972-1986 recalibrated to the FS scale by the results from FS model 01.

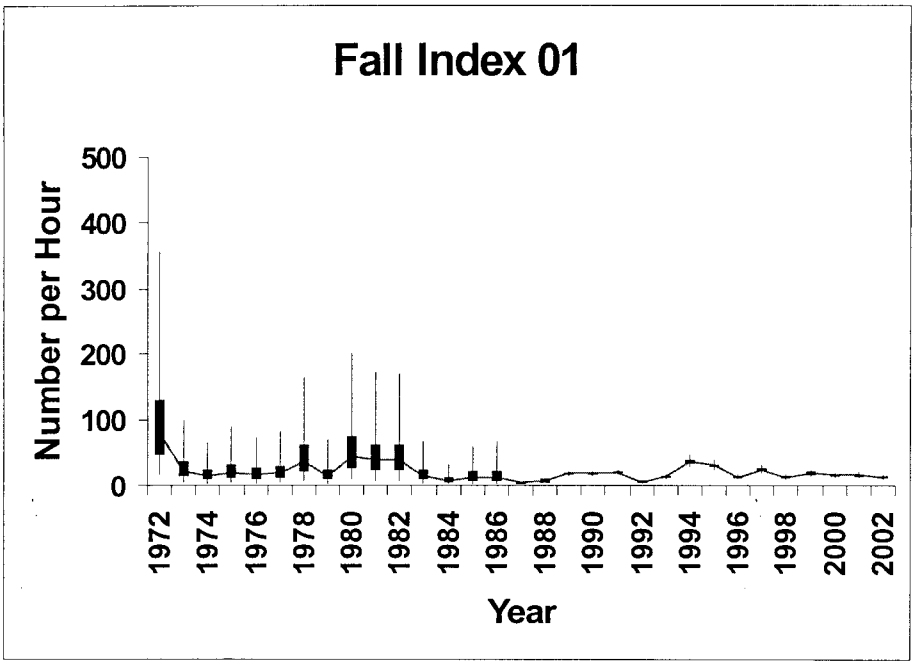

Figure 27. The combined Fall Index based on FS model 02 for 1987-2002, and FG for 1972-1986 recalibrated to the FS scale by the results from FS model 02.

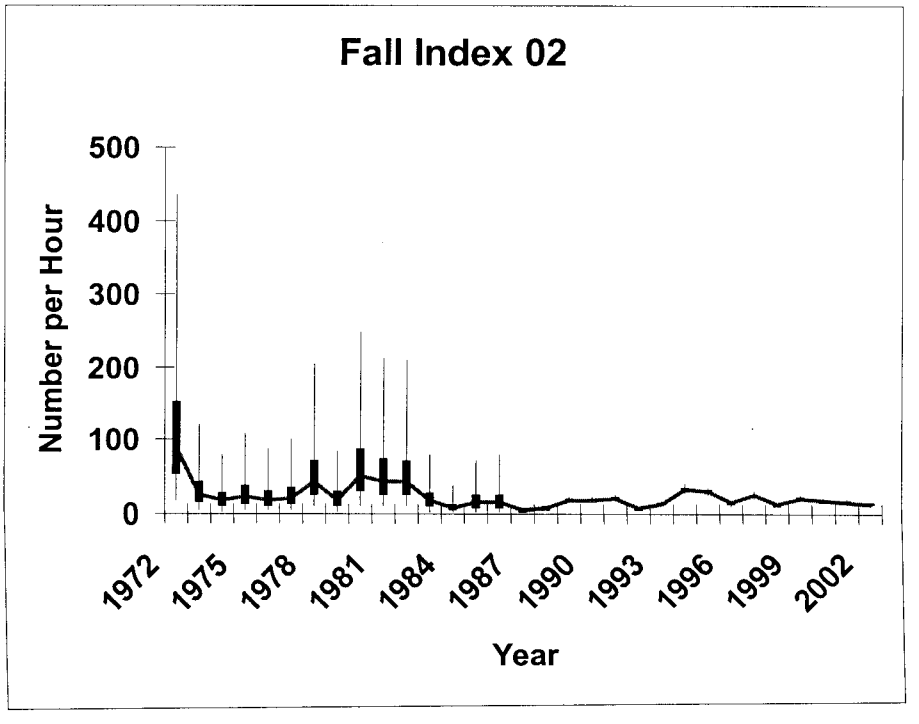

Figure 28. The SS index from model 01. The solid line connects the FS 01 medians. For comparison with other results, the medians from the SS 02 index, and the means of the "Base Index" of Nichols 2004a are also plotted.

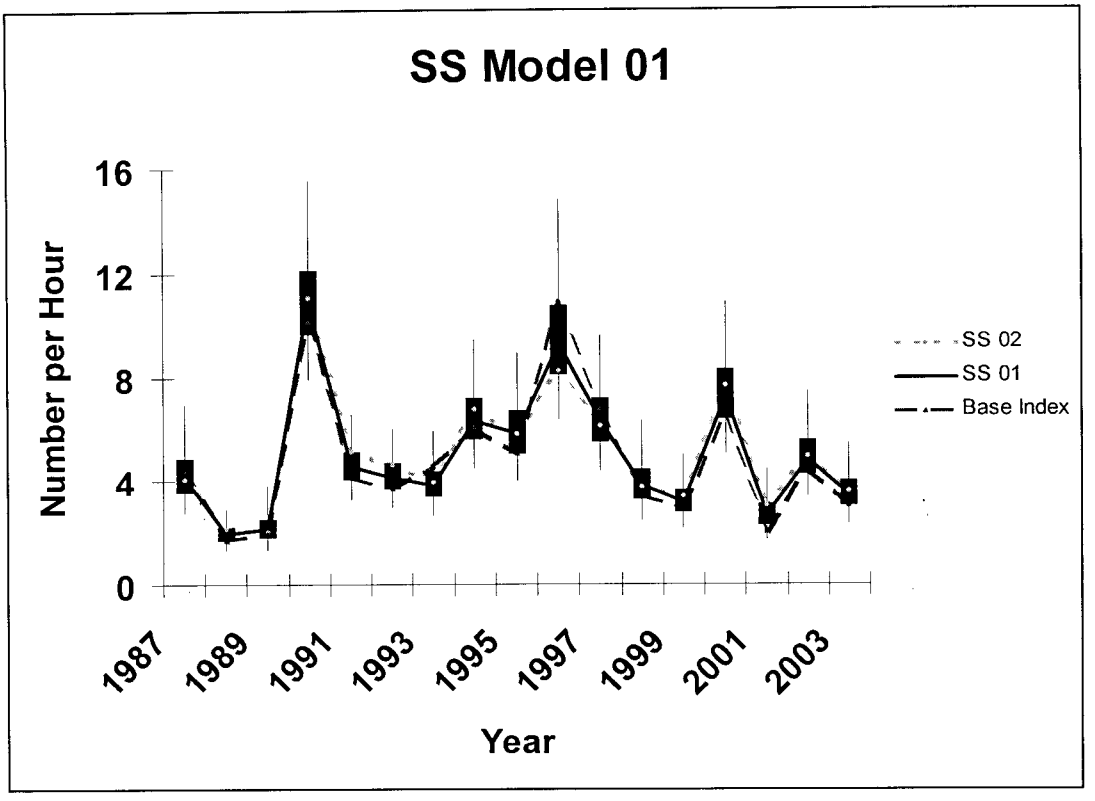

Figure 29. Examples of posterior marginal distribution for the 1990 SS index from model 01. a) arithmetic value. b) log value. The year chosen was just picked to be an example. The shapes for other years are similar, although indexes with smaller medians tend to have some high-side tail extension even in the log.

29a)

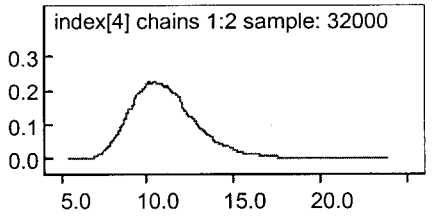

29b)

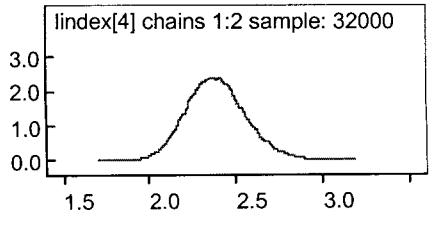

Figure 30. Posterior marginal distributions of the power function paratmeters relating gamma parameter r to predicted abundance in a cell for SS model 01. a) the proportionality parameter. b) the exponent. (b had a normal prior in this version.

30a)

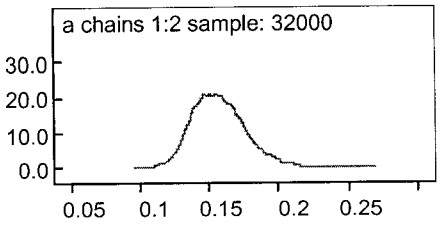

30b)

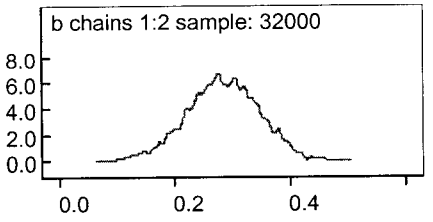

Figure 31. Box plot of the calibration parameter relating SS to ES, model 01. This is an adjustment of the day + night of SS vs night only sampling of ES. The value is the log of the SS index minus the log of an index calculated using only values from the nighttime stratum.

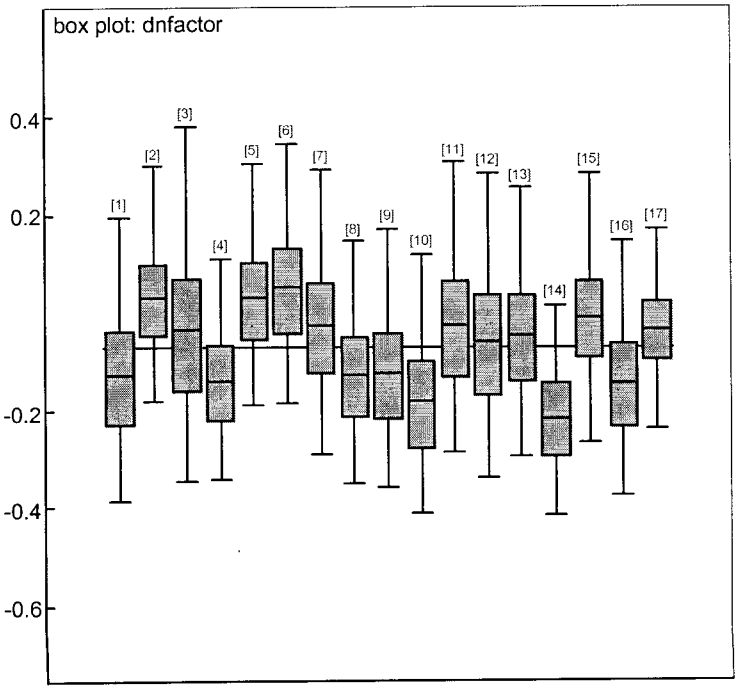

Figure 32. Box plot of calibration parameter relating SS to TC, model 01. The value is the log of the SS index minus the log of an index calculated using only nighttime values from the survey area off Texas, which was all that was covered in the TC survey.

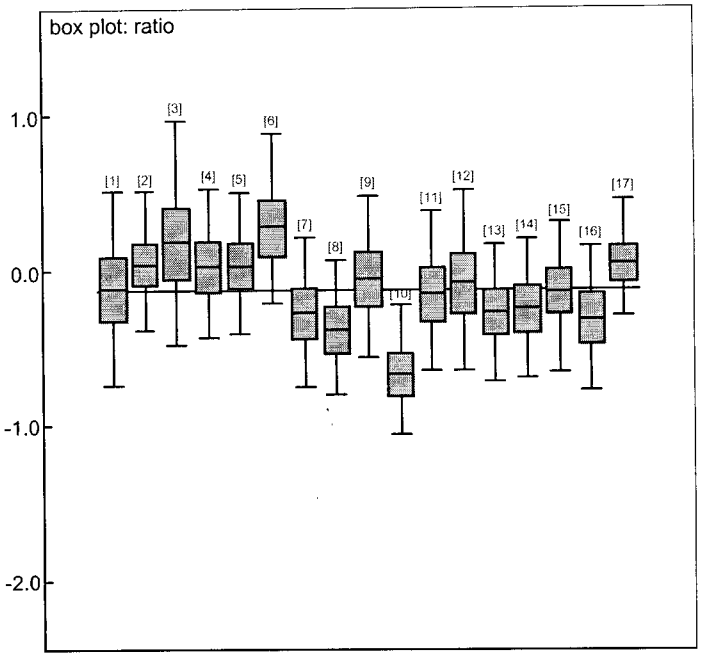

Figure 33. Box plot of the percent of the population estimated to be in the two westernmost alongshore zones (i.e. off Texas) compared to the population in the entire SS survey area. Model 01.

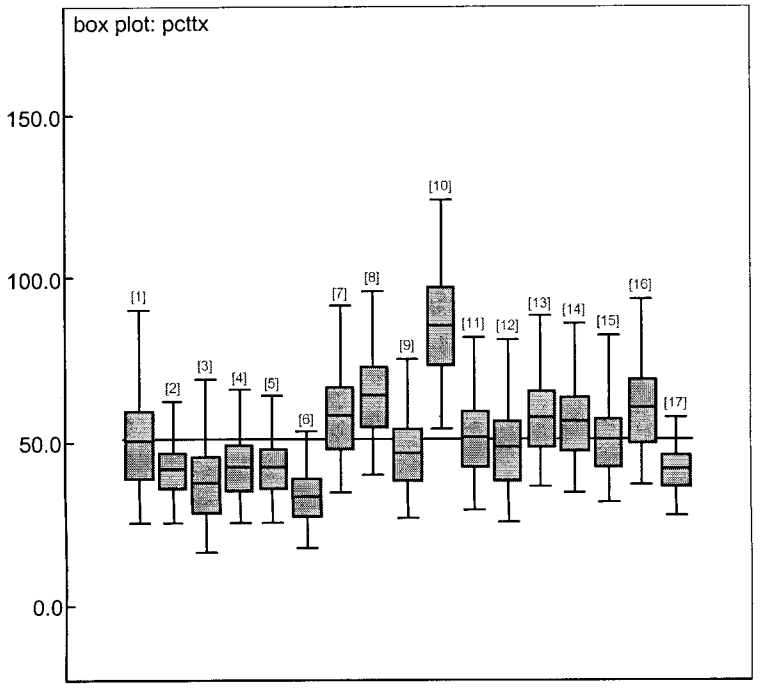

Figure 34. Box plot of the annual precision parameters for the priors of the (log) abundance in each cell. (SS model 01).

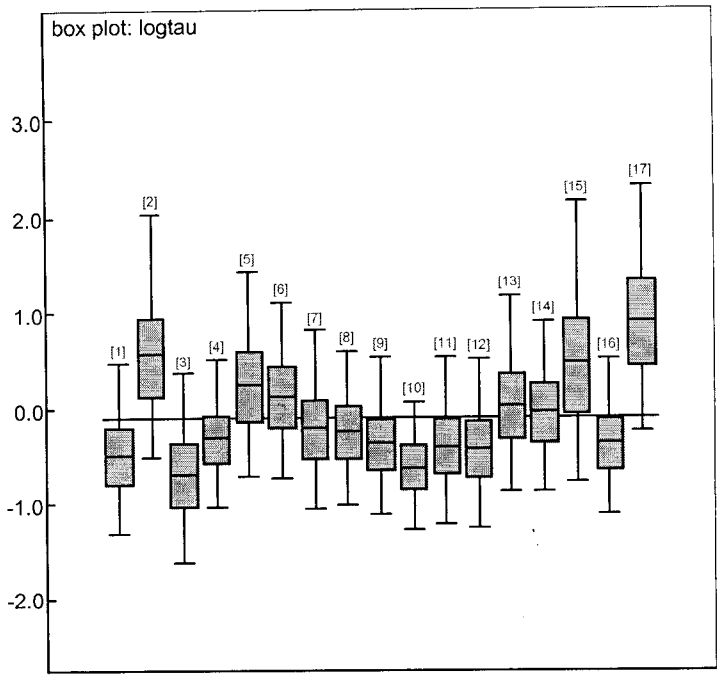

Figure 35. Goodness of fit plot for SS model 01. Predicted abundance vs median of cell observations. Arithmetic scale. The different symbols identify the 6 depth bands of the stratification.

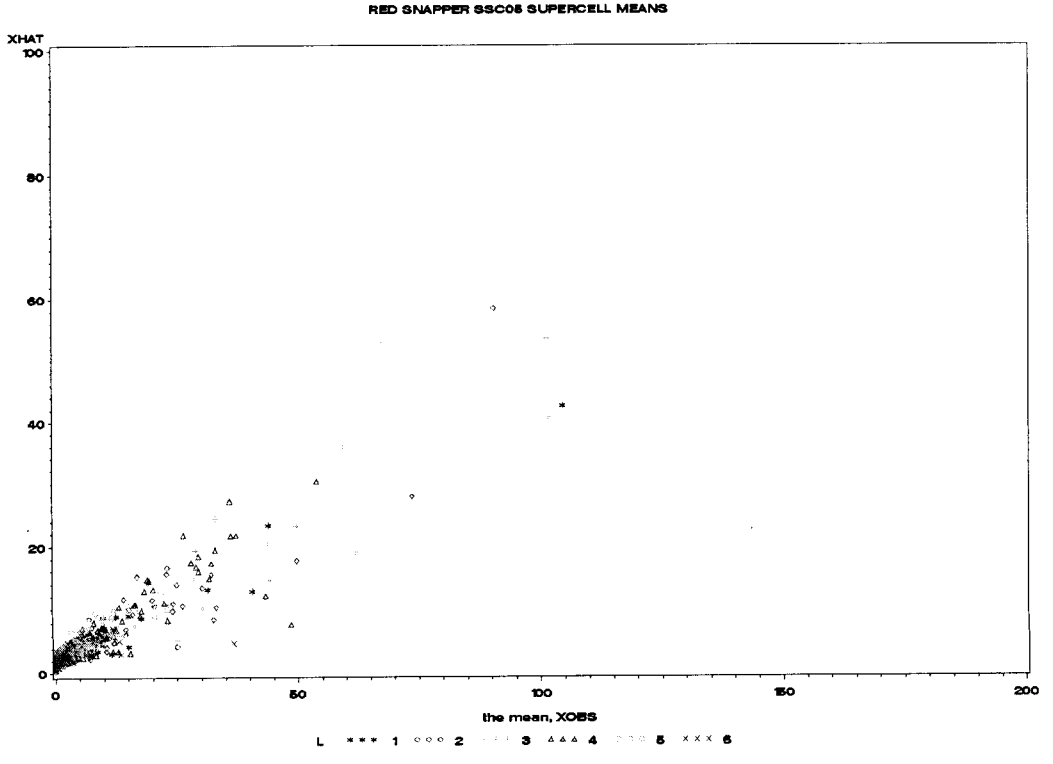

Figure 36. Goodness of fit plot for SS model 01. Predicted abundance vs median of cell observations. Log scale. The different symbols identify the 6 depth bands of the stratification.

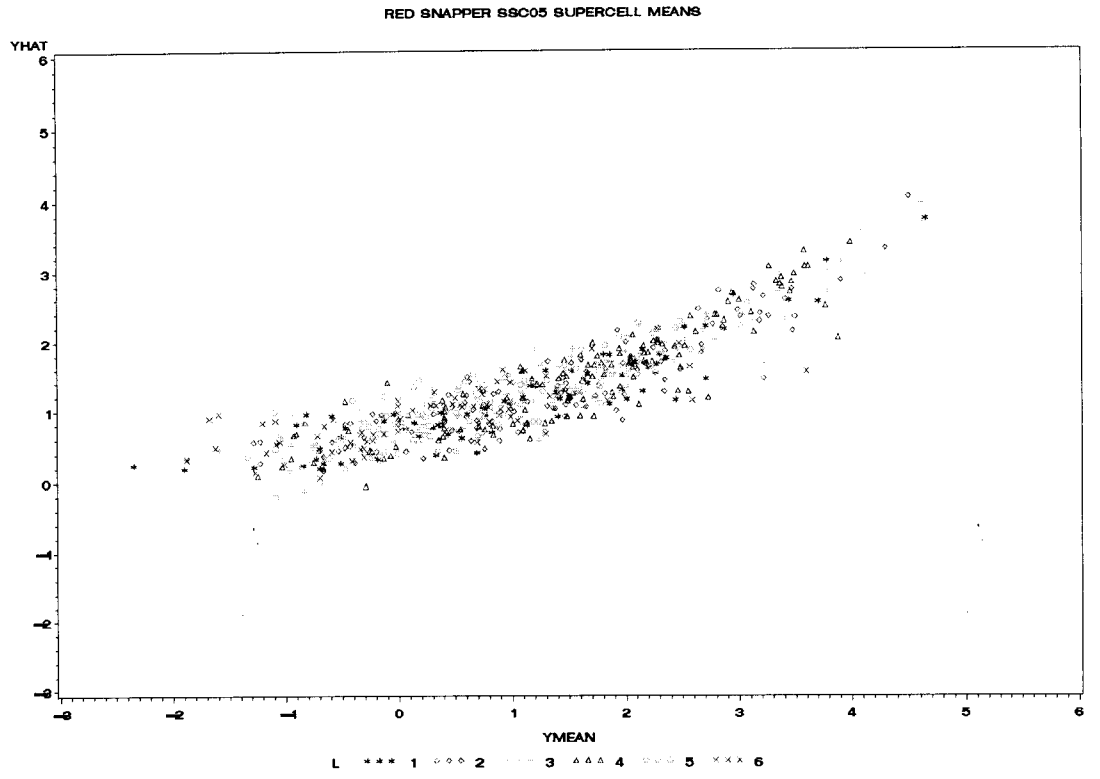

Figure 37. The SS index from model 02. The solid line labeled SS 02 connects the medians. For comparisons with other results, the medians from the FS 01 and the means of the "Base Index" of Nichols 2004a are also plotted.

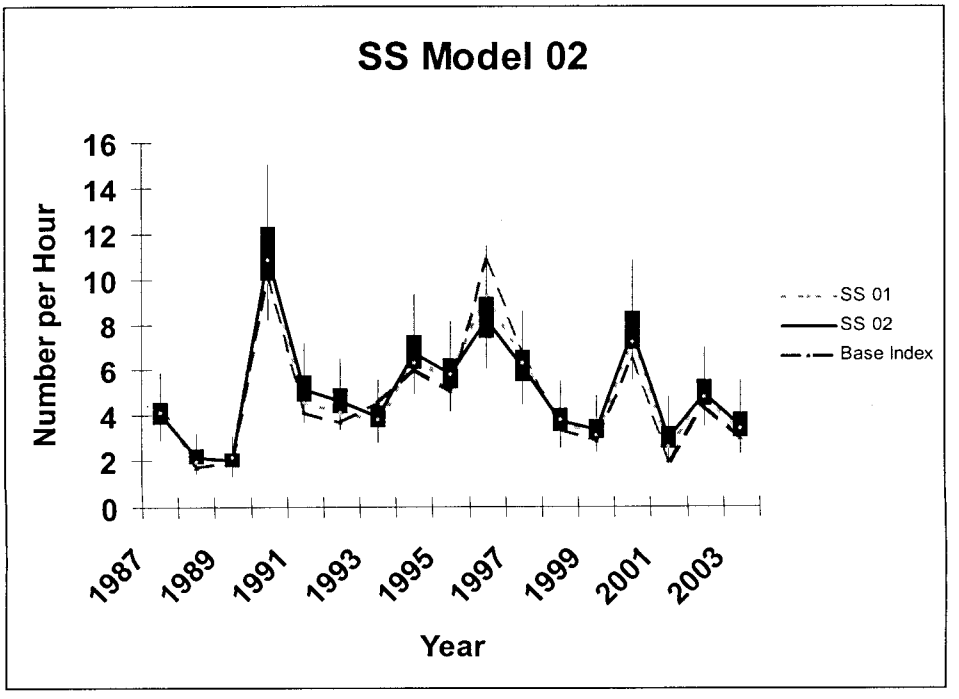

Figure 38. Examples of posterior marginal distributions for the 1990 SS index from model 02. a) arithmetic value. b) log value. The year chosen was just picked to be an example. The shapes of for other years are very similar.

38a)

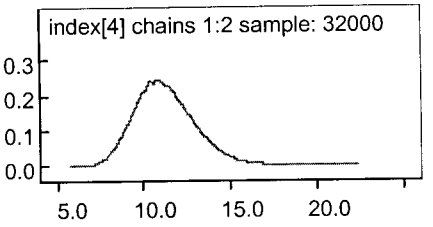

38b)

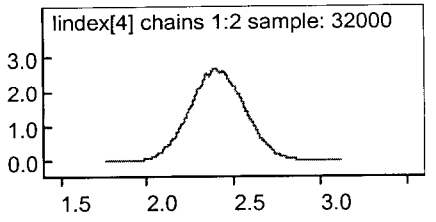

Figure 39. Posterior marginal distributions of the power function parameters relating gamma parameter r to predicted abundance in cell for SS model 02. A functional form $r = a * \text{abundance}^{b}$ is assumed a) the a (proportionality) parameter. b) the b parameter (exponent). (b had a lognormal prior in this version)

39a)

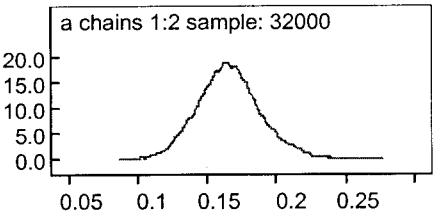

39b)

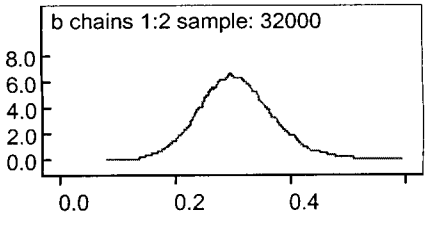

Figure 40. Box plot of marginal posteriors for stratum effects (SS model 02). Stratum numbering system the same as in figure 12.

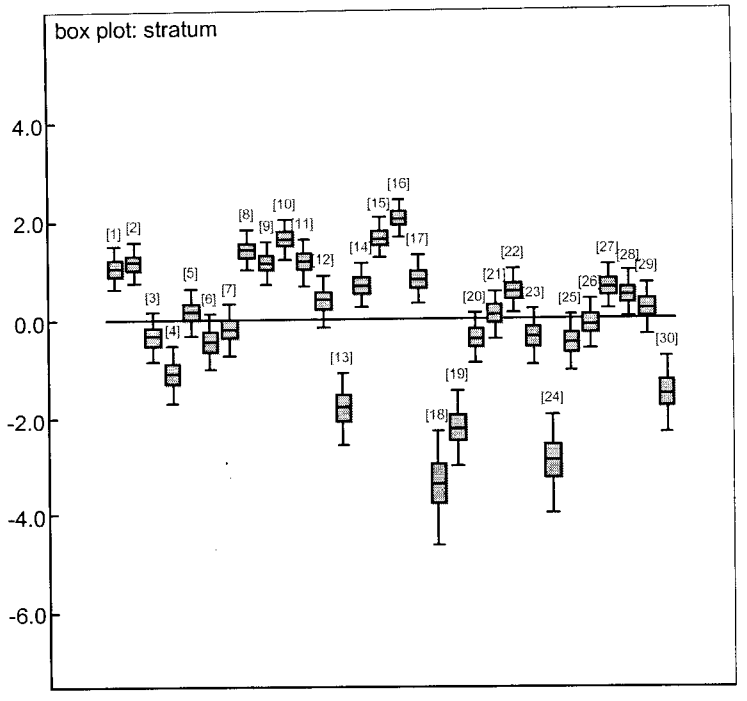

Figure 41. Box plot of the marginal posteriors for the time of day effect (SS model 02). [1] is day; [2] is night.

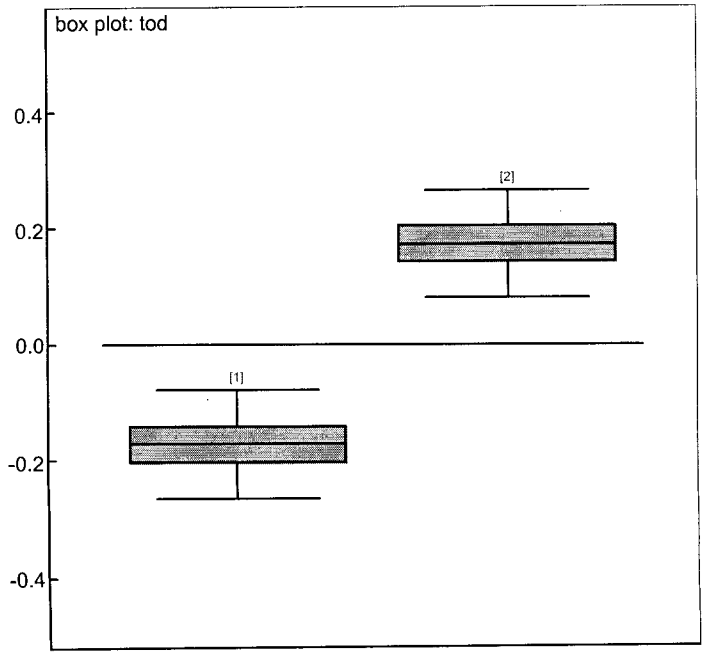

Figure 42. Box plot of the calibration parameter relating SS and ES,model 02. The value is the log of the SS index minus the log of an index calculated using just the night samples. (Both SS and ES had the same spatial range.)

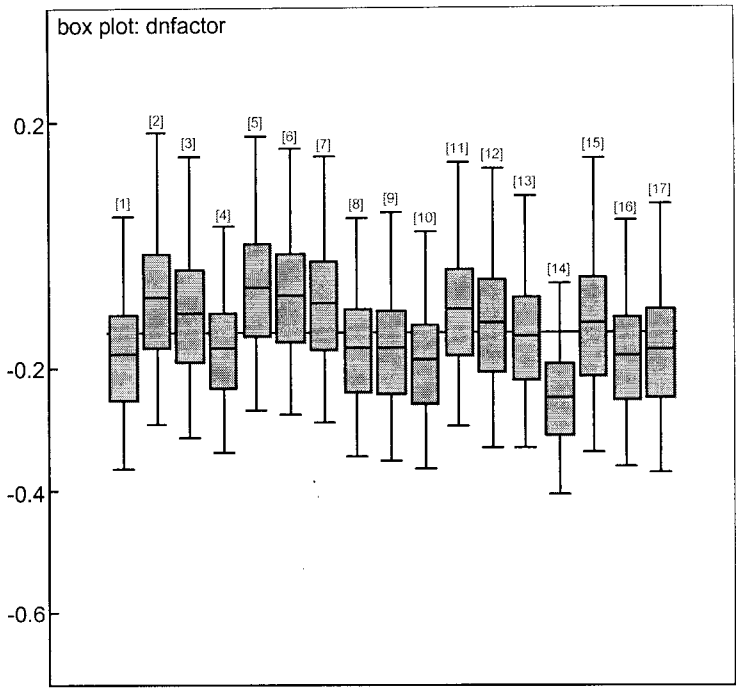

Figure 43. Box plot of the calibration parameter relating SS and TC, model 02. The value is the log of the SS index (full spatial range) minus the log of an index calculated using only night samples for the area covered by the TC survey (off Texas).

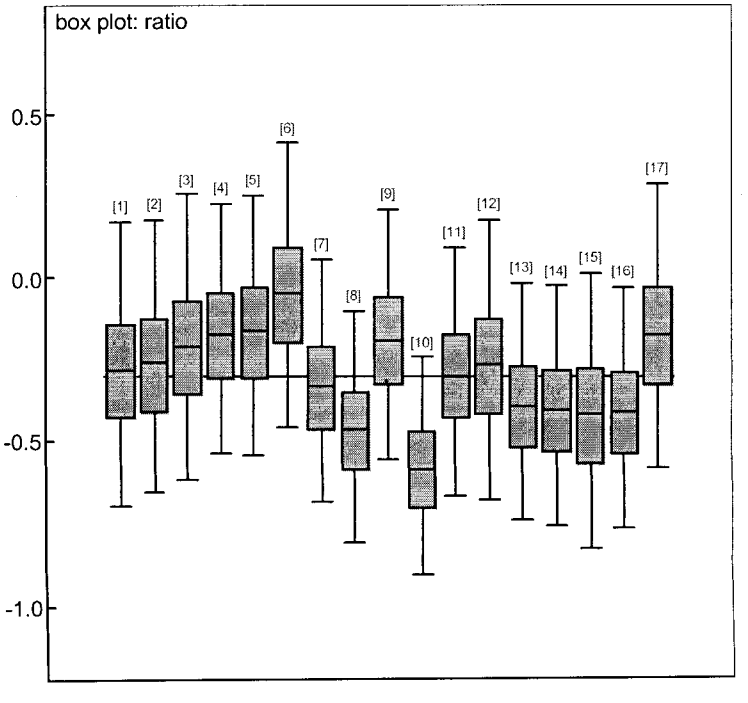

Figure 44. Box plot of the percent of the population estimated to be in the TC survey area, compared to the population in the entire SS survey area (model 02).

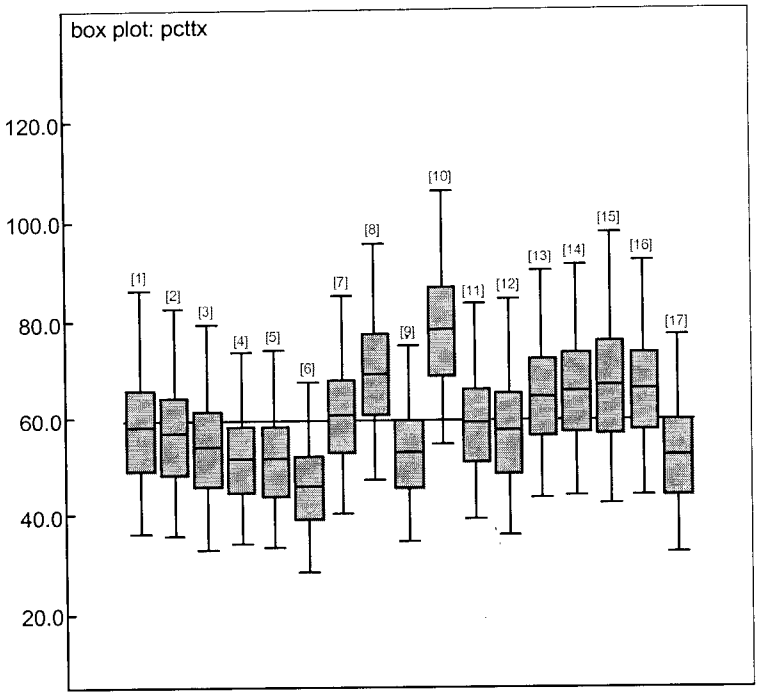

Figure 45. Marginal posterior distribution of the precision parameter for the priors on the Local effects. a) arithmetic scale. b) log scale. The prior on this parameter was lognormal.

45a)

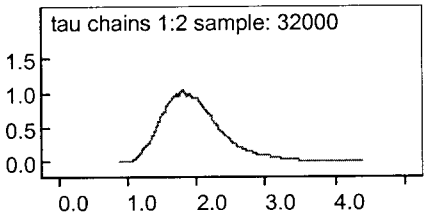

45b)

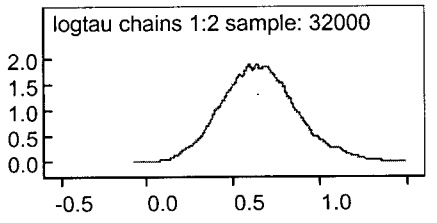

Figure 46. Goodness of fit plot for SS model 02. Predicated abundance vs mean of cell observations. Arithmetic scale. Different symbols identify the 6 depth bands of the stratification.

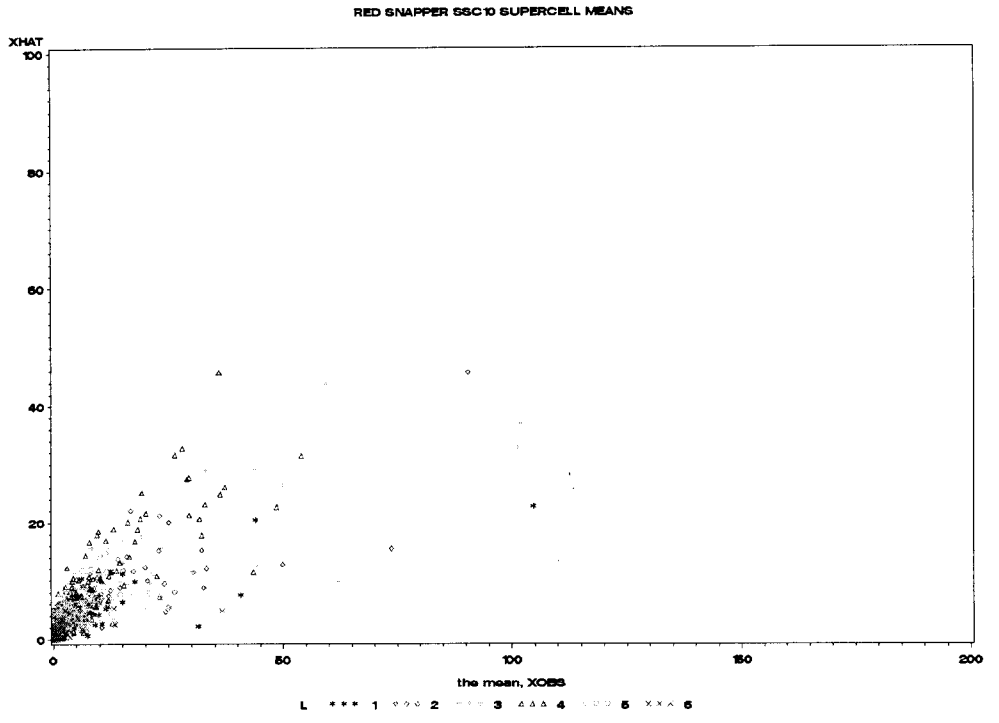

Figure 47. Goodness of fit plot for SS model 02. Predicated abundance vs mean of cell observations. Log scale.

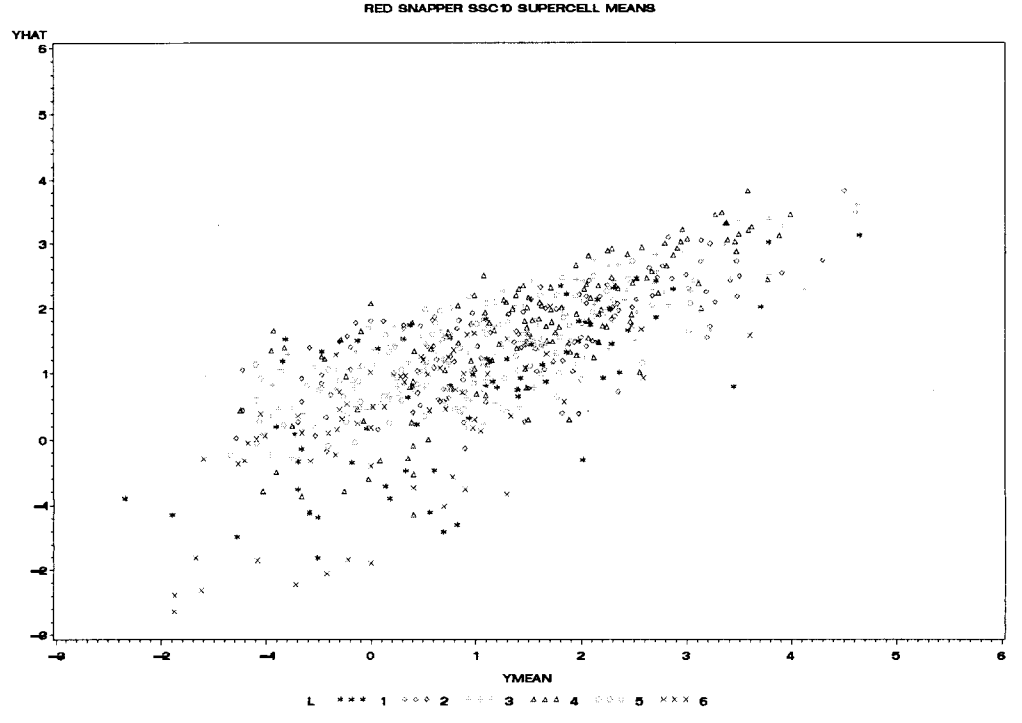

Figure 48. The ES index from model 01. The medians from ES model 02 and the means of the "Base Index" of Nichols 2004a are also plotted.

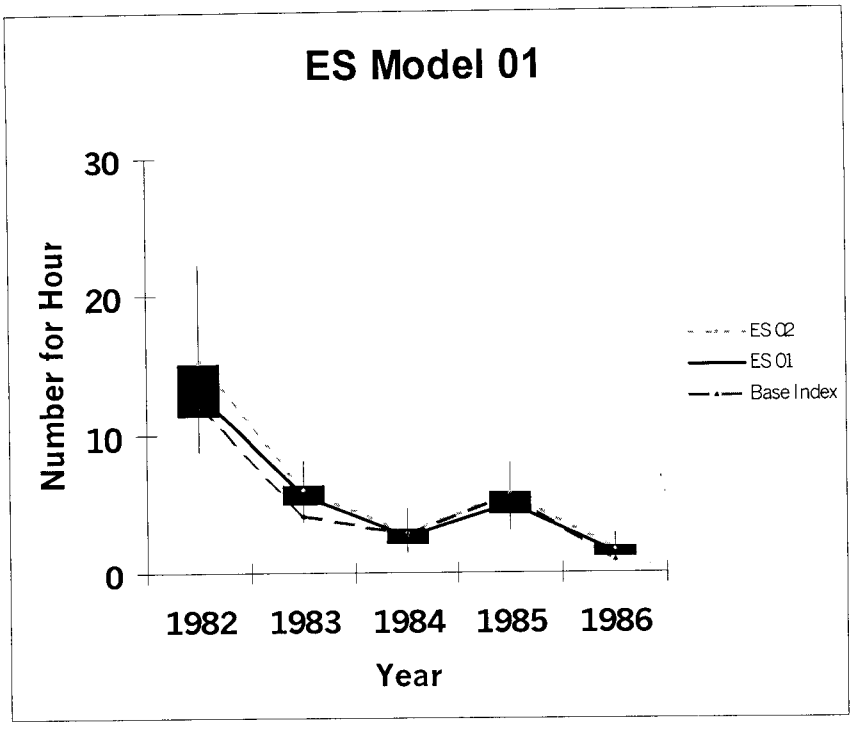

Figure 49. Examples of posterior marginal distributions for the 1985 ES index from model 01. A) arithmetic value. b) log value. The year chosen was just picked to be an example. The shapes for other years are similar.

49a)

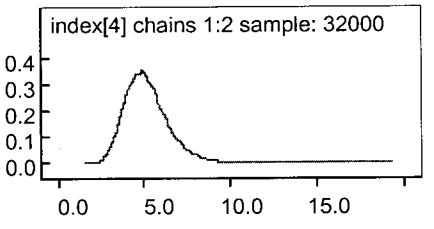

49b)

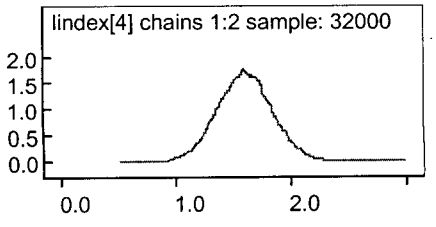

Figure 50. Posterior marginal distributions of the power function parameters relating gamma parameter r to predicted abundance in cell for ES model 01. A functional form r = a * abundance ^{b} is assumed a) the a (proportionality) parameter. b) the b parameter (exponent). (b had a normal prior in this version)

50a)

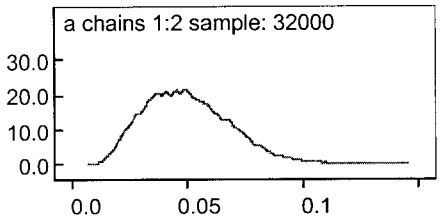

50b)

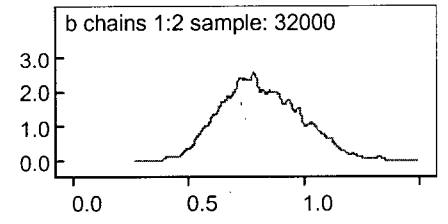

Figure 51. Goodness of fit plot for ES model 01. Predicted abundance vs mean of cell observations. Arithmetic scale. Different symbols identify the 6 depth bands of the stratification.

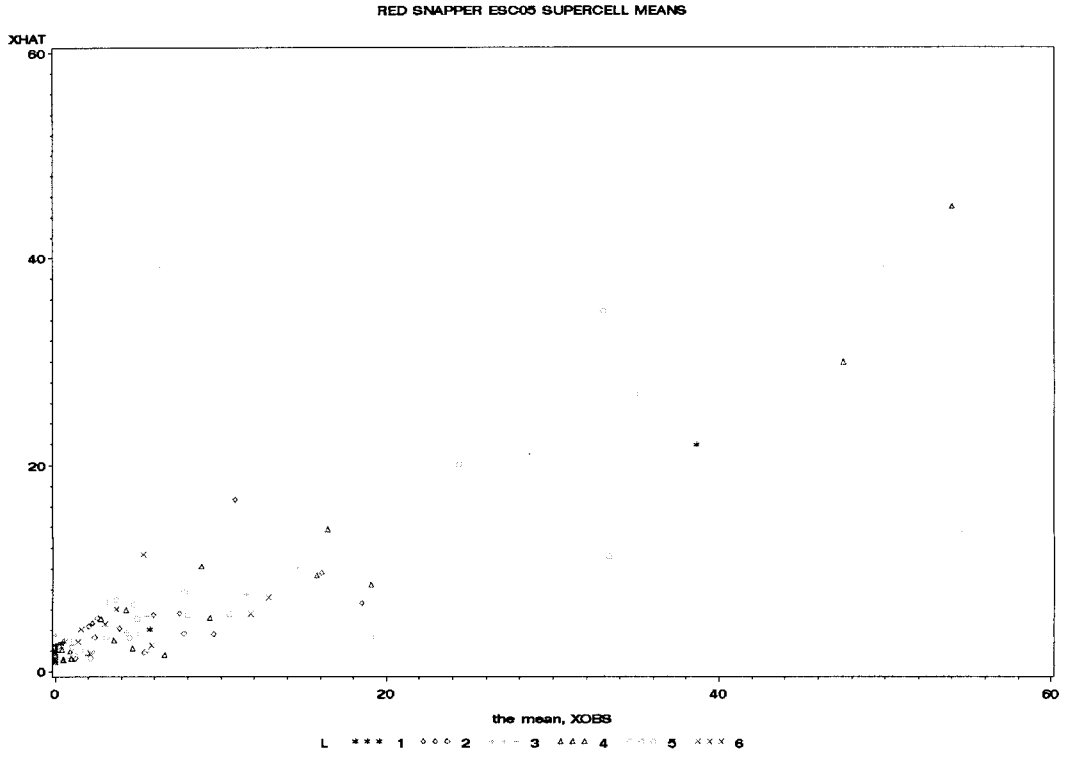

Figure 52. Goodness of fit plot for ES model 01. Predicted abundance vs mean of cell observations. Log scale; means of zero cannot be plotted. Symbols identify depth bands of stratification.

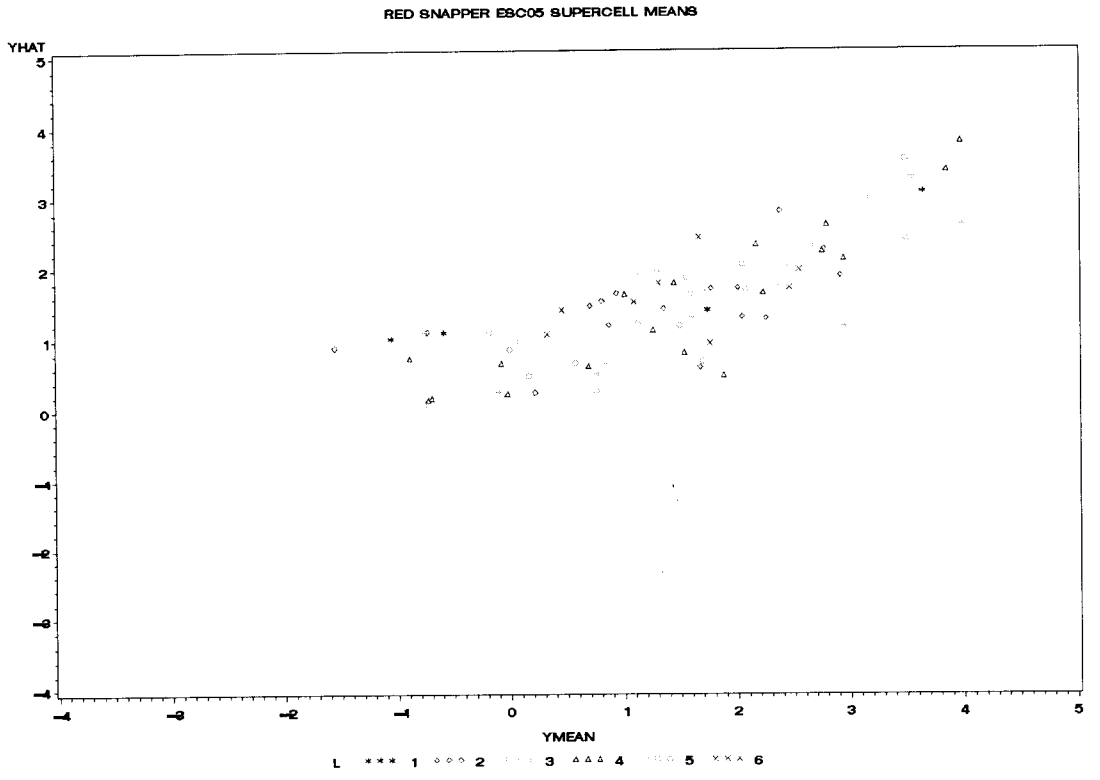

Figure 53. The ES index from model 02. The medians from ES model 01 and the means from the "Base Index" of Nichols 2004a are also plotted.

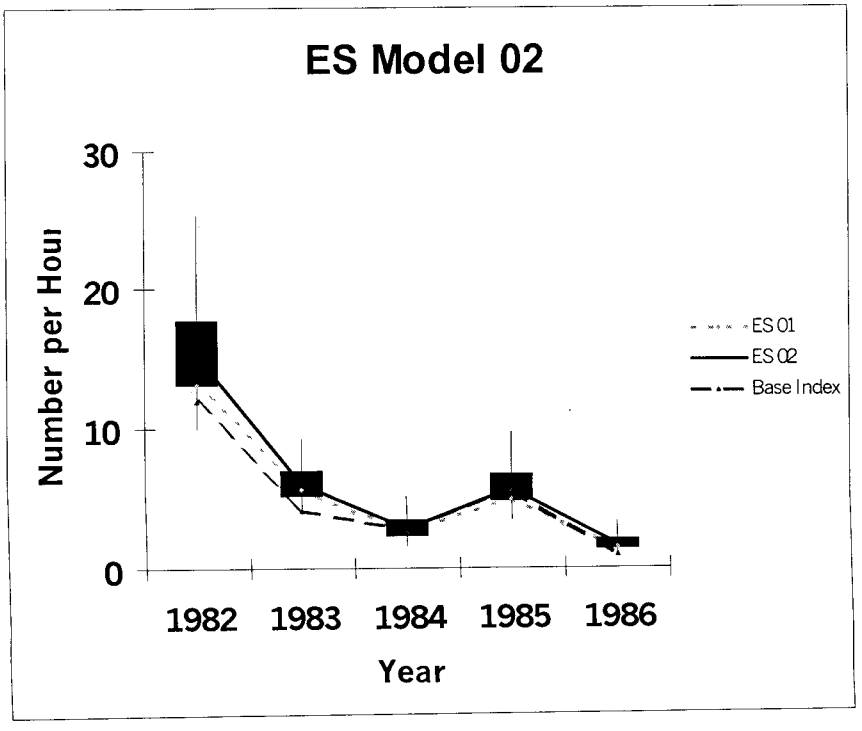

Figure 54. Examples of posterior marginal distributions using the 1985 ES index from model 02. a) arithmetic value. b) log value.

54a)

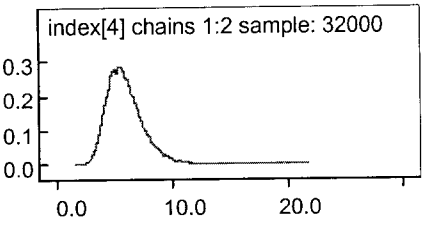

54b)

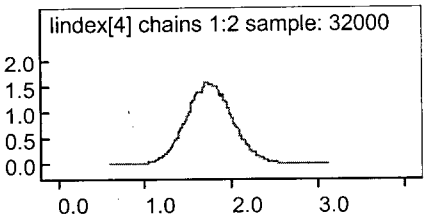

Figure 55. Posterior marginal distributions of the power function parameters relating gamma parameter r to predicted abundance in cell for ES model 02. A functional form r = a * abundance b is assumed a) the a (proportionality) parameter. b) the b parameter (exponent). (b had a lognormal prior in this version)

55a)

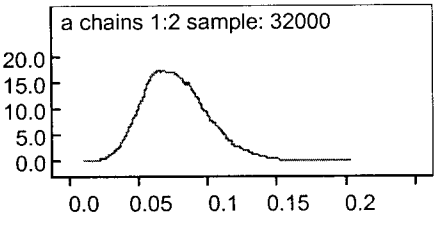

55b)

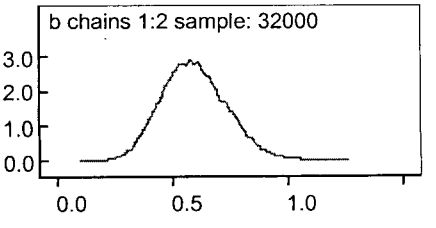

Figure 56. Box plot of marginal posteriors for the stratum effects (ES model 02). Stratum numbering is the same as in figure 12.

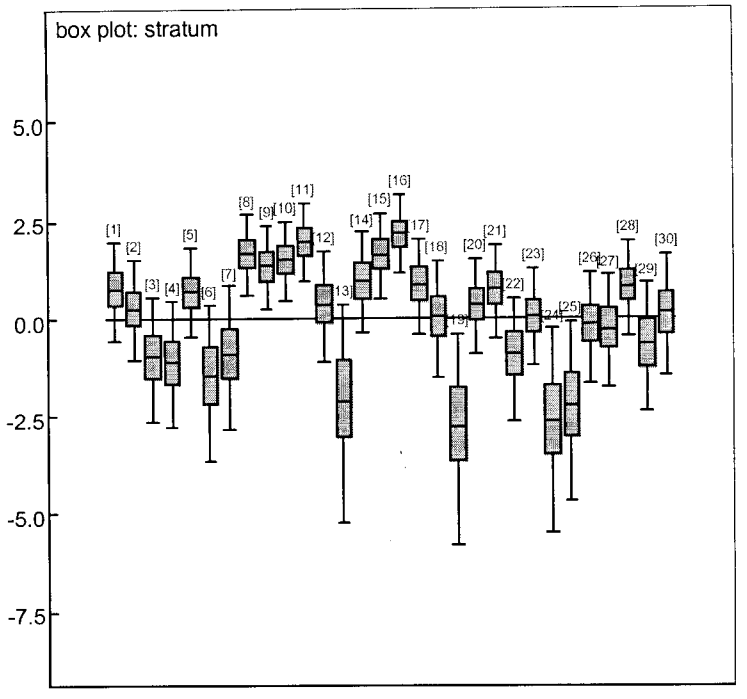

Figure 57. Marginal posterior for the precision parameter for the prior on the Local effects. a) arithmetic scale. b) log scale. The prior on this parameter was lognormal.

57a)

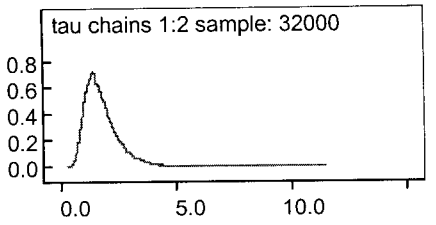

57b)

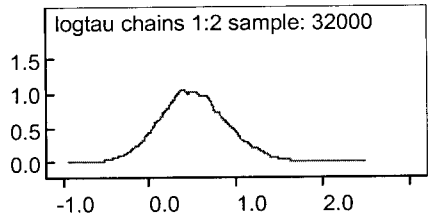

Figure 58. Goodness of fit plot for ES model 02. Predicted abundance vs mean of cell observations. Arithmetic scale. Different symbols identify the 6 depth bands of the stratification.

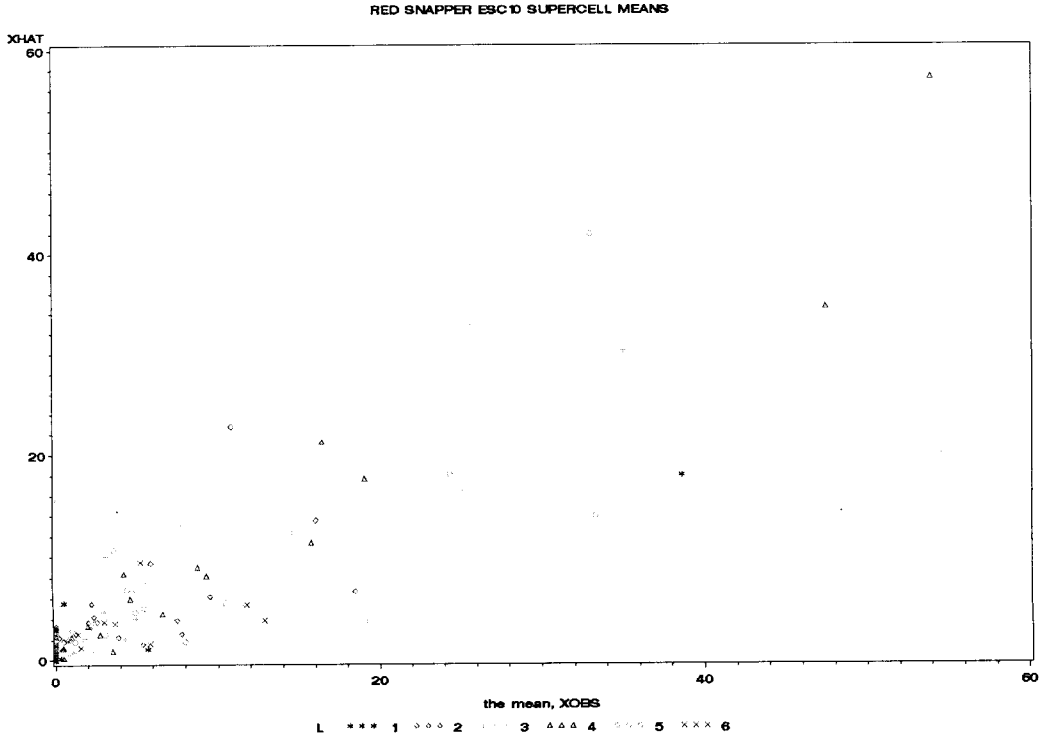

Figure 59. Goodness of fit plot for ES model 02. Predicted abundance vs mean of cell observations. Log scale.

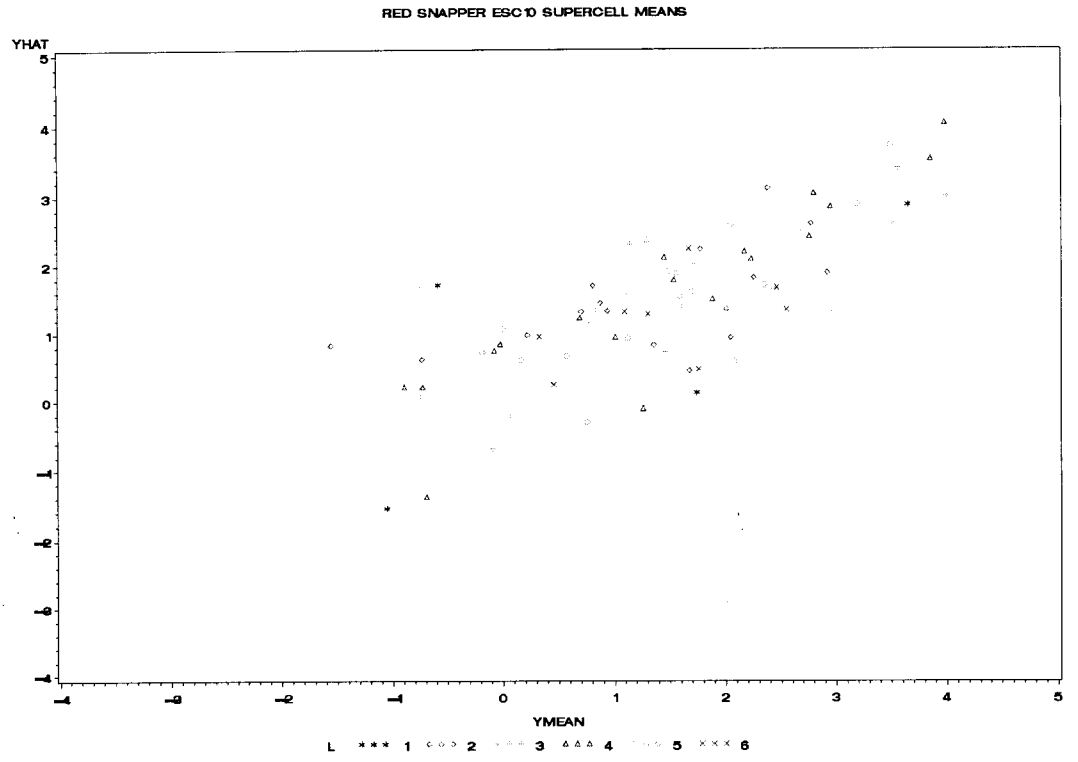

Figure 60. Posterior marginal distributions for the calibration factor to convert ES to the SS scale. a) from the SS 01 model. b) from the SS 02 model.

60a)

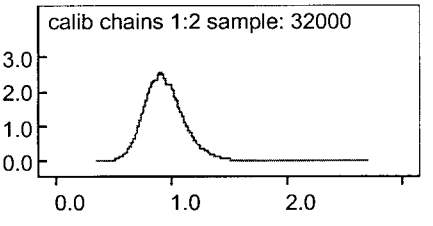

60b)

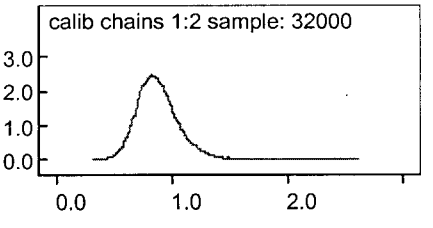

Figure 61. Median values of the ES index, and the rescalings to SS based on ES models 01 and 02. The mean value of the "Base Index" of Nichols 2004a is also shown.

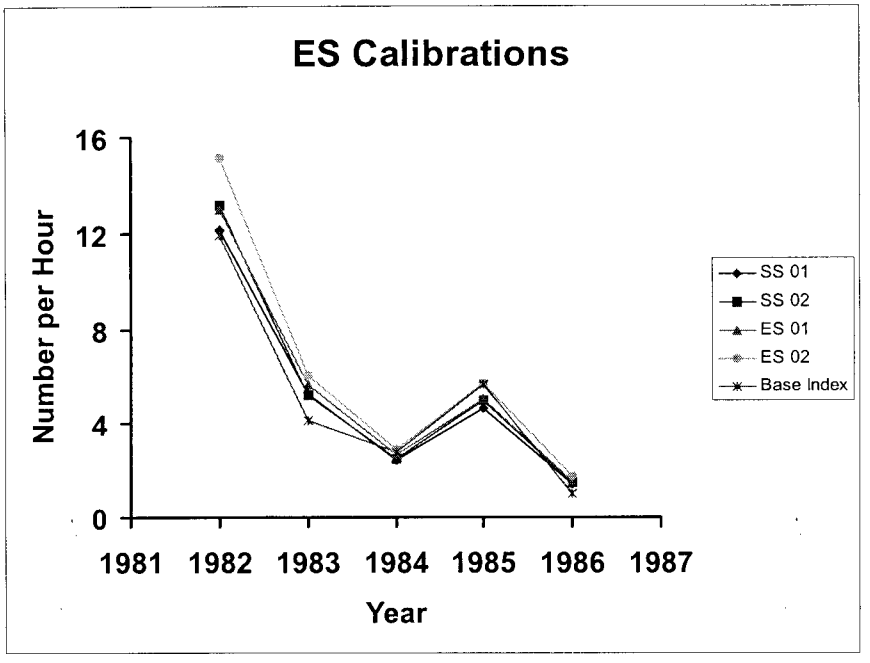

Figure 62. Index value for the TC survey (occurred only in 1981). The only difference between the two models is the normal prior on the "b" parameter in 01 vs the lognormal prior in 02. The angled line connects the medians. The dashed horizontal line is the value of the "Base Index" from Nichols 2004a.

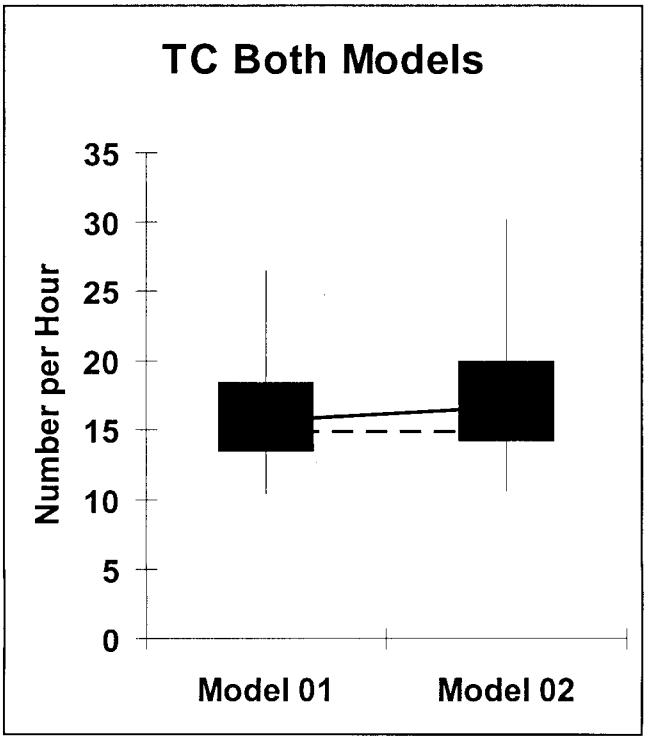

Figure 63. The "a" parameter of the power function relating gamma parameter r to predicted abundance. Marginal posteriors compared with the priors.

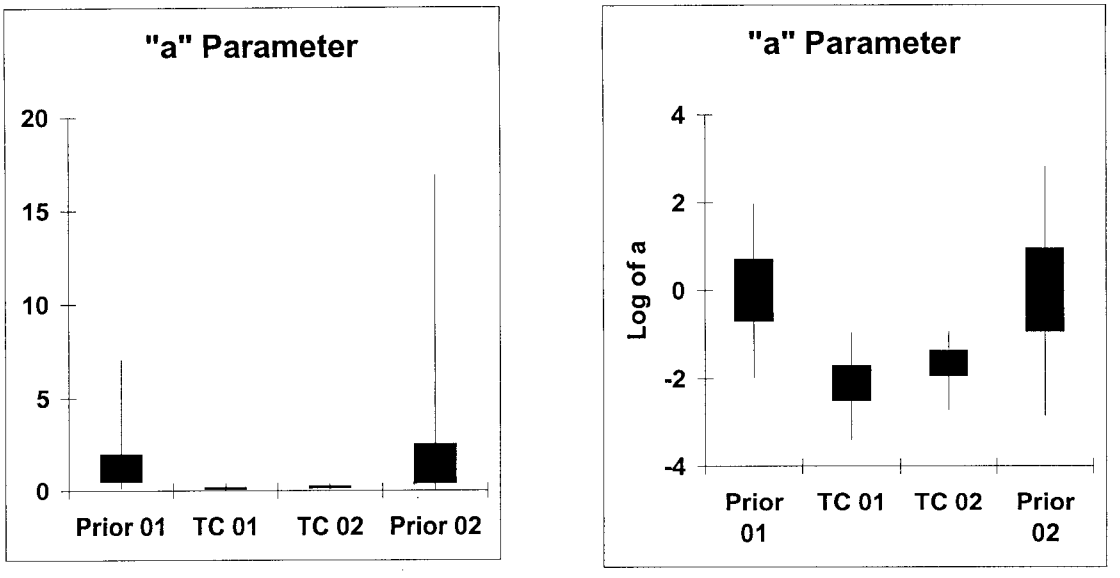

Figure 64. The "b" parameter of the power function relating gamma parameter r to predicted abundance. Marginal posteriors compared with priors. (Log plot not possible due to values below zero in the TC 01 posterior.)

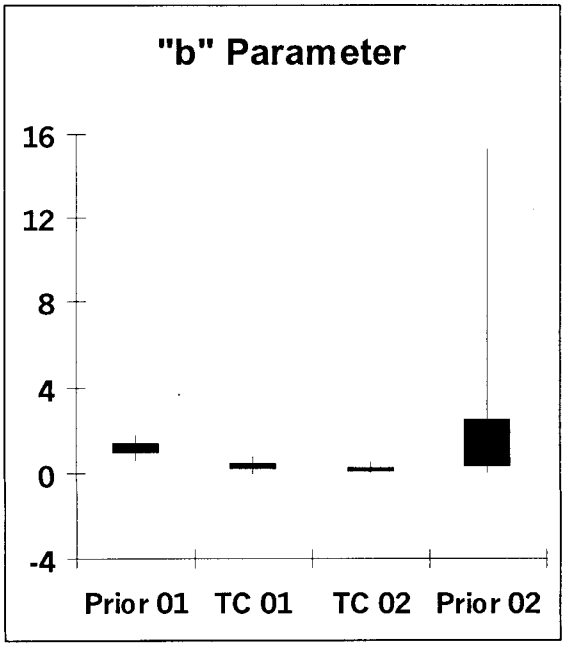

Figure 65. The relationship between mean and variance implied by the two sets of power function parameters of the previous two figures.

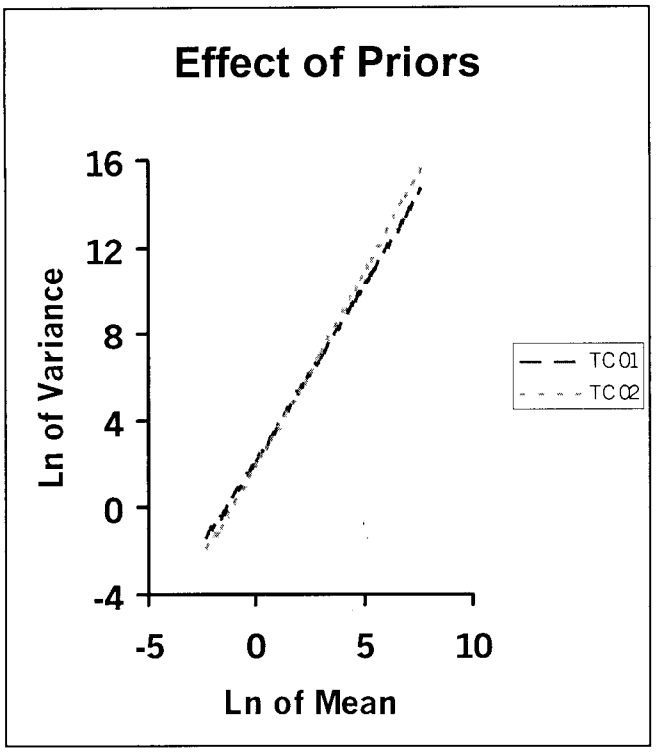

Figure 66. Goodness of fit plot for TC model 01. Arithmetic scale.

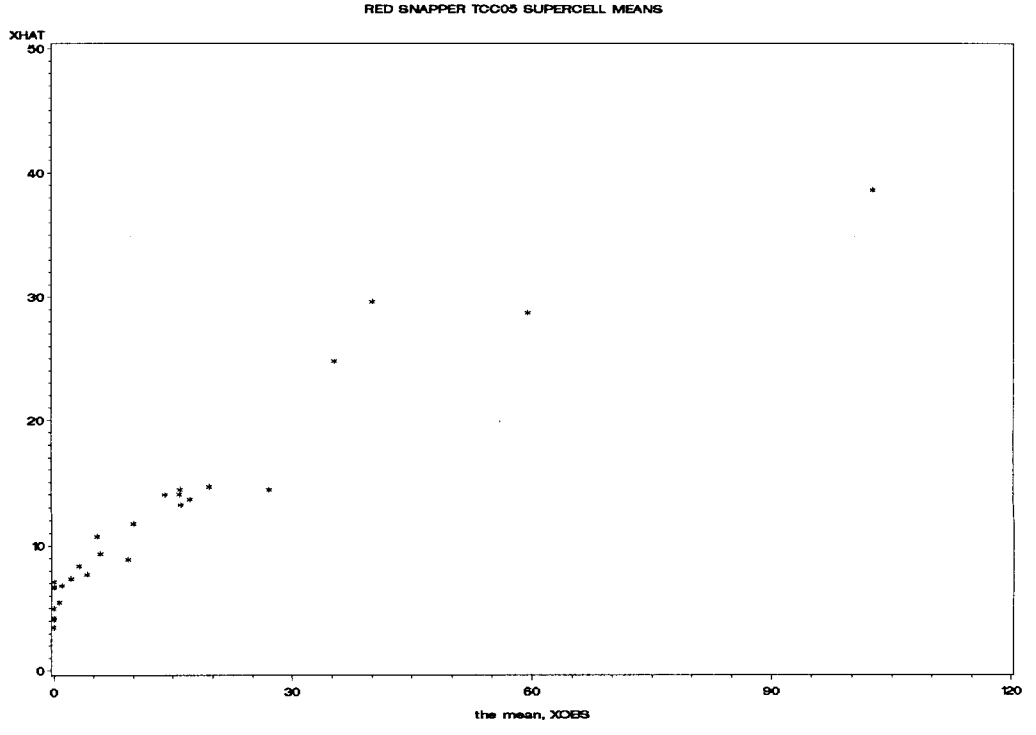

Figure 67. Goodness of fit plot for TC model 01. Log scale.

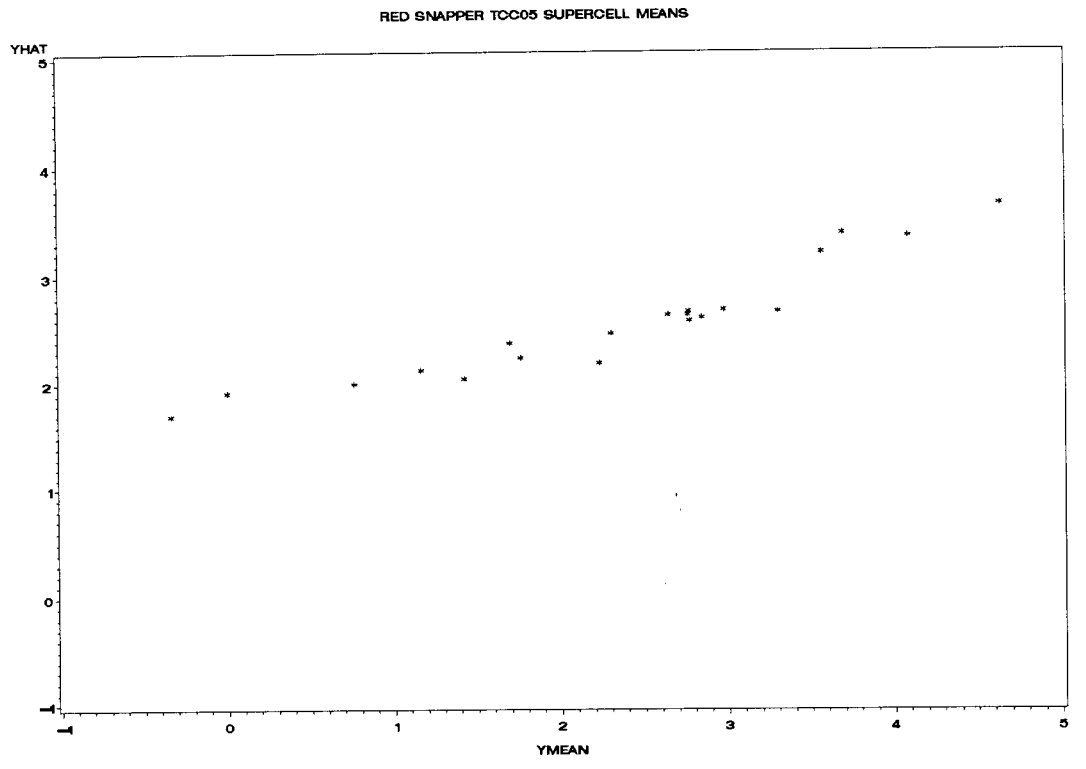

Figure 68. Goodness of fit plot for TC model 02. Arithmetic scale.

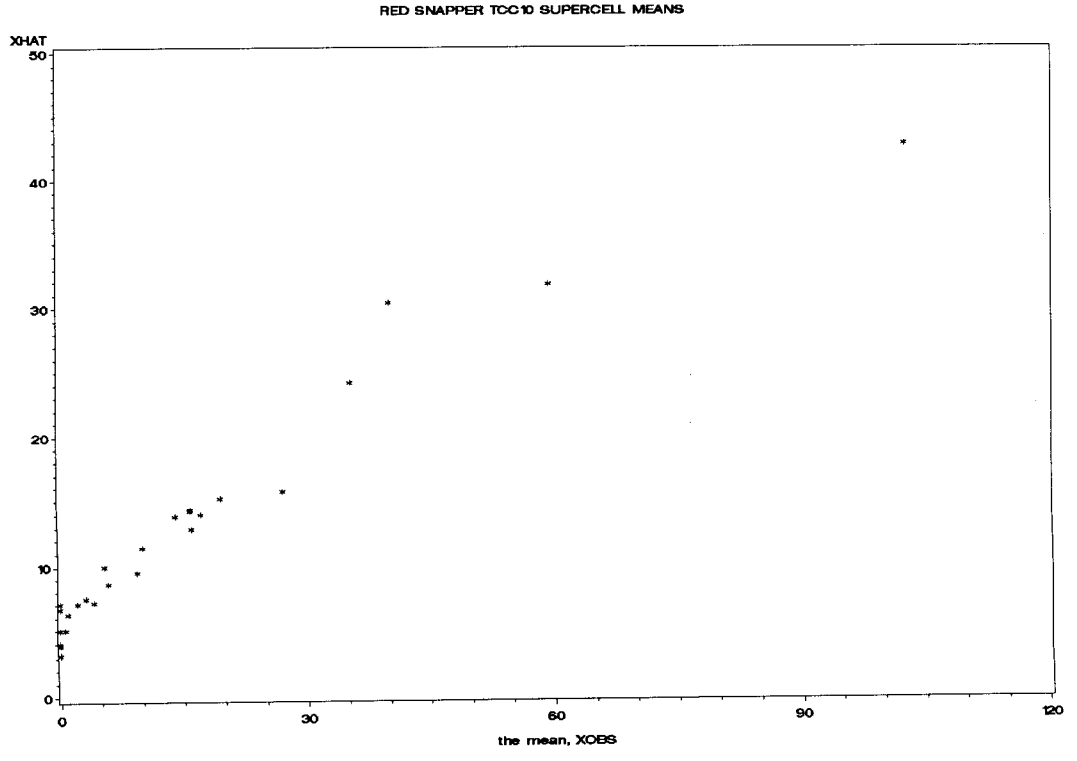

Figure 69. Goodness of fit plot for TC model 02. Log scale.

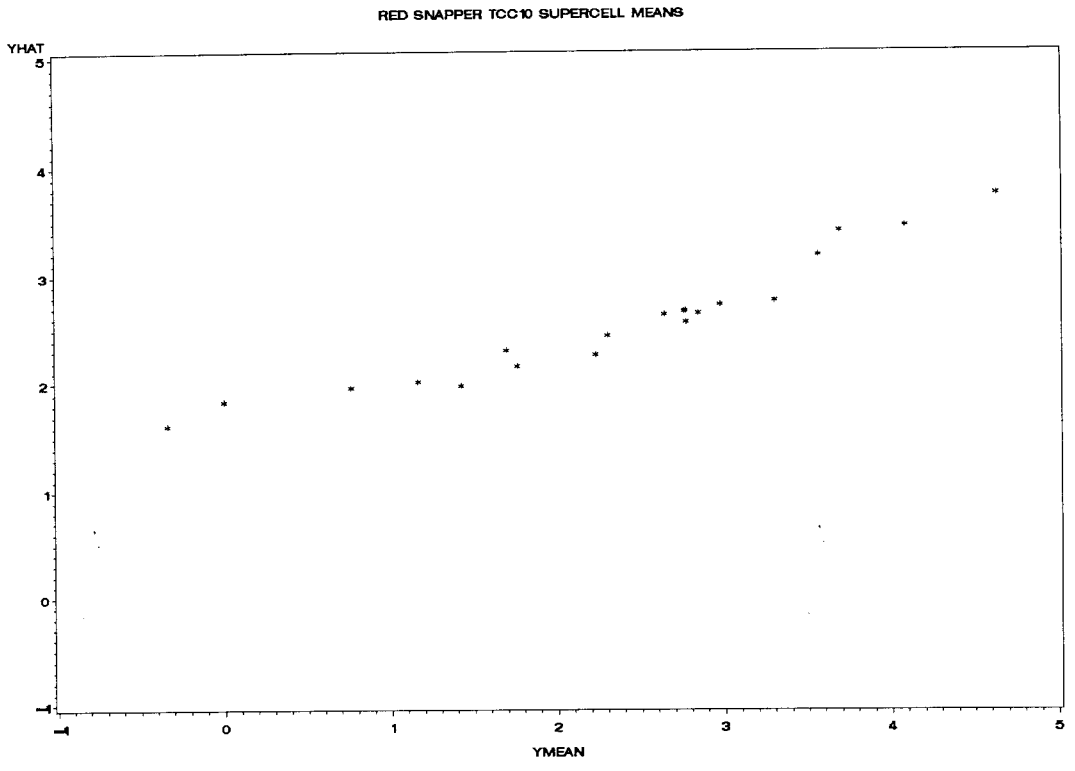

Figure 70. Posterior marginal distributions for the calibration factor to convert TC to the SS scale. a) from the SS 01 model. b) from the SS 02 model.

70a)

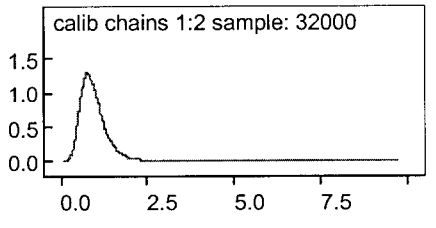

70b)

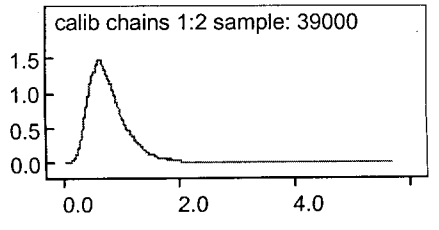

Figure 71. The combined Summer Index based on SS model 01 for 1987-2003, the ES model 01 for 1982-1986, and the TC model 01 for 1981, all calibrated to the SS scale by the results from SS model 01.

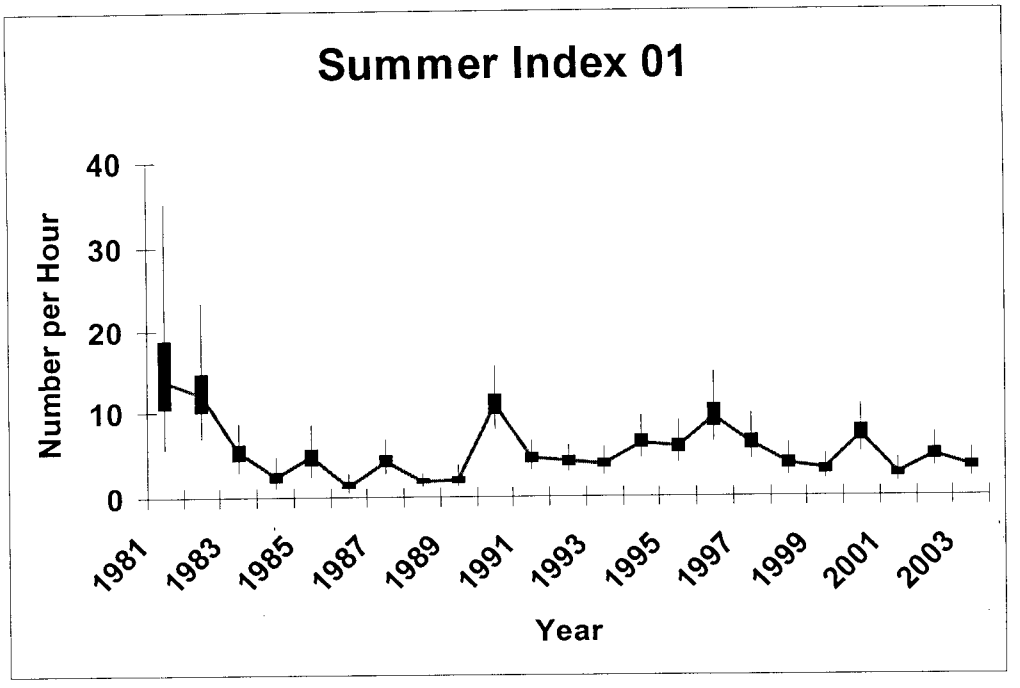

Figure 72. The combined Summer Index based on SS model 02 for 1987-2003, the ES model 02 for 1982-1986, and the TC model 02 for 1981, all calibrated to the SS scale by the results from SS model 02.

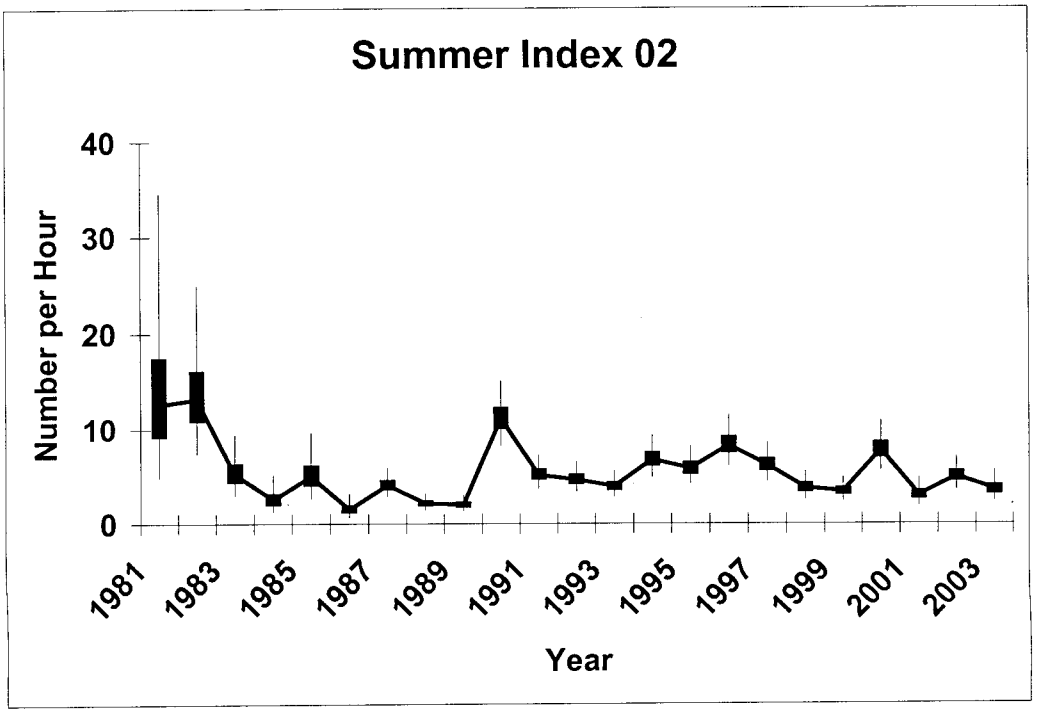

Figure 73. A Fall Index for east of the Mississippi based on the FS and FG 02 models.

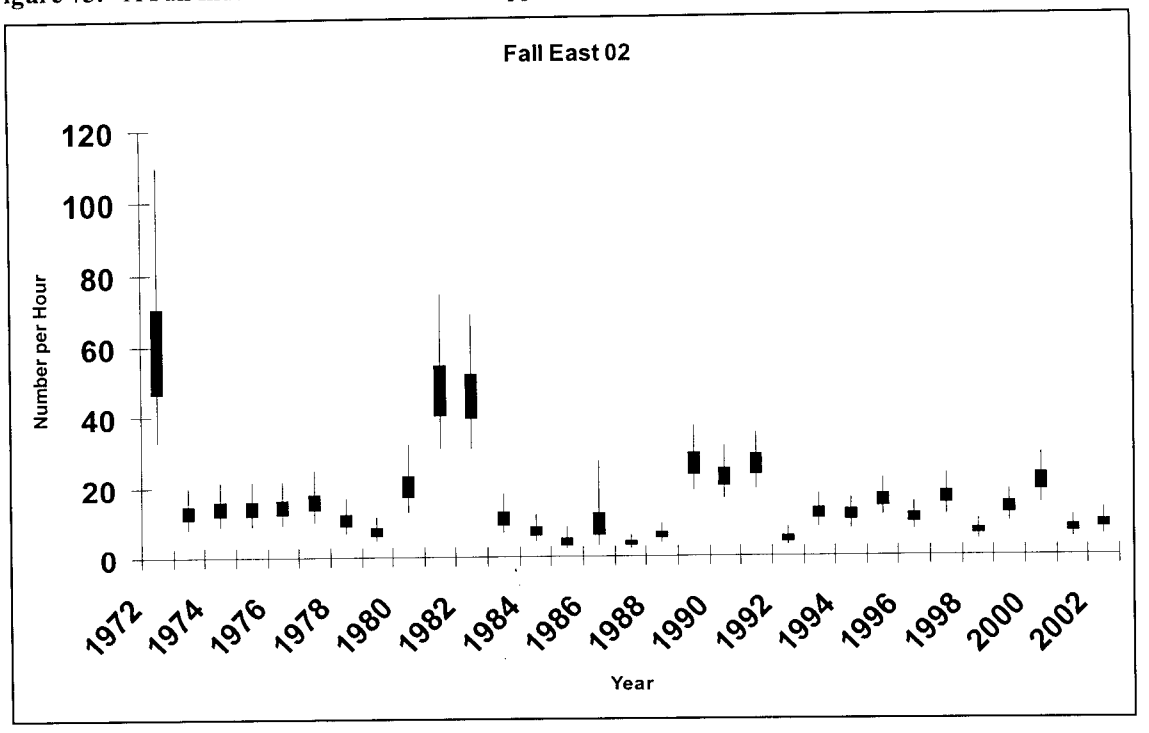

Figure 74. A Fall Index for west of the Mississippi based on the FS and FG 02 models.

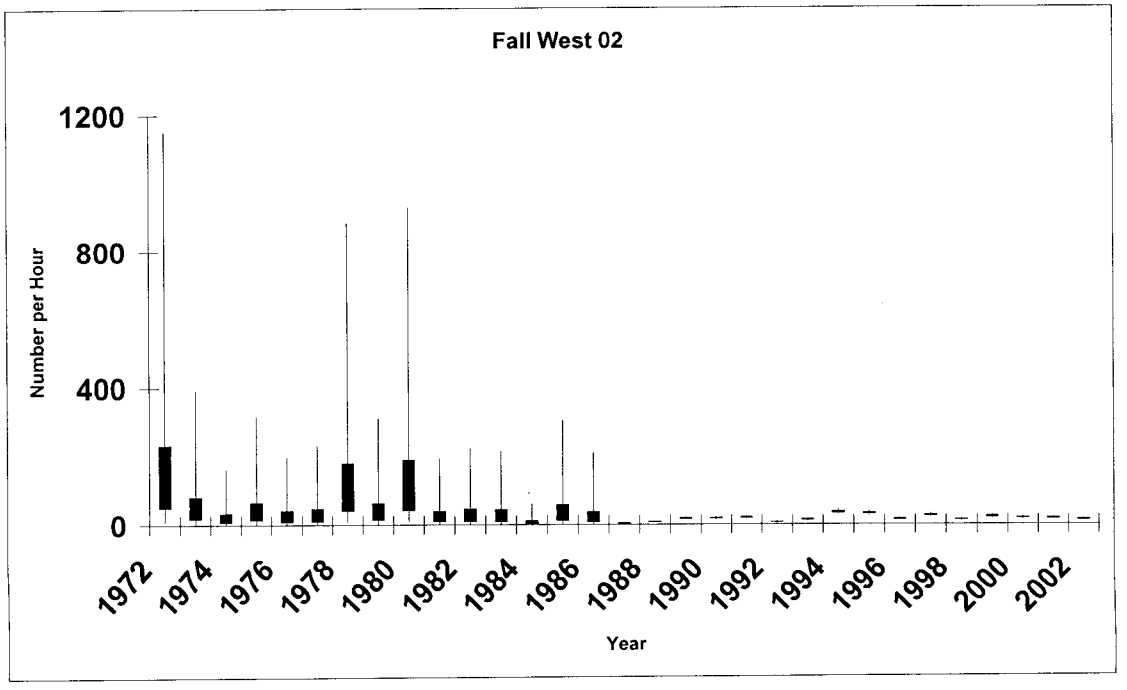

Figure 75. Medians for East and West from the previous two figures, plotted against each other on log scales. (Fall)

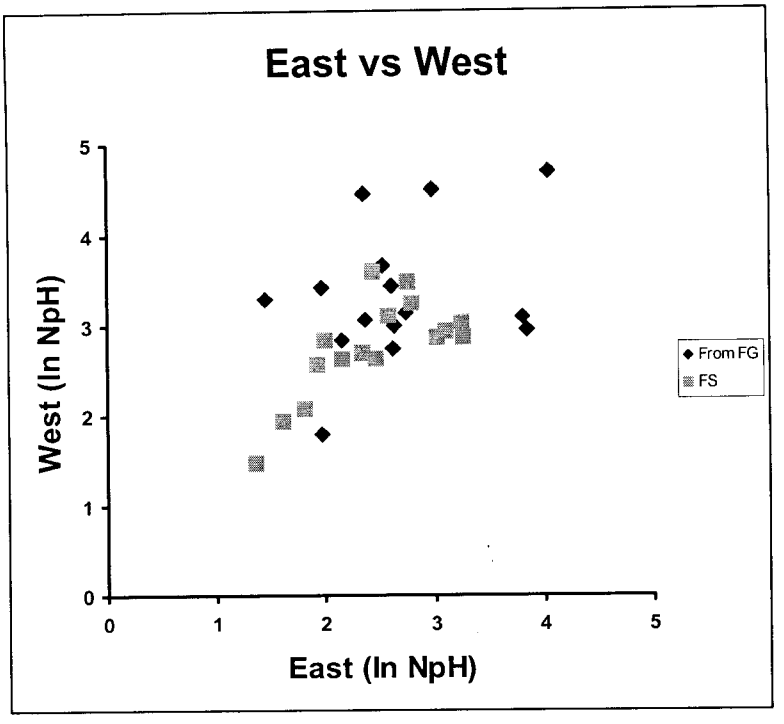

Figure 76. A Summer Index for east of the Mississippi based on the SS and ES 02 models.

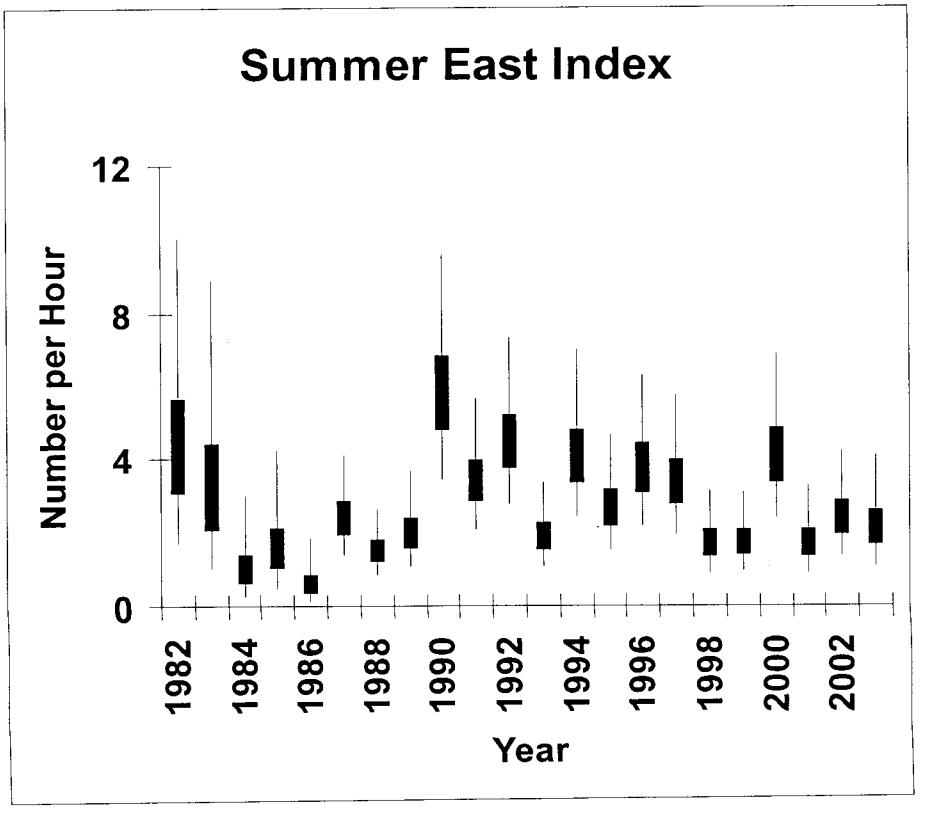

Figure 77. A Summer Index for west of the Mississippi based on the SS, ES, and TC 02 models.

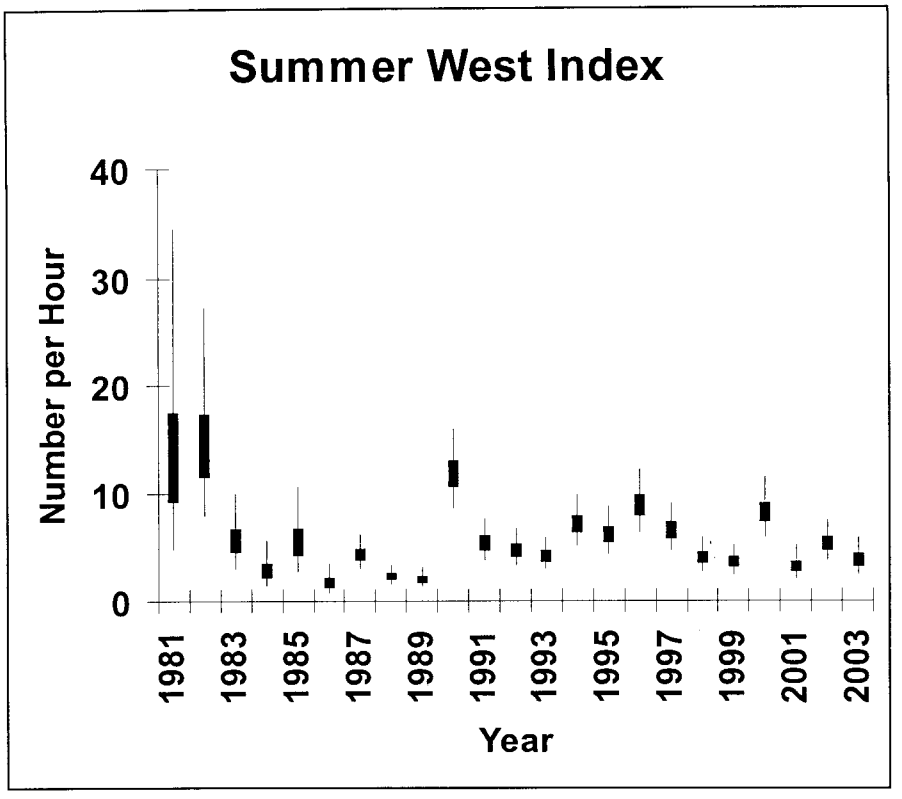

Figure 78. Medians for East and West from the previous two figures, plotted against each other on log scales. (Summer)

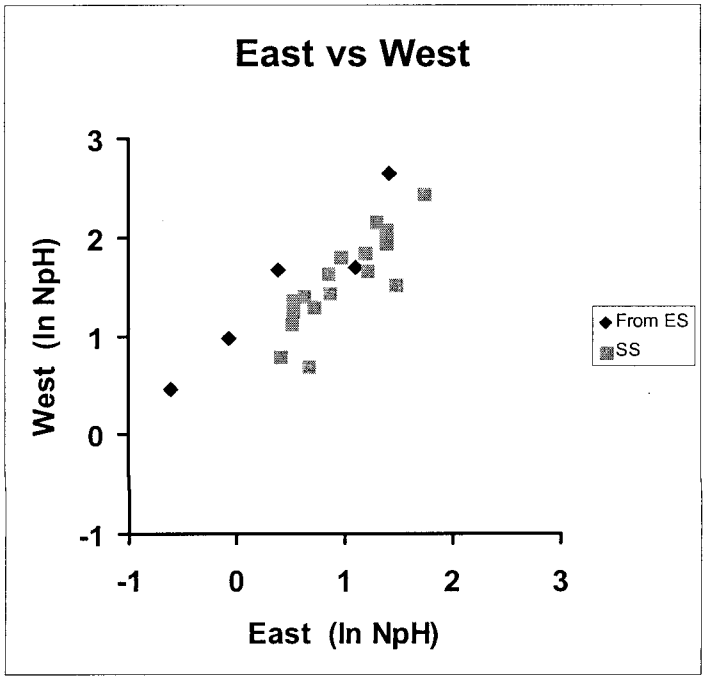

Figure 79. Estimates of Z' based on change in index between fall and summer of successive years. Z' units are year^{-1}.

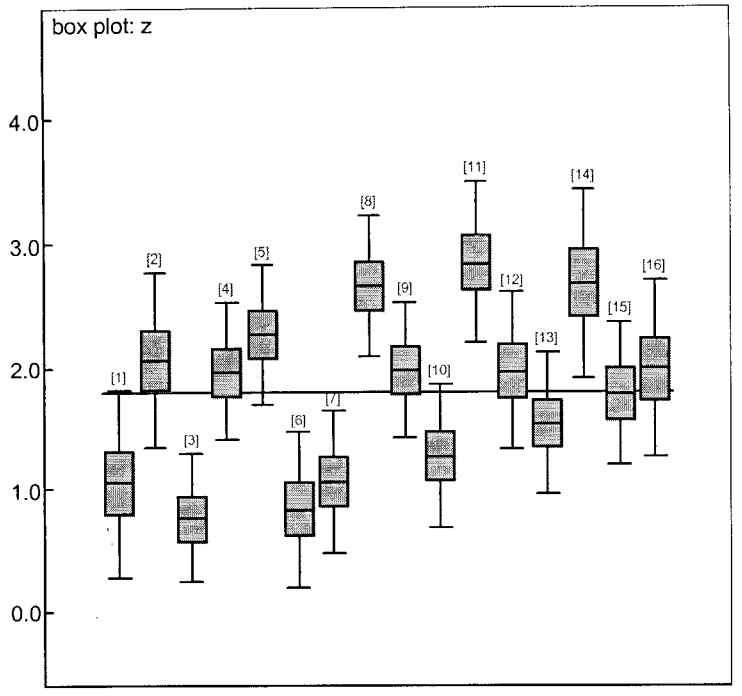

Figure 80. Medians of Z' vs winter/spring shrimping effort (Nov-June, zones 11-21, outside 5 fm).

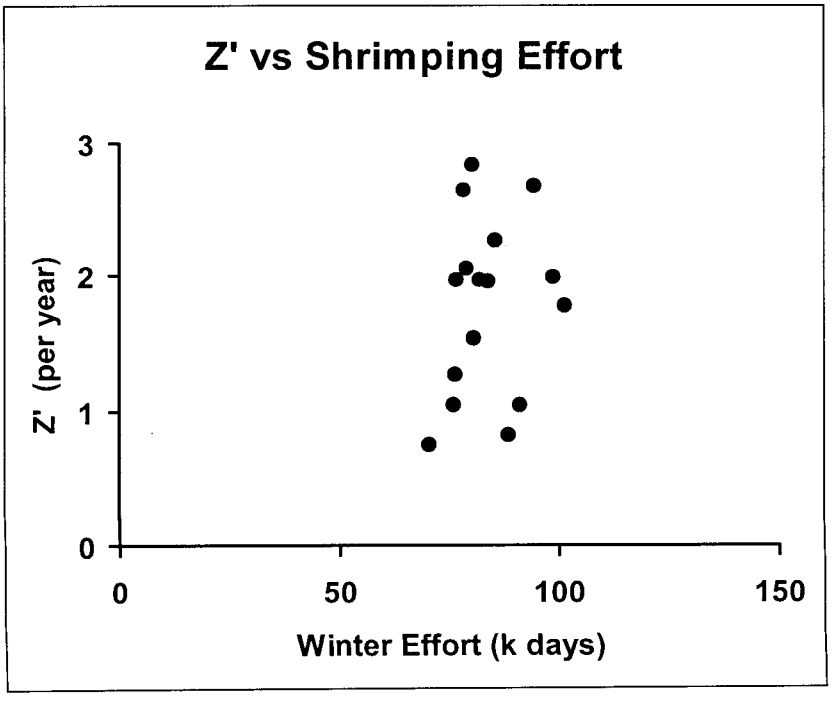

APPENDIX : BUGS Program Listings

BUGS notation is quite compact, and easy to follow once you get used to its idiosyncrasies. The program code does not consist of sequential programing steps like Fortran – instead almost every variable is given a location, with value retained throughout each iteration of the MCMC sampling. BUGS has an annoying convention of specifying statistical distributions by mean and 'precision,' which is variance^{-1} (no doubt a legacy of conjugate priors), rather than using a form like N(mean, variance) in more common usage.

My internal designations of program version reflects several iterations of trials and error corrections. Thus FS model 01 in this paper was conducted with a program titled rsFSc05. I have identified each model by the notation used in this paper above each listing in bold font. Any initial values put into the BUGS run 'by hand' to avoid numerical problems are listed below the actual programs.

Program for FS model 01:

```
model rsFSc05 {

a~dlnorm(0,1)
b~dnorm(1.2,10)

for (i in 1:16) {
 logmean[i]~dnorm(2,0.5)
 tau[i]~dlnorm(0,1)
 logtau[i]<-log(tau[i])
 }
for (i in 1:16) {
 for (j in 1:30) {
  for (k in 1:2)    {
   yhat[i,j,k]~dnorm(logmean[i],tau[i])
   xhat[i,j,k]<-exp(yhat[i,j,k])
   rp[i,j,k]<-a*(pow(xhat[i,j,k],b))
   r[i,j,k]<-max(0.05,rp[i,j,k])
   mu[i,j,k]<-r[i,j,k]/xhat[i,j,k]
   }
  fcell[i,j]<-wate[j]*(xhat[i,j,1]+xhat[i,j,2])/2
  }
 pop[i]<-sum(fcell[i,])
 popwest[i]<-sum(fcell[i,1:24])
 pctwest[i]<-100*popwest[i]/pop[i]
 index[i]<-sum(fcell[i,])/sum(wate[])
 lindex[i]<-log(index[i])
 westindex[i]<-sum(fcell[i,1:24])/sum(wate[1:24])
 eastindex[i]<-sum(fcell[i,25:30])/sum(wate[25:30])
 logwest[i]<-log(westindex[i])
 logeast[i]<-log(eastindex[i])
 westgf[i]<-sum(fcell[i,19:24])/sum(wate[19:24])
 fg[i]<-eastindex[i]*0.4278499 + westgf[i]*0.571501
 ratio[i]<-lindex[i]-log(fg[i])
 ratiosq[i]<-ratio[i]*ratio[i]
 rwest[i]<-logwest[i]-log(westgf[i])
 rwestsq[i]<-rwest[i]*rwest[i]
 }
avgpctwest<-mean(pctwest[])
avgratio<-mean(ratio[2:16])
sdratio<-sqrt((sum(ratiosq[2:16])-avgratio*avgratio/15)/14)
taur<-1/(sdratio*sdratio)
avgindex<-mean(index[])
avgrwest<-mean(rwest[2:16])
sdrwest<-sqrt((sum(rwestsq[2:16])-avgrwest*avgrwest/15)/14)
tauw<-1/(sdrwest*sdrwest)
```

```
for (h in 1:3342) {
 lamb[h]~dgamma(r[yr[h],strat[h],dn[h]],mu[yr[h],strat[h],dn[h]])
 lambda[h]<-lamb[h]*fishtime[h]
 catch[h]~dpois(lambda[h])
 }
}
```

Program for FS model 02:

```
model rsFSc08b {

a~dlnorm(0,1)
b~dnorm(1.2,10)
logmean<-log(10)    # use value near an expected overall mean to center it
tau~dlnorm(0,3)
logtau<-log(tau)

for (i in 1:16) {
 n[i]~dnorm(logmean, 0.3)
 }
for (j in 1:30) {
 sraw[j]~dnorm(0,0.2)
 stratum[j]<-sraw[j]-mean(sraw[])
 }
for (k in 1:2) {
 traw[k]~dnorm(0,1)
 tod[k]<-traw[k]-mean(traw[])
 }
for (i in 1:16) {
 for (j in 1:30) {
  for (k in 1:2)    {
   local[i,j,k]~dnorm(0,tau)
   yhat[i,j,k]<-n[i] + stratum[j] +tod[k]+local[i,j,k]
   xhat[i,j,k]<-exp(yhat[i,j,k])
   rp[i,j,k]<-a*(pow(xhat[i,j,k],b))
   r[i,j,k]<-max(0.05,rp[i,j,k])
   mu[i,j,k]<-r[i,j,k]/xhat[i,j,k]
   }
  fcell[i,j]<-wate[j]*(xhat[i,j,1]+xhat[i,j,2])/2
  }
 pop[i]<-sum(fcell[i,])
 popwest[i]<-sum(fcell[i,1:24])
 poppa[i]<-sum(fcell[i,25:30])+0.62*sum(fcell[i,19:24])
 pctwest[i]<-100*popwest[i]/pop[i]
 pctpa[i]<-100*poppa[i]/pop[i]
 index[i]<-sum(fcell[i,])/sum(wate[])
 lindex[i]<-log(index[i])
 westindex[i]<-sum(fcell[i,1:24])/sum(wate[1:24])
 eastindex[i]<-sum(fcell[i,25:30])/sum(wate[25:30])
 logwest[i]<-log(westindex[i])
 logeast[i]<-log(eastindex[i])
 westgf[i]<-sum(fcell[i,19:24])/sum(wate[19:24])
 fg[i]<-eastindex[i]*0.4278499 + westgf[i]*0.571501
 ratio[i]<-lindex[i]-log(fg[i])
 ratiosq[i]<-ratio[i]*ratio[i]
 rwest[i]<-logwest[i]-log(westgf[i])
 rwestsq[i]<-rwest[i]*rwest[i]
 }
avgpctwest<-mean(pctwest[])
avgpctpa<-mean(pctpa[])
avgratio<-mean(ratio[2:16])
sdratio<-sqrt((sum(ratiosq[2:16])-avgratio*avgratio/15)/14)
taur<-1/(sdratio*sdratio)
avgindex<-mean(index[])
avgrwest<-mean(rwest[2:16])
sdrwest<-sqrt((sum(rwestsq[2:16])-avgrwest*avgrwest/15)/14)
tauw<-1/(sdrwest*sdrwest)
```

```
for (h in 1:3342) {
  lamb[h]~dgamma(r[yr[h],strat[h],dn[h]],mu[yr[h],strat[h],dn[h]])
  lambda[h]<-lamb[h]*fishtime[h]
  catch[h]~dpois(lambda[h])
  }
}

list( tau=1)
list( tau=2)
```

Program for FG model 01:

```
model rsfgc05c {

a~dlnorm(0,0.5)
b~dlnorm(0,0.5)

for (i in 1:15) {
  for (j in 1:2) {
    y[i,j]~dlnorm(2.3,0.3)
    logy[i,j]<-log(y[i,j])
    rp[i,j]<-a*(pow(y[i,j],b))
    r[i,j]<-max(0.05,rp[i,j])
    mu[i,j]<-r[i,j]/y[i,j]
    }
  }
for (k in 1:2990) {
  lamb[k]~dgamma(r[yr[k],st[k]],mu[yr[k],st[k]])
  lambda[k]<-lamb[k]*fishtime[k]
  catch[k]~dpois(lambda[k])
  }
  lcalib~dt(0.4527,2.16,14)                    # avgratio, taur
  calib<-exp(lcalib)
  lcalibwest~dt(0.7218,1.15,14)                        #  avgrwest, tauw
  calibwest<-exp(lcalibwest)

for (i in 1:15) {
  fg[i]<-y[i,1]*0.4278499 + y[i,2]*0.571501
  fs[i]<-fg[i]*calib*3/2.5
  logfs[i]<-log(fs[i])
  logfg[i]<-log(fg[i])
  fswest[i]<-y[i,2]*calibwest*3/2.5
  fseast[i]<-y[i,1]*3/2.5                      # no calib required
  logwest[i]<-log(fswest[i])
  logeast[i]<-log(fseast[i])
  }
}
list( a=0.05, b=0.3)
list( a=0.08, b=0.5)
list( y=structure(.Data=c(
20,20,10,10,20,20,10,10,20,20,10,10,20,20,10,10,20,20,10,10,20,20,10,10,20,20,10,10,20,20),
.Dim=c(15,2)))
list( y=structure(.Data=c(
10,10,20,20,10,10,20,20,10,10,20,20,10,10,20,20,10,10,20,20,10,10,20,20,10,10,20,20,10,10),
.Dim=c(15,2)))
```

Program for FG model 02:

```
model rsfgc08 {
                    # FS 08 same as 05, except calibs are from FS 08
a~dlnorm(0,0.5)
b~dlnorm(0,0.5)

for (i in 1:15) {
 for (j in 1:2)  {
  y[i,j]~dlnorm(2.3,0.3)
  logy[i,j]<-log(y[i,j])
  rp[i,j]<-a*(pow(y[i,j],b))
  r[i,j]<-max(0.05,rp[i,j])
  mu[i,j]<-r[i,j]/y[i,j]
  }
 }
for (k in 1:2990) {
 lamb[k]~dgamma(r[yr[k],st[k]],mu[yr[k],st[k]])
 lambda[k]<-lamb[k]*fishtime[k]
 catch[k]~dpois(lambda[k])
 }
 lcalib~dt(0.5944,1.973,14)          # avgratio, taur
 calib<-exp(lcalib)
 lcalibwest~dt(0.9446,0.9035,14)          # avgrwest, tauw
 calibwest<-exp(lcalibwest)

for (i in 1:15) {
 fg[i]<-y[i,1]*0.4278499 + y[i,2]*0.571501
 fs[i]<-fg[i]*calib*3/2.5
 logfs[i]<-log(fs[i])
 logfg[i]<-log(fg[i])
 fswest[i]<-y[i,2]*calibwest*3/2.5
 fseast[i]<-y[i,1]*3/2.5          # no calib required
 logwest[i]<-log(fswest[i])
 logeast[i]<-log(fseast[i])
 }
}
list( a=0.05, b=0.3)
list( a=0.08, b=0.5)
list( y=structure(.Data=c(
20,20,10,10,20,20,10,10,20,20,10,10,20,20,10,10,20,20,10,10,20,20,10,10,20,20,10,10,20,20),
.Dim=c(15,2)))
list( y=structure(.Data=c(
10,10,20,20,10,10,20,20,10,10,20,20,10,10,20,20,10,10,20,20,10,10,20,20,10,10,20,20,10,10),
.Dim=c(15,2)))
```

Program for SS model 01:

```
model rsSSc05 {

a~dlnorm(0,1)
b~dnorm(1.2,10)

for (i in 1:17) {
 logmean[i]~dnorm(2,0.5)
 tau[i]~dlnorm(0,1)
 logtau[i]<-log(tau[i])
 }
for (i in 1:17) {
 for (j in 1:30) {
  for (k in 1:2)   {
   yhat[i,j,k]~dnorm(logmean[i],tau[i])
   xhat[i,j,k]<-exp(yhat[i,j,k])
   rp[i,j,k]<-a*(pow(xhat[i,j,k],b))
   r[i,j,k]<-max(0.05,rp[i,j,k])
   mu[i,j,k]<-r[i,j,k]/xhat[i,j,k]
   }
```

```
  fcell[i,j]<-wate[j]*(xhat[i,j,1]+xhat[i,j,2])/2
  ncell[i,j]<-wate[j]*xhat[i,j,2]
  }
 pop[i]<-sum(fcell[i,])
 index[i]<-sum(fcell[i,])/sum(wate[])
 lindex[i]<-log(index[i])
 eastindex[i]<-sum(fcell[i,25:30])/sum(wate[25:30])
 westindex[i]<-sum(fcell[i,1:24])/sum(wate[1:24])
 logeast[i]<-log(eastindex[i])
 logwest[i]<-log(westindex[i])
 nindex[i]<-sum(ncell[i,])/sum(wate[])
 lndx[i]<-log(nindex[i])
 poptx[i]<-sum(ncell[i,1:12])
 txindex[i]<-sum(ncell[i,1:12])/sum(wate[1:12])
 logtx[i]<-log(txindex[i])
 ratio[i]<-lindex[i]-logtx[i]
 ratiosq[i]<-ratio[i]*ratio[i]
 pcttx[i]<-100*poptx[i]/pop[i]
 dnfactor[i]<-lindex[i]-lndx[i]
 dnfsq[i]<-dnfactor[i]*dnfactor[i]
 rwest[i]<-logwest[i]-logtx[i]
 rwestsq[i]<-rwest[i]*rwest[i]
 neast[i]<-sum(ncell[i,25:30])/sum(wate[25:30])
 nwest[i]<-sum(ncell[i,1:24])/sum(wate[1:24])
 rne[i]<-logeast[i]-log(neast[i])
 rnw[i]<-logwest[i]-log(nwest[i])
 rnesq[i]<-rne[i]*rne[i]
 rnwsq[i]<-rnw[i]*rnw[i]
 }
avgratio<-mean(ratio[])
avgdnf<-mean(dnfactor[])
sdratio<-sqrt((sum(ratiosq[])-avgratio*avgratio/17)/16)
sddnf<-sqrt((sum(dnfsq[])-avgdnf*avgdnf/17)/16)
taur<-1/(sdratio*sdratio)
taud<-1/(sddnf*sddnf)
avgindex<-mean(index[])
avgtx<-mean(txindex[])
avgnindex<-mean(nindex[])
avgeast<-mean(eastindex[])
avgwest<-mean(westindex[])
avgrwest<-mean(rwest[])
sdrwest<-sqrt((sum(rwestsq[])-avgrwest*avgrwest/17)/16)
tauw<-1/(sdrwest*sdrwest)
avgrne<-mean(rne[])
avgrnw<-mean(rnw[])
sdrne<-sqrt((sum(rnesq[])-avgrne*avgrne/17)/16)
sdrnw<-sqrt((sum(rnwsq[])-avgrnw*avgrnw/17)/16)
taune<-1/(sdrne*sdrne)
taunw<-1/(sdrnw*sdrnw)

for (h in 1:3382) {
  lamb[h]~dgamma(r[yr[h],strat[h],dn[h]],mu[yr[h],strat[h],dn[h]])
  lambda[h]<-lamb[h]*fishtime[h]
  catch[h]~dpois(lambda[h])
  }
}
```

Program for SS model 02:

```
model rsSSc10 {

a~dlnorm(0,0.5)
b~dlnorm(0,0.5)
logmean<-log(10)    # use value near an expected overall mean to center it
tau~dlnorm(0,3)
logtau<-log(tau)

for (i in 1:17) {
  n[i]~dnorm(logmean, 0.3)
```

```
 }
for (j in 1:30) {
 sraw[j]~dnorm(0,0.2)
 stratum[j]<-sraw[j]-mean(sraw[])
 }
for (k in 1:2) {
 traw[k]~dnorm(0,1)
 tod[k]<-traw[k]-mean(traw[])
 }
for (i in 1:17) {
 for (j in 1:30) {
  for (k in 1:2)    {
   local[i,j,k]~dnorm(0,tau)
   yhat[i,j,k]<-n[i] + stratum[j] +tod[k]+local[i,j,k]
   xhat[i,j,k]<-exp(yhat[i,j,k])
   rp[i,j,k]<-a*(pow(xhat[i,j,k],b))
   r[i,j,k]<-max(0.05,rp[i,j,k])
   mu[i,j,k]<-r[i,j,k]/xhat[i,j,k]
   }
  fcell[i,j]<-wate[j]*(xhat[i,j,1]+xhat[i,j,2])/2
  ncell[i,j]<-wate[j]*xhat[i,j,2]
  }
 pop[i]<-sum(fcell[i,])
 index[i]<-sum(fcell[i,])/sum(wate[])
 lindex[i]<-log(index[i])
 eastindex[i]<-sum(fcell[i,25:30])/sum(wate[25:30])
 westindex[i]<-sum(fcell[i,1:24])/sum(wate[1:24])
 logeast[i]<-log(eastindex[i])
 logwest[i]<-log(westindex[i])
 nindex[i]<-sum(ncell[i,])/sum(wate[])
 lndx[i]<-log(nindex[i])
 poptx[i]<-sum(ncell[i,1:12])
 txindex[i]<-sum(ncell[i,1:12])/sum(wate[1:12])
 logtx[i]<-log(txindex[i])
 ratio[i]<-lindex[i]-logtx[i]
 ratiosq[i]<-ratio[i]*ratio[i]
 pcttx[i]<-100*poptx[i]/pop[i]
 dnfactor[i]<-lindex[i]-lndx[i]
 dnfsq[i]<-dnfactor[i]*dnfactor[i]
 rwest[i]<-logwest[i]-logtx[i]
 rwestsq[i]<-rwest[i]*rwest[i]
 neast[i]<-sum(ncell[i,25:30])/sum(wate[25:30])
 nwest[i]<-sum(ncell[i,1:24])/sum(wate[1:24])
 rne[i]<-logeast[i]-log(neast[i])
 rnw[i]<-logwest[i]-log(nwest[i])
 rnesq[i]<-rne[i]*rne[i]
 rnwsq[i]<-rnw[i]*rnw[i]
 }
avgratio<-mean(ratio[])
avgdnf<-mean(dnfactor[])
sdratio<-sqrt((sum(ratiosq[])-avgratio*avgratio/17)/16)
sddnf<-sqrt((sum(dnfsq[])-avgdnf*avgdnf/17)/16)
taur<-1/(sdratio*sdratio)
taud<-1/(sddnf*sddnf)
avgindex<-mean(index[])
avgtx<-mean(txindex[])
avgnindex<-mean(nindex[])
avgeast<-mean(eastindex[])
avgwest<-mean(westindex[])
avgrwest<-mean(rwest[])
sdrwest<-sqrt((sum(rwestsq[])-avgrwest*avgrwest/17)/16)
tauw<-1/(sdrwest*sdrwest)
avgrne<-mean(rne[])
avgrnw<-mean(rnw[])
sdrne<-sqrt((sum(rnesq[])-avgrne*avgrne/17)/16)
sdrnw<-sqrt((sum(rnwsq[])-avgrnw*avgrnw/17)/16)
taune<-1/(sdrne*sdrne)
taunw<-1/(sdrnw*sdrnw)
```

```
for (h in 1:3382) {
 lamb[h]~dgamma(r[yr[h],strat[h],dn[h]],mu[yr[h],strat[h],dn[h]])
 lambda[h]<-lamb[h]*fishtime[h]
 catch[h]~dpois(lambda[h])
 }
}

list( tau=1, a=0.5, b=0.5)
list( tau=2, a=0.4, b=0.4)
```

Program for ES model 01:

```
model rses05 {

a~dlnorm(0,1)
b~dnorm(1.2,10)

for (i in 1:5) {
 meen[i]~dlnorm(2,0.5)
 lgm[i]<-log(meen[i])
 tau[i]~dlnorm(0,1)
 logtau[i]<-log(tau[i])
 }
for (i in 1:5) {
 for (j in 1:30) {
    xhat[i,j]~dlnorm(lgm[i],tau[i])
    yhat[i,j]<-log(xhat[i,j])
    rp[i,j]<-a*(pow(xhat[i,j],b))
    r[i,j]<-max(0.05, rp[i,j])
    mu[i,j]<-r[i,j]/xhat[i,j]
    fcell[i,j]<-wate[j]*xhat[i,j]
    }
 index[i]<-sum(fcell[i,])/sum(wate[])
 lindex[i]<-log(index[i])
 eastindex[i]<-sum(fcell[i,25:30])/sum(wate[25:30])
 westindex[i]<-sum(fcell[i,1:24])/sum(wate[1:24])
 logeast[i]<-log(eastindex[i])
 logwest[i]<-log(westindex[i])
 }
for (h in 1:523) {
 lamb[h]~dgamma(r[yr[h],strat[h]],mu[yr[h],strat[h]])
 lambda[h]<-lamb[h]*fishtime[h]
 catch[h]~dpois(lambda[h])
 }
lcalib~dt(-0.06934,34,16)     # these are avgdnf
calib<-exp(lcalib)
lcalw~dt(-0.06477,31.04,16)  # these are rne and rnw
lcale~dt(-0.03169,10.46,16)
calibwest<-exp(lcalw)
calibeast<-exp(lcale)
for (i in 1:5) {
 fs[i]<-index[i]*calib
 logfs[i]<-log(fs[i])
 fseast[i]<-eastindex[i]*calibeast
 fswest[i]<-westindex[i]*calibwest
 logfseast[i]<-log(fseast[i])
 logfswest[i]<-log(fswest[i])
 }
}
list(
b=0.4,
a=0.1,
meen=c(5,2,5,2,5),
tau=c(1,1,1,1,1)
)
```

```
list(
b=0.5,
a=0.2,
meen=c(2,5,2,5,2),
tau=c(2,2,2,2,2)
)
```

Program for ES model 02:

```
model rses10 {

a~dlnorm(0,0.5)
b~dlnorm(0,0.5)

logmean<-log(10)    # use value near overall mean
tau~dlnorm(0,3)
logtau<-log(tau)

for (i in 1:5) {
  n[i]~dnorm(logmean, 0.3)
  }
for (j in 1:30) {
  sraw[j]~dnorm(0,0.2)
  stratum[j]<-sraw[j]-mean(sraw[])
  }
for (i in 1:5) {
  for (j in 1:30) {
    local[i,j]~dnorm(0,tau)
    yhat[i,j]<-n[i] + stratum[j] + local[i,j]
    xhat[i,j]<-exp(yhat[i,j])
    rp[i,j]<-a*(pow(xhat[i,j],b))
    r[i,j]<-max(0.05,rp[i,j])
    mu[i,j]<-r[i,j]/xhat[i,j]
    fcell[i,j]<-wate[j]*xhat[i,j]
    }
  index[i]<-sum(fcell[i,])/sum(wate[])
  lindex[i]<-log(index[i])
  eastindex[i]<-sum(fcell[i,25:30])/sum(wate[25:30])
  westindex[i]<-sum(fcell[i,1:24])/sum(wate[1:24])
  logeast[i]<-log(eastindex[i])
  logwest[i]<-log(westindex[i])
  }
for (h in 1:523)  {
  lamb[h]~dgamma(r[yr[h],strat[h]],mu[yr[h],strat[h]])
  lambda[h]<-lamb[h]*fishtime[h]
  catch[h]~dpois(lambda[h])
  }
lcalib~dt(-0.1439,28.17,16)     # these are avgdnf
calib<-exp(lcalib)
lcalw~dt(-0.142,27.49,16)  # these are rne and rnw
lcale~dt(-0.1358,15.36,16)
calibwest<-exp(lcalw)
calibeast<-exp(lcale)
for (i in 1:5)  {
  fs[i]<-index[i]*calib
  logfs[i]<-log(fs[i])
  fseast[i]<-eastindex[i]*calibeast
  fswest[i]<-westindex[i]*calibwest
  logfseast[i]<-log(fseast[i])
  logfswest[i]<-log(fswest[i])
  }
}
list(
b=0.4,
a=0.1,
tau=1
)
list(
```

```
b=0.5,
a=0.2,
tau=2
)
```

Program for TC model 01:

```
model rstc05 {

a~dlnorm(0,1)
b~dnorm(1.2,10)
meen~dlnorm(0,0.5)
lgm<-log(meen)
tau~dlnorm(0,1)
logtau<-log(tau)

for (j in 1:27) {
  xhat[j]~dlnorm(lgm,tau)
  yhat[j]<-log(xhat[j])
   rp[j]<-a*(pow(xhat[j],b))
   r[j]<-max(0.05, rp[j])
   mu[j]<-r[j]/xhat[j]
   fcell[j]<-wate[j]*xhat[j]
   }
index<-sum(fcell[])/sum(wate[])
lindex<-log(index)

for (h in 1:85) {
  lamb[h]~dgamma(r[strat[h]],mu[strat[h]])
  lambda[h]<-lamb[h]*effort[h]
  catch[h]~dpois(lambda[h])
  }
lcalib~dt(-0.1252,7.421,16) # avgratio
calib<-exp(lcalib)
fs<-index*calib
logfs<-log(fs)
lcalw~dt(-0.112,8.299,16)   # avgrwest
calibw<-exp(lcalw)
fswest<-index*calibw
logfswest<-log(fswest)
}

list(
b=0.7,
a=0.03,
meen=5,
tau=1
)
list(
b=0.8,
a=0.04,
meen=7,
tau=2
)
```

Program for TC model 02:

```
model rstc10 {

a~dlnorm(0,0.5)
b~dlnorm(0,0.5)
meen~dlnorm(0,0.5)
lgm<-log(meen)
tau~dlnorm(0,1)
logtau<-log(tau)
```

```
for (j in 1:27) {
  xhat[j]~dlnorm(lgm,tau)
  yhat[j]<-log(xhat[j])
   rp[j]<-a*(pow(xhat[j],b))
   r[j]<-max(0.05, rp[j])
   mu[j]<-r[j]/xhat[j]
   fcell[j]<-wate[j]*xhat[j]
   }
index<-sum(fcell[])/sum(wate[])
lindex<-log(index)

for (h in 1:85) {
  lamb[h]~dgamma(r[strat[h]],mu[strat[h]])
  lambda[h]<-lamb[h]*effort[h]
  catch[h]~dpois(lambda[h])
  }
lcalib~dt(-0.2998,6.549,16) # avgratio
calib<-exp(lcalib)
fs<-index*calib
logfs<-log(fs)
lcalw~dt(-0.2624,7.787,16)   # avgrwest
calibw<-exp(lcalw)
fswest<-index*calibw
logfswest<-log(fswest)
}

list(
b=0.7,
a=0.03,
meen=5,
tau=1
)
list(
b=0.8,
a=0.04,
meen=7,
tau=2
)
```

Program for estimating Z':

```
model z {

sdmult<-1

for (i in 1:16) {
  ftau[i]<-1/(sdmult*sdmult*fsd[i]*fsd[i])
  stau[i]<-1/(sdmult*sdmult*ssd[i]*ssd[i])
  fs[i]~dt(fmeen[i],ftau[i],30)
  ss[i]~dt(smeen[i],stau[i],30)
  z[i]<-12*(fs[i]-ss[i])/8
  }
avgz<-mean(z[])
}

list(
fmeen=c(1.47,2.068,2.911,2.943,3.046,1.924,2.613,3.529,3.434,2.665,3.224,2.527,3.071,2.885,
2.786,2.595),
fsd=c( 0.1655,0.1186,0.09844,0.09594,0.09498,0.1296,0.1149,0.09283,0.09451,0.1079,
0.09698,0.1188,0.1032,0.1029,0.1095,0.1102),
smeen=c(0.7673,0.6969,2.408,1.639,1.536,1.372,1.912,1.758,2.116,1.818,1.325,1.218,2.047,
1.099,1.601,1.274),
ssd=c(0.2024,0.2109,0.1528,0.1687,0.1695,0.1729,0.1636,0.1704,0.1635,0.1669,0.1954,0.1845,
0.1689,0.2416,0.173,0.2196)
)
```